IRAM Annual Report 2014

iram
Institut de
Radioastronomie
Millimétrique

IRAM Annual Report 2014

Published by IRAM © 2014
Director of publication Karl-Friedrich Schuster
Edited by Sabine König, Catherine Berjaud and Karin Zacher

With contributions from:
Sébastien Blanchet, Walter Brunswig, Isabelle Delaunay, Bertrand Gautier, Olivier Gentaz, Frédéric Gueth, Carsten Kramer, Bastien Lefranc, Alessandro Navarrini, Santiago Navarro, Roberto Neri, Juan Peñalver, Karl-Friedrich Schuster

Contents

Introduction

2014 has been a good year for IRAM. After years of planning and project preparation numerous important undertakings have come to be reality.

First of all, NOEMA, the Northern Extended Millimeter Array, has seen its first antenna (Ant. 7) completed, and other new and important pieces of hardware such as the new phase reference system have been installed at the observatory. In September 2014, the completion of the first NOEMA antenna was celebrated with great attention from IRAM's partner organizations as well as from local, regional and national representatives. During the celebration event the IRAM partner organizations CNRS, MPG and IGN reconfirmed their enthusiastic support for IRAM as one of the most successful international astronomy collaborations in Europe. While in France this support for IRAM has been underlined by the 2014 INSU science prospective exercise, which placed NOEMA in the highest priority category, the German partner MPG has announced that additional funds have been identified for future upgrades.

Reaching the important milestone of the completion of Ant. 7 indicates that the long-term efforts of IRAM's highly motivated staff has paid off and many challenges were successfully overcome. Moreover, the collected experience generated a very steep learning curve which will form a solid base and generate confidence for the years to come. Towards the end of 2014 the assembly of the next antenna (Ant. 8) has already been started. The next challenges will now be to progress as foreseen with the receiver upgrades, and the development of POLYFIX, the powerful and innovative next-generation correlator for NOEMA.

The second very important achievement concerns the access to the NOEMA observatory. During the last months of 2014, the new cable car to the Plateau de Bure was completed, with commissioning and start of operations scheduled for spring 2015. As one can imagine, this project has been complex not only due to the exceptional site, the important costs of the project and the interaction with the ongoing upgrade of the observatory, but in particular also with respect to the tragic events in IRAM's history. The reestablishment of a safe, reliable and efficient access was and is a necessary condition for the bright future of the NOEMA project, and IRAM as a whole.

IRAM is in the exceptional position that, in parallel to the very important efforts for NOEMA, the development of NIKA-2 (Neel-IRAM-KID-Array 2), a major facility instrument for the IRAM 30-meter telescope, has been possible through collaboration with local French and European partners. NIKA-2 will be a unique and extremely powerful dual band millimeter imager for the 2 and 1.1 mm bands, including a polarimetry option. In 2014, the project has entered the phase where the different components such as the cryostat were assembled and detector prototype arrays have been fabricated. The detector development program has greatly profited from the French LABEX program FOCUS. The wide field of view of NIKA-2 requires important upgrades in the 30-meter telescope Nasmyth optics. During 2014, these upgrades have been thoroughly prepared with work at the telescope foreseen for spring 2015. The precursor visiting instruments NIKA-1 and GISMO have not only helped to pave the way for NIKA-2, but also delivered exquisite science clearly demonstrating the scientific potential of large scale continuum mapping with the IRAM 30-meter telescope. It has been a particular pleasure and a very positive experience for the IRAM staff to collaborate with the highly professional GISMO team from NASA Goddard.

Science programs with IRAM continued to be extremely successful and productive. The unique variety of instruments at the IRAM facilities provides users with the tools to study the whole bandwidth of topics in modern astronomy, from planetary and solar system science to cosmology. A central subject for many highly successful programs remains the aspect of star formation on all spatial scales while ultra-wide bandwidth, high-resolution spectroscopy observations with IRAM's receivers have started to revolutionize astrochemistry. IRAM's facilities are essential for the analysis, transformation and completion of the Herschel and Planck data heritage. The strategy of a close interaction and

synergy of IRAM and ALMA is now clearly confirmed. A phenomenon which underlines this situation is the sharp increase in pressure on IRAM facilities from non-IRAM countries which have recently obtained access to ALMA through ESO.

I would like to thank the IRAM staff for their continuous work of highest quality which allowed to cope with the many challenges which had to be overcome to reach the current success. This annual report will only give a partial view on all the things going on at IRAM but it will certainly also give you a flavor of the many exiting things to come.

Karl-Friedrich Schuster
Director

Left: Official inauguration of the 1st NOEMA antenna (from left to right): Bertrand Gautier (NOEMA station manager), Karl Schuster (IRAM Director), Reinhard Genzel (MPE Director), Richard Bonneville (French Ministry for Research), Martin Stratmann (MPG President), Klaus Ranner (Consul General of the Federal Republic of Germany), David Musial (German Ambassy), Pascale Delecluse (INSU Director), Denis Mourard (INSU Vice Director), Brigitte Indigo (IRAM), Jesus Gomez-Gonzalez (Vice Director Spanish IGN), Markus Schleier (MPG), Linda Tacconi (IRAM SAC Member), Susanne Wasum-Rainer (Ambassadress of the Federal Republic of Germany), Milda Krasauskaite (MPG). Credits: Edyta Tolwinska

Below left: Pascale Delecluse (INSU Director) and Martin Stratmann (MPG President) clear the way for the 1st NOEMA antenna. Credits: Edyta Tolwinska.

Below: MPE Director Reinhard Genzel presenting future research possibilities with NOEMA. Credits: Ludovic Fortoul.

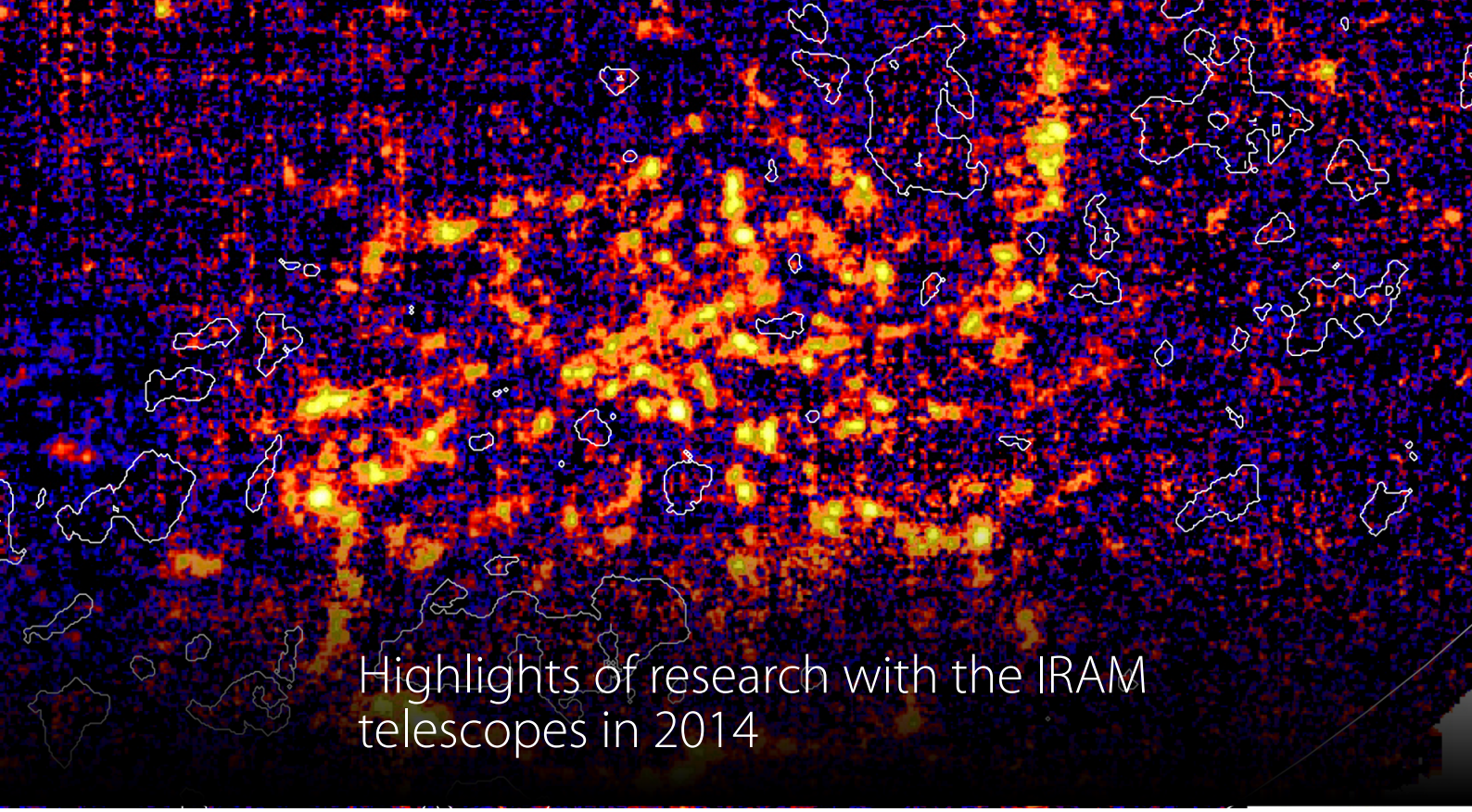

Highlights of research with the IRAM telescopes in 2014

NEW INSIGHTS TO THE FORMATION OF MASSIVE STARS

One of the challenges in understanding how stars form is how massive clouds of gas and dust fragment to produce the direct progenitors of individual stars. In order to shed new light on the formation of stars more than 10 times the mass of our Sun, an international team of astronomers led by Nicolas Peretto (Cardiff University) has used the IRAM 30-meter telescope in Spain.

Stars form in some of the coldest (~10 Kelvin) regions of the Universe, deep inside large clouds of molecular gas. Observations at wavelengths from the FIR to millimeter of star-forming regions have revealed that these clouds are sub-structured into complex networks of clumps, filaments and cores. These central cores are the direct progenitors of individual stars. Despite their importance, how these cores form and evolve remains unclear in several aspects. In particular the temperature of these cores is too low to prevent them from fragmenting into small pieces. A different source of pressure support is therefore necessary to form super-Sun progenitors.

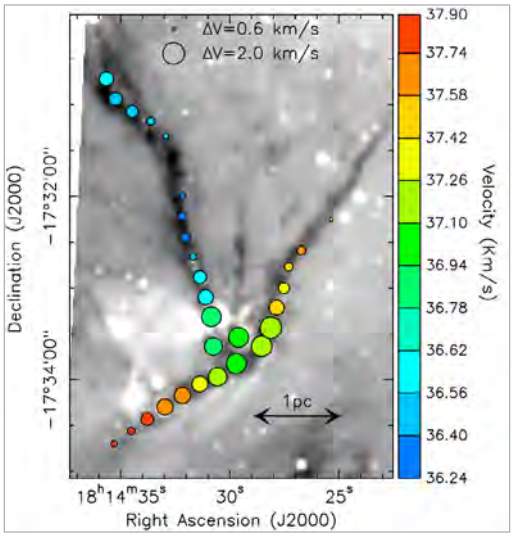

Spitzer 8 µm image of SDC13 in grey scale with the results of the N_2H^+(1-0) HFS fitting as circles. The color of the circles codes the gas velocity while their sizes code the gas velocity dispersion.
Work by Peretto et al. 2014, A&A, 561, A83

By observing the structure and motion of a set of infrared dark interstellar filaments, the researchers have found for the first time clear evidence that in-falling streams of dense gas can set the conditions for the formation of super-Sun progenitors.

Peretto and collaborators investigated SDC13, a Spitzer identified Dark Cloud region consisting in a small network of infrared dark filaments with total mass ~1000 $M_\odot$. The darkness of these dense filamentary clouds ensures that the initial conditions for the formation of stars are still imprinted in the gas properties.

The observations revealed the presence of two intermediate-mass cores, ~80 $M_\odot$ each, sitting at the junction of the long dark filaments. Complementary observations obtained with the EMIR heterodyne receiver at the IRAM 30-meter telescope further showed that the gas within the filaments exhibits correlated velocity and internal motion gradients, the largest internal motions being measured at the center of the system, near the cores.

Comparison with a simple model suggests that these filaments are collapsing along their length. The effect of this collapse is two-fold: it channels material to the

center of the system and the cores, and it provides in addition the energy that allows super-Sun progenitor cores to form.

According to the authors this finding bridges the gap between what is known about the formation of solar-type stars and the formation of the most massive stars in the Galaxy. As more and more massive progenitors are found and studied, it seems that the impact of large-scale gas dynamics becomes increasingly important. These results point towards a picture of star formation that researchers have been arguing over for the past decade.

CALYPSO PROVIDES A FIRST IN-DEPTH LOOK AT COMS

Along the path leading to the formation of solar-type stars, the Class 0 phase is the main accretion phase during which most of the final stellar mass is accreted onto the central protostellar object. It is therefore of paramount importance to study the properties of the infalling envelope material on all scales during the Class 0 phase. Ultimately, this will allow us to constrain the efficiency of the accretion/ejection process to build solar-type stars and to shed light on the initial conditions for the formation of protoplanetary disks and planets around stars like our own.

On small spatial scales (≤50-200 AU) where the progenitors of the protoplanetary disks are assembled, most envelope tracers like ^{12}CO and N_2H^+ are optically thick or chemically destroyed. As this makes it difficult to probe the physical properties of the inner envelope on scales where accretion actually proceeds, Anaëlle Maury (Harvard/ESO/Laboratoire AIM) and collaborators embarked on CALYPSO (Continuum And Lines in Young ProtoStellar Objects), an IRAM Plateau de Bure Large Program to observe various complex organic molecules (COMs) towards a statistically significant sample of low-mass Class 0 protostars. These molecules are likely to trace the warm inner envelope heated by the central protostellar object, and hence are excellent candidates to study the infall and accretion of circumstellar material down to the very vicinity of the protostar. The aim of CALYPSO is to determine if the COM emission lines trace an embedded disk, shocks from the protostellar jet, or the warm inner parts of the protostellar envelope.

First results obtained on NGC 1333-IRAS2A show that the emission of numerous COMs originates from a region of ~60 AU around the protostar, that there is no evidence for a preferential elongation of the COMs along the jet, and hence that COM emission is not arising from shocked envelope material at the base of the jet. Down to similar sizes, the dust emission is well reproduced with a single power-law envelope model, and thus does not favor the hypothesis that COM emission arises from the thermal sublimation of grains embedded in a circumstellar disk. Finally, the COM emission is consistent with the size of the inner envelope where a dust temperature >100 K is expected. This strongly suggests that COMs trace the warm inner envelope where the icy mantles of dust grains evaporate.

These results obtained in the frame of CALYPSO program suggest that the analysis of spectral emission lines from COMs could become a powerful tool for tracing the protostellar kinematics during the disk formation epoch, on scales where protoplanetary disks are observed at later evolutionary stages.

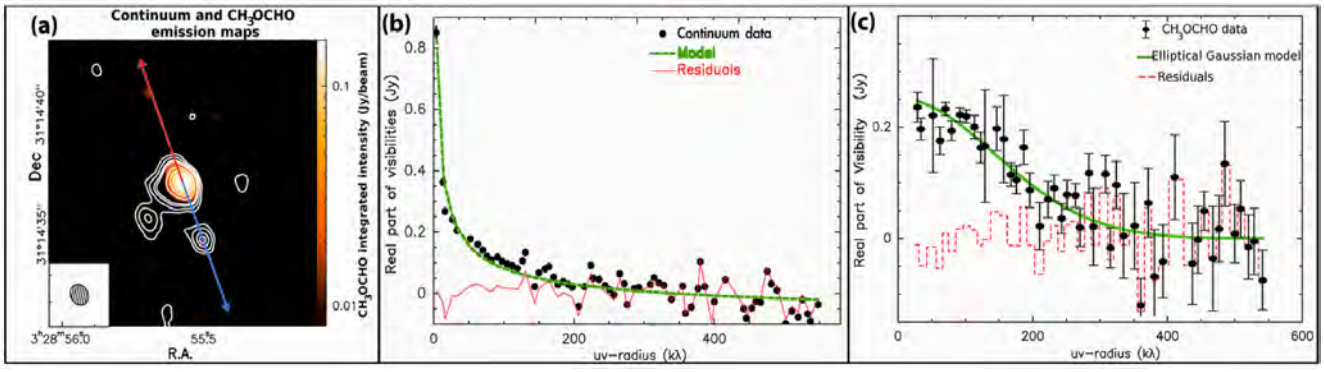

CH_3OCHO at 217 GHz (background) and continuum (contours) emission maps towards IRAS2A. The synthesized beam is 0.80″ × 0.68″. The red and blue arrows show the direction of the jet; b) continuum visibilities averaged over baseline bins of 10m, power-law model (green) and residuals (red); c) CH_3OCHO visibilities, Gaussian model (FWHM 0.47″×0.40″, green line) and residuals (red).
Work by Maury et al. 2014, A&A, 563, L2

PROTOSTELLAR ACCRETION, DISK AND JET IN IRAS 20126+4104

The quest for disks around newly formed early-type stars is one of the challenges of modern astronomy. While there is general consensus that solar-type stars form through disk-mediated accretion, it is still debated whether a scaled-up version of the same formation mechanism holds for high-mass stars. These stars reach the zero-age main sequence while they still undergo mass accretion from their parental core. Under these circumstances, the powerful radiation pressure of the star is expected to halt the infalling material, thus preventing further growth of the stellar mass. This so called radiation pressure problem has recently found a solution that involves accretion through a circumstellar disk.

To date, only a handful of disk candidates are known, and basically all of them are associated with early B-type stars, whereas disks around the most massive, O-type stars appear elusive. The best-known disk candidate around a B-type star is IRAS 20126+4104. To investigate the structure of the disk around this star and its relationship with the jet, Riccardo Cesaroni (INAF, Italy) and collaborators performed observations with the interferometer. They mapped several rotational transitions of $CH_3{}^{12}CN$ and of the $CH_3{}^{13}CN$ isotopologue with ~0.4" (~660 AU) resolution. Their findings confirm the existence of a disk rotating around a ~7–10 $M_\odot$ B-type protostar with the velocity increasing at small radii. The dramatic improvement in sensitivity and spectral and angular resolution of the IRAM interferometer with respect to previous observations allowed to establish that higher excitation transitions are emitted closer to the protostar than the ground state lines, which demonstrates that the gas temperature is increasing towards the center.

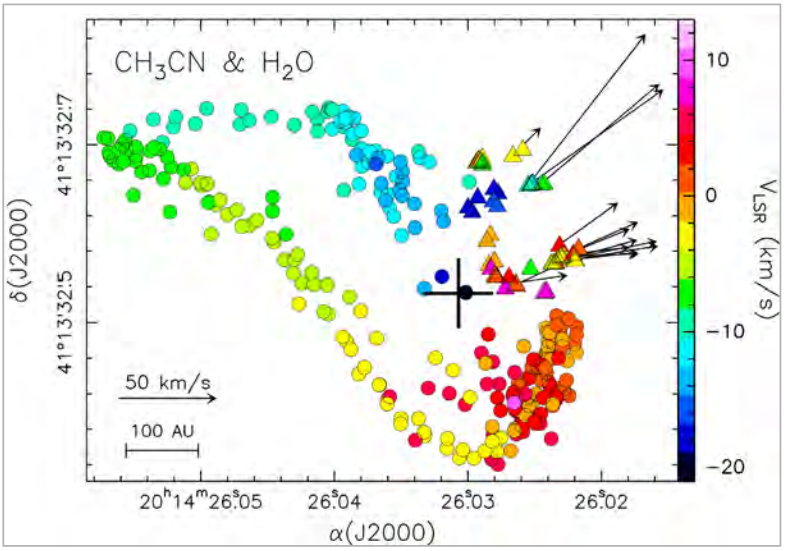

Map of the peaks of the CH_3CN K = 2, 3, 4 line emission (circles) and water maser spots (triangles) from Moscadelli et al. (2000, 2005) and Edris et al. (2005). The color indicates the LSR velocity. The arrows indicate the proper motions measured by Moscadelli et al. (2005). The cross marks the position of the continuum emission peak.
Work by Cesaroni et al. 2014, A&A, 566, A73

The results also reveal that the material is asymmetrically distributed in the disk. The authors argue that this is further evidence to support the view that B-type stars may form through disk-mediated accretion as their low-mass siblings do, and suggest that the disk structure may be significantly perturbed by tidal interactions with companions, even in a relatively poor cluster such as the one associated with IRAS 20126+4104. This might explain why disks around O-stars, surrounded by rich clusters, have been until now so elusive. It is to expect that in the long term NOEMA's high sensitivity and broader range of capabilities will greatly help to expand the discovery space opened by ALMA to explore the diversity and the evolution of disks around a large number of B- and O-type protostars.

Finally, comparison between previous H_2O maser data tracing the jet and the CH_3CN data reveal that the jet is rotating about its axis. This finding not only constrains the genesis of the jet, but also provides further evidence that the velocity gradient observed in CH_3CN is indeed tracing rotation about the jet axis and that the jet emitted along the disk axis is co-rotating with the disk.

NEW GIANT PLANET ON EDGE OF DISCOVERY?

The formation of planets around multiple stars is probably trickier than around single stars. As numerical simulations suggest not all orbital paths around binary stars are dynamically stable, and as such the formation of planets around binary stars is likely to be confined to a few orbital niches. In a close binary star, theory predicts the presence of circumstellar disks around each star, and an outer disk around the binary star surrounding a gravitationally cleared inner cavity. Given that the inner disks are depleted by accretion onto the stars on timescales of a few thousand years, any replenishing material must be flowing through the disk cavities from the outer reservoir. Replenishment for a time longer than the accretion lifetime is therefore likely to indicate an increase in the probability for planets to form.

To investigate the dynamics of the replenishment flows of dust and gas from the outer disk reservoir of a multiple star system, observations were performed towards GG Tau A. Building on a collaboration between LAB/IPAG/IRAM (France), CRyA (Mexico), Colgate University/STScI/Stony Brook University

(USA), and ASIAA (Taiwan), Anne Dutrey from the Laboratoire d'Astrophysique de Bordeaux (France) mapped the emission of the dust continuum, ^{12}CO(6-5) and ^{12}CO(2-1) towards GG Tau A. By combining submillimeter, millimeter (ALMA and IRAM) and infrared (VLTI/ESO) observations, the authors were able to shed new light on the complex dynamics within this triple star system. They thus detected for the first time that planets could form not only around one of the members of the triple star system but also in the outer disk.

The researchers lifted part of the veil on the distribution of matter and the dynamics inside the cavity. The images show filamentary gas fragments stretching from the outer disk to the inner regions. The amount of gas proves to be sufficient to power the internal disk around GG Tau Aa, one of the stars. From the kinematics and the amount of gas channeled through the cavity, the researchers conclude that the flow is strong enough to supply gas to the inner disk beyond the accretion lifetime, leaving enough time for planets to form.

These results show the complexity of planet formation around multiple stars and confirm the general picture predicted by numerical simulations. The CO emission maps also reveal a remarkable feature at the outer edge of the outer disk around the triple star system. The team investigations show that the material at the edge is twice as hot as the surrounding environment and that this is possibly the signature of a giant planet in the making. It is suggested that the planet would be digging out a path in the outer disk but the evidence for the existence of such planet will have to wait for NOEMA to be completed.

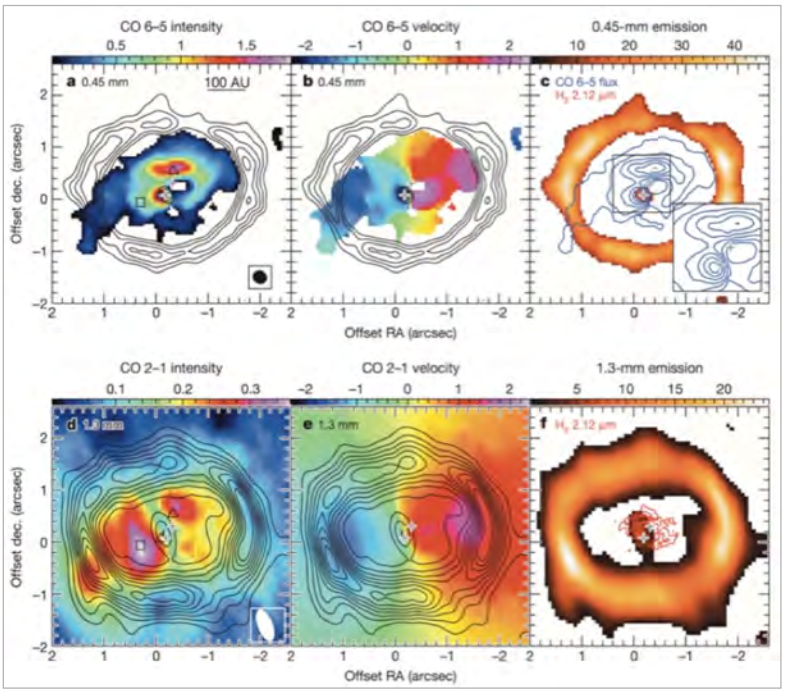

ALMA (top) and IRAM (bottom) interferometer images of GG Tau A in the thermal continuum at 0.45mm and 1.3mm, and in the lines of CO(6-5) and CO(2-1). The H_2 2.12µm emission map by Beck et al. 2012 is shown in red. Contours show either continuum or line emission. Crosses show the locations of the stars.
Work by Dutrey et al. 2014, Nature, 514, 600

EMIR TAKES A CHEMICAL INVENTORY OF COMETS ISON AND LOVEJOY

Comets are probably the least evolved bodies from the origin of the solar system, and presumably one of the best tracers to gain a better understanding of the formation and evolution of the solar system. New observational constraints on their chemical composition are of paramount importance to place tight constraints on the primordial solar system and hence on the origin of life. Bright comets are fairly rare, hard to predict, and are of utmost importance to understand how they might have delivered the seeds of life to Earth.

To explore the molecular chemistry in comets C/2012 S1 (ISON) and C/2013 R1 (Lovejoy), Marcelino Agúndez (LAB/Bordeaux) and collaborators from LESIA (Paris) and CSIC (Granada) performed spectroscopic observations using the EMIR 230 GHz dual polarization receiver at the IRAM 30-meter telescope. They obtained robust detections of molecular lines such as HCN, HNC and CH_3OH in various rotational transitions in both comets, in addition to detecting HCO^+ in comet ISON and a few weak unidentified lines in comet Lovejoy, one of which might be assigned to methylamine (CH_3NH_2).

The team was able to report a tenfold enhancement of the intensity of the HCN (3-2) line in comet ISON on November 14 at 10 UT. The event, which was accompanied by an outburst of activity, is potentially related to a breakup of part of the comet's nucleus.

The researchers estimated the kinetic temperature of the CH_3OH transitions to 90K in comet ISON and

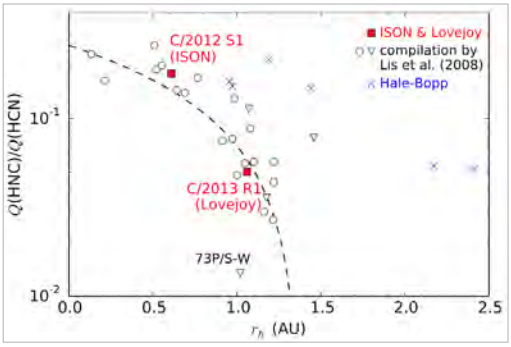

HNC/HCN ratios observed in comets as a function of heliocentric distance. Values derived in comets ISON and Lovejoy are indicated as red squares. Ratios (empty circles) and upper limits (empty triangles) derived from a sample of moderately active comets are from Lis et al. (2008). Values derived at various heliocentric distances before perihelion in comet Hale-Bopp are shown as blue crosses.
The empirical relation found by these authors is shown as a dashed line.
Work by Agúndez et al. 2014, A&A, 564, L2

60K in comet Lovejoy. The HNC/HCN ratios were derived to be 0.18 in ISON and 0.05 in Lovejoy, and were found to be similar to those found in most comets and are consistent with the HNC enhancement expected for a comet approaching the Sun. Phosphine (PH_3) is most likely one of the major carriers of phosphorus in comets but its fundamental transition remained again undetected. According to Agúndez and collaborators the 3σ upper limits lead to PH_3/H_2O ratios 4–10 times above the solar P/O elemental ratio and thus do not allow to conclude whether or not PH_3 is the main phosphorus compound in comets.

COSMIC RAYS IONIZATION NEAR SNR W28

Cosmic rays (CR) are an essential ingredient in the evolution of the interstellar medium, as they dominate the ionization of the dense molecular gas, where stars and planets form. However, since they are efficiently scattered by the galactic magnetic fields, many questions remain open, such as where exactly they are accelerated, what is their original energy spectrum, and how they propagate into molecular clouds.

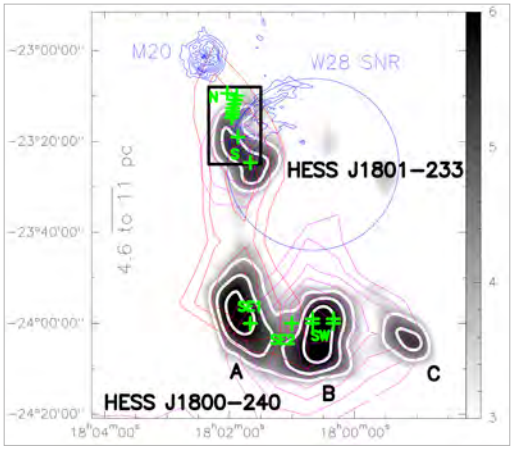

TeV emission by HESS (greyscale) towards the SNR W28 complex, CO(1-0) emission by Dame et al. 2001 (red and magenta), and 20cm free-free emission by Yusef-Zadeh et al. 2000 (blue). Crosses (green) show the positions observed with the IRAM 30-meter telescope. Work by Vaupré et al. 2014, A&A, 568, A50

To provide new insights on cosmic rays of low energy, a French consortium of researchers from the Institute of Astrophysics and Planetology (IPAG), the laboratory AstroParticule and Cosmology (APC) and the Institut d'Astrophysique (IAP) pioneered a new approach based upon the spectroscopic analysis of molecular gas close to supernova remnants (SNR). To measure the CR ionization rate towards a supernova remnant, Solenn Vaupré (IPAG) and collaborators used the IRAM 30-meter telescope to observe two molecular regions to the northeast and south of the mixed-morphology SNR known as W28. Vaupré's team performed observations in the lines of CO, HCO^+, and DCO^+ and compared them with the predictions of radiative transfer and chemical models. While the CO observations were used to constrain the density, temperature, and column density of the molecular environment, the DCO^+/HCO^+ abundance ratios provided constraints on the electron fraction and, consequently, on the CR ionization rate.

These observations provide for the first time clear evidence for the presence of low energy CR in the near vicinity of the shock of the SNR. The authors find that the CR ionization rates towards most of the clouds near W28 are much larger (≳100) than in standard galactic clouds. Their observations support the hypothesis that the gamma rays observed around W28 have a hadronic origin. In addition, based on CR diffusion estimates, they find that the ionization of the gas is likely due to CR of 0.1−1 GeV. Finally, Vaupré et al. suggest that their observations are in agreement with the global picture of CR diffusion, in which the low-energy tail of the CR population diffuses at smaller distances than the high-energy counterpart.

Clearly, these results provide new and excellent perspectives for the study of the origins and properties of CRs in the Galaxy and to better constrain the intensity of CRs in star and planet forming regions.

HERA PROVIDES A COMPLETE CENSUS OF MOLECULAR CLOUDS IN M33

Understanding the interstellar medium (ISM) and the interplay between the atomic and molecular components in a low-metallicity environment is undoubtedly one of the key research areas in observational astrophysics. Spiral galaxies near enough to resolve individual molecular clouds are ideally suited to investigate the dependence of star formation on the physical conditions across the disk of the galaxy.

In a concerted effort to better understand the physical and dynamical links between atomic and molecular gas, Clement Druard (LAB, Bordeaux) and collaborators used HERA at the IRAM 30-meter telescope to observe the Local Group spiral M33 in the frame of an IRAM Large Program. They obtained a complete $^{12}CO(2\text{-}1)$ high angular (~50 pc, GMC size scale) and high spectral resolution (2.6 km/s) census of the molecular clouds in the disk of this galaxy. A

cut in the ^{12}CO (1–0) line along the major axis of the disk complements the data obtained in the ^{12}CO(2–1) line. The total ^{12}CO(2–1) luminosity was estimated to 2.8 10^7 K.km/s pc^2 and found to follow the spiral arms in the inner disk. The line intensity is found to decrease nearly exponentially with a scale length of 2.1 kpc. The total molecular gas mass in the disk of M33 was estimated to be 3.1 10^8 $M_\odot$. The ^{12}CO(2–1)/(1–0) intensity ratio, which was ~0.8 on average, was found to show no significant variations with galactocentric distance.

The IRAM 30-meter telescope data also show 1) the velocity dispersion between the atomic and molecular gas is very low, 2) the linewidths of both components decrease with galactocentric distance, and 3) the CO(2–1) peak temperature follows very closely the atomic gas peak brightness. These findings taken together suggest a tight connection between the atomic and molecular components. Druard and collaborators conclude that the probability density function of the H_2 column density, as traced by the CO emission, shows a log-normal profile with considerable excess in the high column density regime, presumably owing to the onset of the gravitational contraction phase of the galaxy.

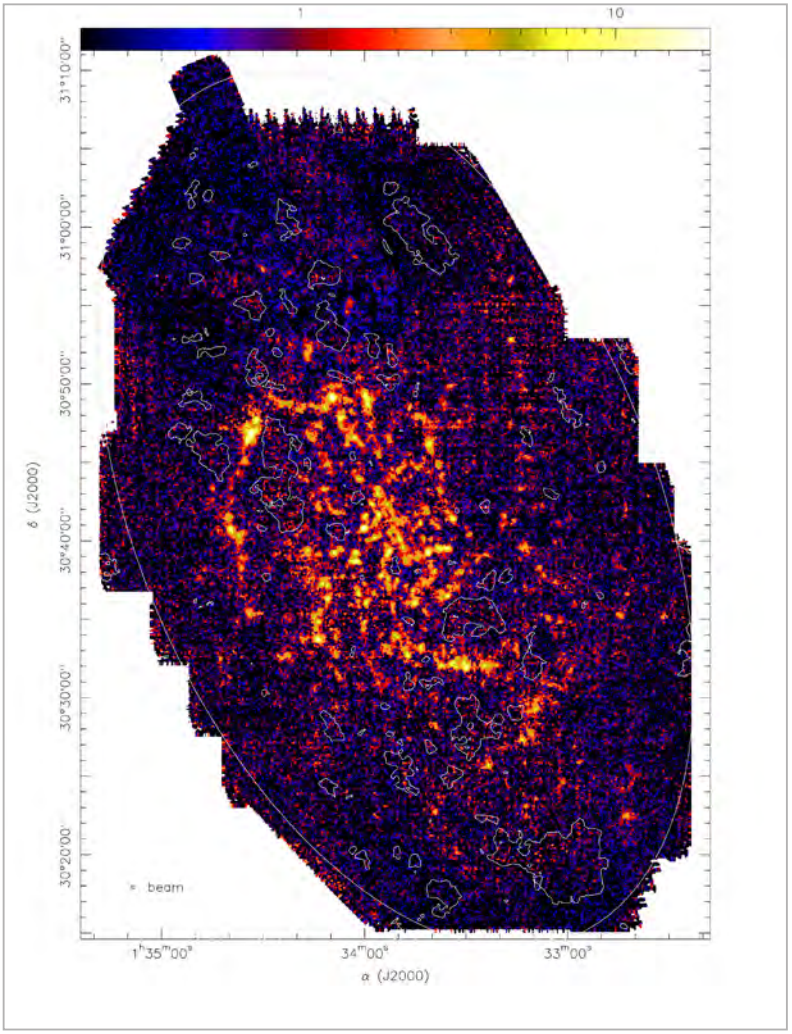

^{12}CO(2–1) integrated intensity map in K km/s. The contours (grey) show HI-poor regions where the HI line does not reach 10 K. The beam size is shown in the lower left corner of the figure. The white ellipse outlines the galaxy's 7.2 kpc radius.
Work by Druard et al. 2014, A&A, 567, A118

MASSIVE GALACTIC-SCALE OUTFLOWS SHAPE THE EVOLUTION OF GALAXIES

Massive, highly energetic, galactic-scale molecular outflows in local AGN hosts and ultra-luminous infrared galaxies (ULIRGs) have provided strong evidence for negative feedback on star formation. The major breakthrough achieved by recent studies is the confirmation that, regardless of the driving mechanism, these outflows affect the phase of the interstellar medium out of which stars forms and hence the overall evolution of the galaxy.

To study the properties of a sample of local AGN and ULIRGs and investigate their impact on galaxy evolution, an international collaboration led by Claudia Cicone (University of Cambridge) performed IRAM interferometer ^{12}CO(1–0) observations of local ULIRGs and quasar-hosts: a clear signature of massive and energetic molecular outflows, extending on kiloparsec-scales, is found in the CO(1–0) kinematics of four out of seven sources, with measured outflow rates of several 100 $M_\odot$/yr. By combining these observations with data from the literature, the authors find that starburst-dominated galaxies have an outflow rate comparable to their star formation rate (SFR), or even higher by a factor of ~2–4, implying that starbursts can indeed be effective in removing cold gas from galaxies. Their analysis also suggests that the presence of an active galactic nucleus (AGN) can boost the outflow rate by a large factor, which is found to increase with the L_{AGN}/L_{Bol} ratio. The gas depletion time scales due to molecular outflows are anti-correlated with the presence and luminosity of an AGN in these galaxies, and range from a few hundred million years in starburst galaxies down to just a few million years in galaxies hosting powerful AGNs. In quasar hosts, the depletion time scales due to the outflow are much shorter than the depletion time scales due to star formation. Cicone et al. estimate the outflow kinetic power and find that, for galaxies hosting powerful AGNs, it corresponds to about 5% of the AGN luminosity,

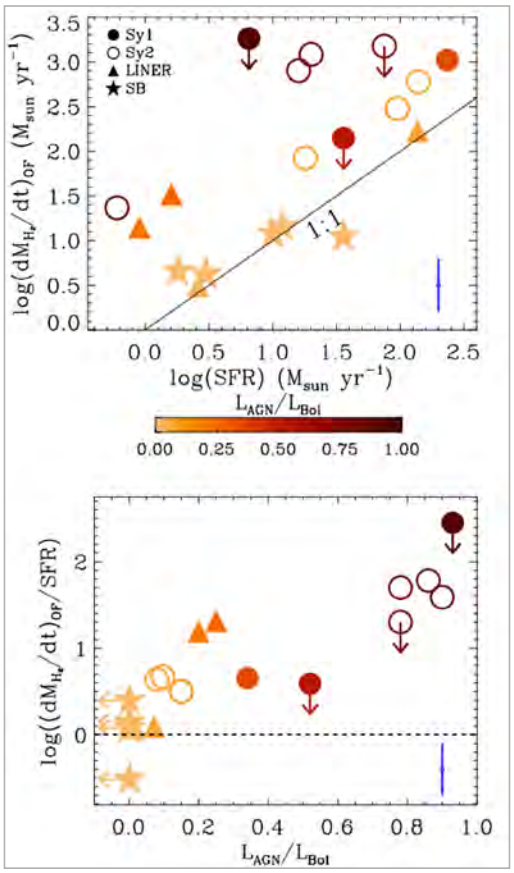

Top: outflow mass-loss rate as a function of the SFR for a sample of unobscured (filled circles) and obscured (open circles) AGNs, LINERs (triangles) and starburst galaxies (stars). Symbols are colour coded according to L_{AGN}/L_{Bol}. Below: positive correlation between the outflow mass loading factor and L_{AGN}/L_{Bol}.
Work by Cicone et al. 2014, A&A, 562, A21

as expected by models of AGN feedback. Moreover, they find that momentum rates of about 20 L_{AGN}/c are common among the AGN dominated sources in their sample. For pure starburst galaxies, the data tentatively support models in which outflows are mostly momentum-driven by the radiation pressure from young stars onto dusty clouds.

Overall, the results indicate that, although starbursts are effective in powering massive molecular outflows, the presence of an AGN may strongly enhance such outflows, and hence have a profound feedback effect on the evolution of galaxies by efficiently removing fuel for star formation.

FIRST DEEP NIKA EXPOSURES OF THE THERMAL SZ-EFFECT

Galaxy clusters are gravitationally bound ensembles of up to thousands of galaxies. Most of the cluster baryons, however, reside between the galaxies in an extremely hot and tenuous gas. The plasma is heated to high temperatures under its own gravity and as a result emits X-rays through bremsstrahlung emission. Even though one can search for galaxy clusters through their emission in various wavelengths, there is another approach of doing so using the thermal Sunyaev-Zeldovich (tSZ) effect, a tiny spectral distortion of a few micro-K in the CMB. This method is unique in that it is independent of redshift.

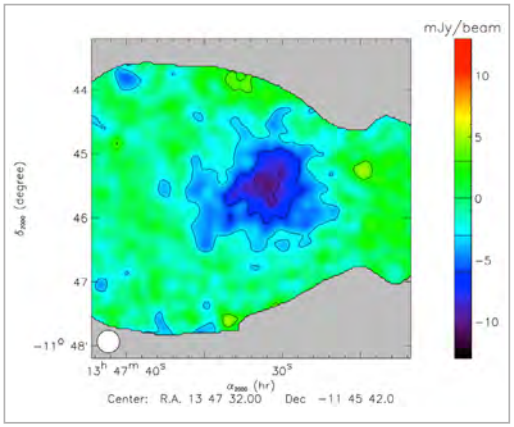

NIKA map of RX J1347.5-1145 at 140 GHz. The beam is shown on the bottom left corner of the map, accounting for both the 18.5" beam and the extra 10" Gaussian smoothing. Contours are in steps of 3σ. The Compton parameter at the minimum is $y \cong 10^{-3}$.
Work by Adam et al. 2014, A&A, 569, A66

To assess the performance of NIKA (New IRAM Kids Array), a dual-band camera with 132 kinetic inductance detectors at 140GHz and 224 detectors at 240GHz, and to demonstrate the potential of NIKA2, observations were performed at the IRAM 30-meter telescope to measure the tSZ effect towards RX J1347.50-114, the most luminous X-ray cluster of galaxies known to date (z=0.45).

The NIKA maps of RX J1347.50-114 are the result of a large international collaboration led by Rémi Adam (LPSC, Grenoble). The results show that RX J1347.50-114 presents a decrement at the cluster position consistent with the tSZ nature of the signal. The authors used the 140 GHz map to study the pressure distribution of the cluster by fitting a gNFW model to the data. Subtracting this model from the map, they confirm previous tSZ measurements of Mustang and X-ray observations of XMM according to which RX J1347.5-1145 is a spherical, relaxed cool-core cluster, which is undergoing a merger event. As expected from the overpressure caused by an ongoing galaxy merger, the map shows a strong southeast extension that corresponds to the merger shock. The tSZ extension is also observed in the radial flux profile of the cluster but the peak of the tSZ is not found to be spatially coincident with the centroid of the

X-ray emission. The generalized NFW fit of the north-western region enabled Adam and collaborators to constrain the cluster pressure profile parameters $\theta_s = 70''$ and $P_0 = 3.29$ KeV/cm^3. The pressure profile derived from X-ray agrees within the uncertainrties with the tSZ best-fit model.

It is clear that the future NIKA2 camera with ~5000 detectors and a field of view of ~6.5' will be particularly well-suited for in-depth studies of the intra-cluster medium at intermediate to high redshift, and that it will thus support the characterization of clusters detected by the Planck satellite.

WITNESSING THE GALACTIC BLOW OUT PHASE OF GALACTIC EVOLUTION

Starburst galaxies can drive molecular gas outflows through stellar radiation pressure. Molecular gas is the phase of the interstellar medium from which stars form, so these outflows curtail stellar mass growth in galaxies. Previously known outflows, however, involve small fractions of the total molecular gas content and are restricted to sub-kpc scales. While feedback from active galactic nuclei is in at least some cases dynamically important, feedback from stars is generally considered incapable of aggressively terminating star formation on galactic scales. Extraplanar molecular gas has been detected in the archetype starburst galaxy M82, but so far there has been no evidence that starbursts can propel significant quantities of cold molecular gas to the same galactocentric radius (~10 kpc).

As part of a recent NOEMA interferometer campaign to investigate galaxies characterized by very intense star formation in which the galactic gas reservoirs are forming stars at the Eddington limit, James Geach (University of Hertfordshire) and collaborators reported the detection of strong CO(2-1) emission towards the ultra-compact starburst galaxy J090523+5759 (z=0.712). The SFR surface density of this galaxy is likely >5000 $M_\odot$/yr. In addition to revealing a main CO emission line, the researchers found a clear but intriguing feature in the spectrum – a very broad (~1000 km/s) component, reminiscent of the line profiles associated with the molecular outflow in Mrk 231 and some other quasars. They find that one third of the molecular gas has a velocity of up to 1000 km/s, that it is spatially extended on a scale of approximately 10 kpc, and that the kinetic power (~2.6 10^{36} W) associated with this high-velocity component is consistent with the momentum flux (~4.8 10^{30} N) available from stellar radiation pressure. Clearly, this result demonstrates that nuclear bursts of star formation are capable of ejecting large amounts of cold gas from the central regions of galaxies, thereby strongly affecting their evolution. Geach and collaborators are not ruling out the possibility that the outflow was launched by an AGN that has since switched off, but the current observations indicate that the outflow is compatible with pure stellar feedback.

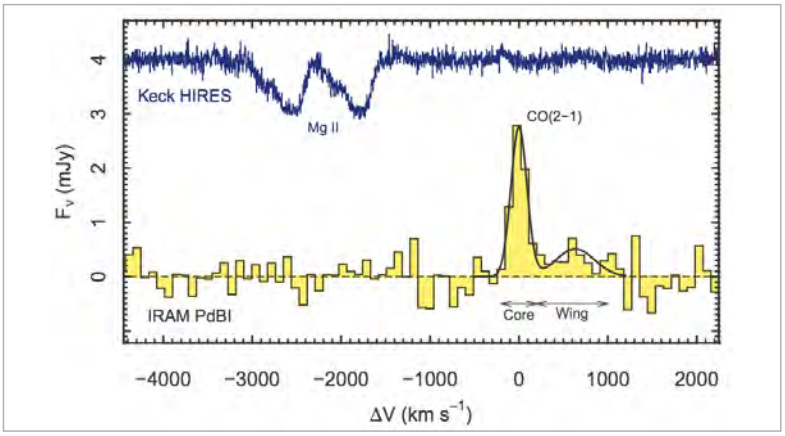

2 mm spectrum of SDSS J0905+57 obtained with the IRAM interferometer. The ^{12}CO(2–1) line peaks at a redshift consistent with the stellar absorption lines. There is evidence for significant CO emission in a high velocity wing that extends up to 1000 km/s from the core line. J0905+57 is also driving a high-velocity outflow of ionized gas, as revealed by the strongly blue-shifted Mg II λ2796, λ2803 Å doublet absorption observed in the Keck HIRES rest-frame ultraviolet spectrum. Work by Geach et al. 2014, Nature, 516, 68

A scenario in which a compact, Eddington-limited starburst is observed to expel its own molecular gas supply and thus is regulating star formation during the assembly phase of the inner regions of a galaxy bulge, is a critically important testcase for models of feedback that are required by current theories of galaxy evolution to truncate the growth of stellar bulges. The results obtained by Geach and collaborators are therefore a major advance in this area.

NEW LIGHT ON BLACK HOLES OF THE EARLY UNIVERSE?

Observations of the early Universe have shown that the most distant galaxies discovered so far host black holes that are extremely massive. These objects, known with the name of quasars, are generally discovered through the intense X-ray radiation they emit, but the mechanism responsible for the formation of the black holes is still not known. To unveil this mystery and better understand their origin and evolution, it would be necessary to detect their lower mass ancestors. However, the early phase of a quasar life is characterized by the production of huge amounts of dust that absorbs X-ray radiation and thus hampers the detection of black holes.

In an attempt to address this question, Simona Gallerani (CSNS, Italy) and collaborators from the University of Cambridge (UK) and IRAM (France), have recently discovered the emission line of

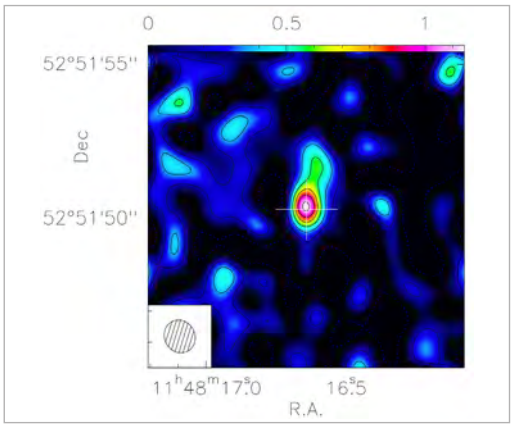

Map of the velocity-integrated emission line of ^{12}CO(17-16) observed with the IRAM interferometer.
Work by Gallerani et al. 2014, MNRAS, 445, 2848

^{12}CO(17-16) towards J114816.64+525150.3. Contrary to X-ray radiation, this line has the property of passing undisturbed through dusty regions. The serendipitous detection of this line in this *z*=6.4 quasar has the promising potential to open a new pathway for the discovery and the study of the evolution of the first black holes in the early Universe.

According to Gallerani and collaborators the ^{12}CO(17–16) line was detected with a high level of confidence, although it possibly is contaminated by OH^+ emission that may account for 35–60% of the total flux observed. In trying to draw comparisons with shock-dominated sources like M82 and NGC1068, and merger systems like NGC6240, the researchers found that the energy distribution of the ^{12}CO transitions appears exceedingly flat in these galaxies and that none of them shows the large high-J flux densities observed in J114816.64+525150.3. This suggests that is very unlikely that the ^{12}CO(17-16) line is excited by shocks. In the same line of reasoning, it appears that models of photodissociation regions (PDR) alone cannot reproduce the high luminosity of the line relative to the low-J CO transitions and that the presence of an X-ray-dominated region (XDR) is required. By adopting a composite PDR+XDR model, the authors derive molecular cloud and radiation field properties in the nuclear region of J114816.64+525150.3 and conclude that the highly excited lines of ^{12}CO represent a sensitive and possibly unique tool to indirectly infer the presence of X-ray regions in weaker or dust-enshrouded progenitors of supermassive black hole in galaxies of the early universe.

A DEEP MOLECULAR LINE SCAN IN THE HUBBLE DEEP FIELD NORTH

While significant progress in deep field studies has been made, current knowledge of the formation of the general galaxy population is based almost exclusively on optical, near–IR and cm–radio deep field surveys of stars, star formation, and ionized gas. Observations of the molecular gas content, which is key to the cosmic star formation history, have to date been limited to follow–up studies of galaxies that are pre–selected from optical/NIR and sub–millimeter continuum surveys. In order to obtain an unbiased census of the molecular gas content in high–z galaxies, there is a clear need for a blind search of molecular gas down to mass limits characteristic of the normal star forming galaxy population. Such a molecular deep field has been out of reach using past instrumentation, both in terms of sensitivity and instantaneous bandwidth.

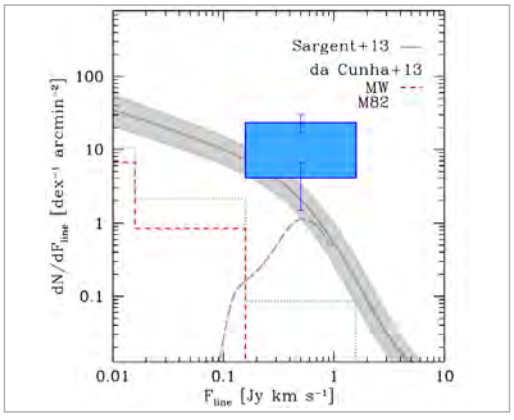

Comparison between the observed number of CO line candidates (shaded box), and the expectations from the empirical predictions in the case of Milky Way-like CO excitation and in the case of M82-like excitation. The gray shading shows the 1σ uncertainties in the predictions by Sargent et al. (2013).
Work by Decarli et al. 2014, ApJ, 782, 78 and Walter et al. 2014, ApJ, 782, 79

A project led by researchers Roberto Decarli and Fabian Walter (MPIA, Germany) tackled the challenge and performed a systematic blind search for CO in the Hubble Deep Field North (HDF-N) using the interferometer. The line scan, which surveys the entire 3mm band from 79.7 to 114.8 GHz, covers a cosmic volume of ~7000 Mpc^3 and redshift ranges $z < 0.45$, $1.01 < z < 1.89$ and $z > 2$. Using different search algorithms Decarli and collaborators identified 17 possible line candidates (including 2 secure detections) with typical fluxes in the range 0.16-0.56 Jy.km/s and linewidths in the range 110-500 km/s. The absence of a second line at the position of any of the candidates suggests the lines belong to galaxies at low redshift ($z < 3$). Combined with the multiwavelength and spectroscopic database of the HDF-N, the authors were able to put constraints on the CO luminosity function and on the resulting evolution of the H_2 molecular gas density as a function of lookback time and out of redshifts $z \sim 3$ in the HDF-N. The authors conclude that the contribution of the blind detections to the cosmic molecular gas density already constitute a major contribution to current empirical predictions and models. As a consequence, accounting for the contribution of yet undetected sources (at lower or higher CO luminosities) would give values that lie above the predictions.

The 30-meter telescope

Image: Nicolas Billot

OVERVIEW

Aside from supporting observations of about 200 astronomical projects, work focussed on preparing for the installation of new optics in the receiver cabin and the arrival of the new, large field-of-view camera NIKA-2, both scheduled for 2015. The holographic measuring system of the antenna dish was re-installed and tested. Spurious lines, which are occasionally encountered in spectral line observations with the wide bandwidths offered by the Eight Mixer Receiver (EMIR), were investigated.

One of the various science highlights was the detection of pulsar signals at 3mm and 2mm wavelengths. In close collaboration with the pulsar group at the MPIfR in Bonn, two radio pulsars were observed and detected at 3mm and 2mm wavelengths. For these experiments, the hardware and the software of the broad-band continuum backend (BBC) were improved. This new acquisition system is now connected to the telescope reference clock from which all critical timings are derived, ensuring a known and stable sampling frequency, as well as timestamps with improved accuracy of less than 10 μsec. The software was also adapted to allow very high data recording at rates of 1 kHz. For 2015, it is planned to further improve this new observing mode.

Due to a somewhat reduced staff, the support of visiting astronomers at the 30-meter telescope by astronomers on duty (AoDs) has not always been on-site at the Pico Veleta as in the past, but occasionally remotely from Granada. Newly installed tools to monitor the progress of observations from Granada and new means of communication helped to soften the impact of this measure, while at the same time allowing staff astronomers to spend more time on technical projects, some of which are listed below or elsewhere in this report. Visiting astronomers were contacted in advance of their observing runs to prepare observing scripts. Newcomers to the 30-meter telescope were in general introduced to the 30-meter telescope on-site.

From observations of planets and other primary calibrators between 80 and 360 GHz, the mean deviations of the main mirror from a perfect parabola are known to be 50μm rms. To create maps of the 30-meter telescope surface error distribution, the 39.4 GHz beacon of the ESA Alphasat communication satellite was used. This satellite had been launched in July 2013. Its beacon is mapped with two dedicated frontends installed in the prime focus cabin of the 30-meter telescope, one pointing towards the satellite, the other pointing towards the 30-meter dish. Cross-correlating the two signals allows to measure the amplitude and phase distribution of the beam pattern in the far-field. A simple fourier-transform then allows to derive the surface error map. This method, called phase coherent holography, had been applied until 2001 using the Italsat satellite, which had however been switched-off back then. Using the Alphasat satellite, a slightly revised hardware and a newly designed, automated data processing pipeline, as part of the clic/gildas software, has allowed to create first maps. Significant progress was made in adapting the drive program of the New Control System (NCS) and

the observing software to the fast tracking of the satellite. Further debugging and observations under stable night time conditions are planned for 2015 to obtain a map of good quality, as one mandatory step before the primary surface can be repainted. This is needed as described further below.

ASTRONOMICAL PROJECTS

During the year 2014, a total of 193 projects were scheduled at the 30-meter telescope. This number includes two large programs, five projects for director's time, and 10 VLBI projects. A quarter of these projects was scheduled in observing pools, including the continuum pools with GISMO and NIKA. About 10% of the scheduling units, mainly the shorter ones of less than 10 hours, were observed remotely.

During the scheduling year, 148 astronomers visited the telescope, 48 of which came to support the observing pools. In addition, two groups of four master students came to the Pico Veleta to observe short educational projects as part of their training courses.

The program committee received 32 TNA (Trans National Access)-eligible proposals, and recommended 17 for observations at the 30-meter. Among those, 15 could be scheduled at the telescope for a total of 416 hours, and 10 European astronomers were granted travel support to Granada for observing their project.

During more than 70% of the scheduled observing time, EMIR was used. The remaining time was split-up between HERA (7%), GISMO (9%), and NIKA (13%). Almost 60% of the observing time was dedicated to Galactic research, while about a quarter of the time was used for observing nearby galaxies, and about 20% of the time was dedicated to more distant objects.

Left: Time distribution of science categories observed in 2014.
Right: Usage of EMIR bands.

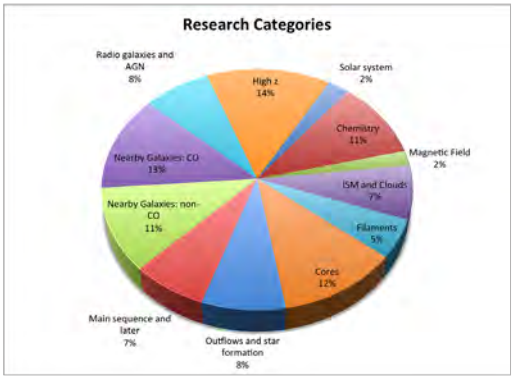

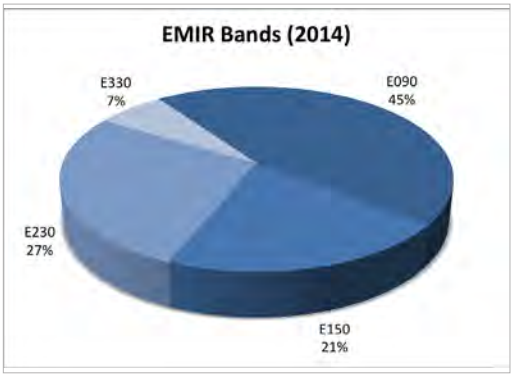

TELESCOPE OPERATION

Similar as in previous years, 68% of the total time was used for observations, while about 9% of the time was used for technical projects and the regular maintenance. About 23% of the time was lost due to adverse meterological conditions, including one storm with wind speeds of more than 216 km/h. The time lost due to unforeseen technical problems was in total only less than 12 hours. The observing efficiency in terms of number of hours of observations varies strongly over the year. It was highest in August when 87% of the total time was spent on astronomical observations, while it was lowest in February when less than 40% could be spent on-sky, due to long periods of poor weather conditions.

In preparation for NIKA-2, measurements of inclination angles and vibrations have been carried out at selected places in the receiver cabin, in particular at the positions of the new mounts of the tertiary mirror and the fourth mirror (M4). A new mount for the beam switching blade has been constructed. And the current beam switching optics have been readjusted. The separation between on and off position are now 170".

The paint on the main reflector surface is slowly degrading after more than 30 years of operation. In 2014, work focussed on getting holographic measurements of the antenna surface working again, (as described above). The gradual loss of paint thickness was monitored at a number of measurement points in the dish. Discussion with the companies VERTEX and MTM on possible ways to repaint were started.

In the past years, several measures were taken to reduce the electrical consumption of the

observatory without affecting the observations. About half of the reduced consumption is due to changes in the antenna air conditioning system, in particular by switching off the cooling system, which is not needed. The other half of the reduction is due to switching off the heating of the antenna tower, modifications in the air conditioning system in the computer room, new operator rules on the times and strengths of the applied de-icing power, and the installation of energy efficient lamps in the observatory.

Radio-electric protection of the observatory is an area of rising concern, due to the expected introduction of new car and helicopter radar systems working at frequencies around 77 GHz. In an effort coordinated with the Yebes observatory and with the spectrum manager of the European Committee on Radio Astronomy Frequencies (CRAF), the interests of the millimeter astronomical community in Spain have been stated.

Several measures have been taken to further improve safety at the 30-meter telescope. As part of the bi-yearly cycle, a training course on fire extinguishing was given by the Granada fire brigade. The working state of the emergency videoconference system at the telescope to the emergency services 061 in Granada is now tested every 4 weeks, with the participation of the operator-on-duty.

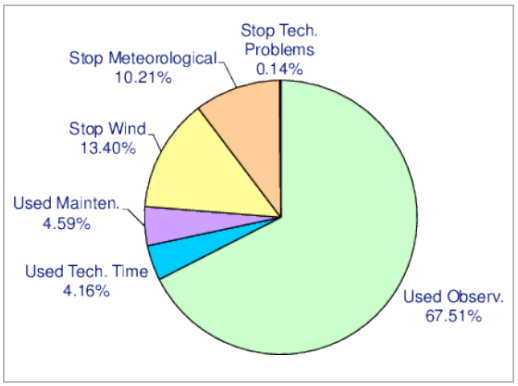

Distribution of the total time in 2014.

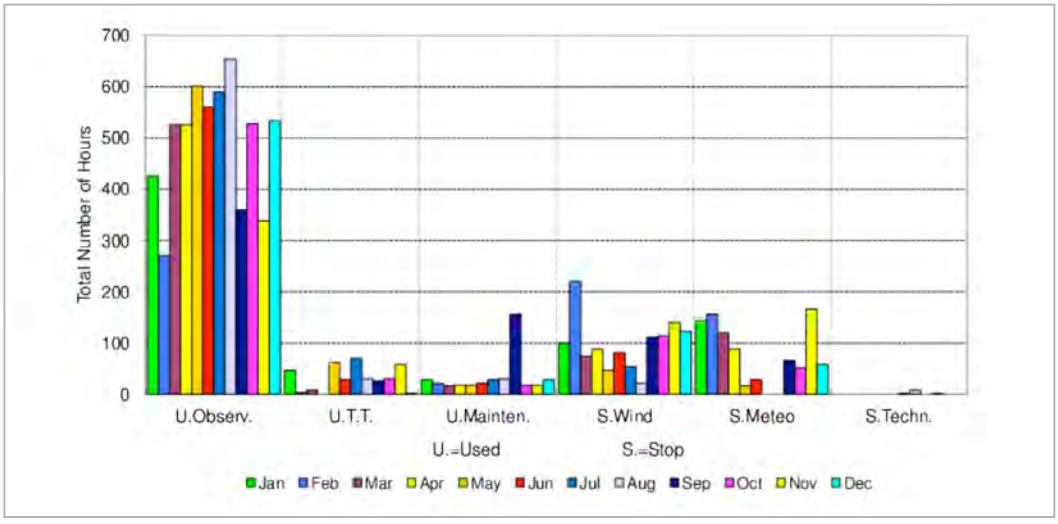

Monthly time distribution of observing time, technical projects (T.T.), maintenance, time lost due to high wind speeds, or other adverse meteorological conditions, or technical issues.

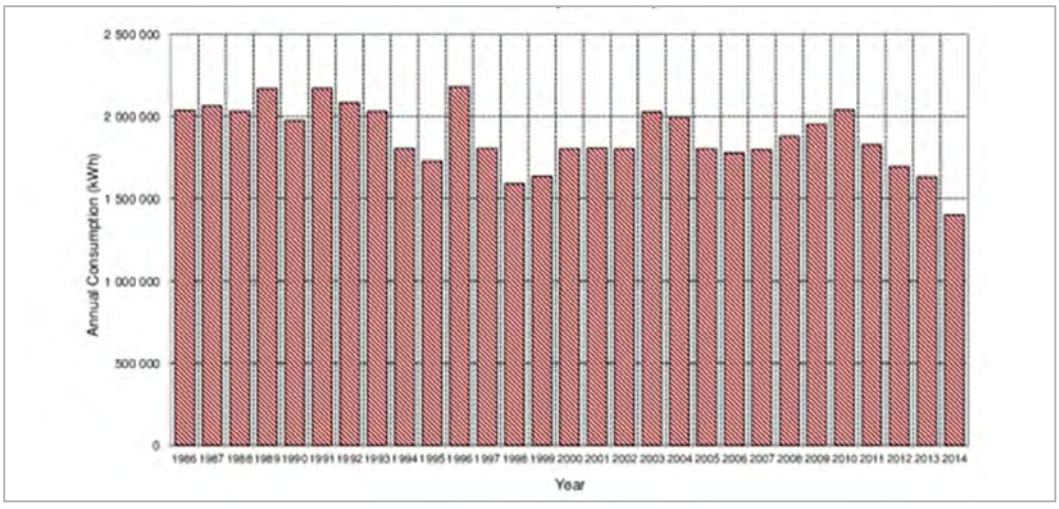

Total annual electrical consumption.

FRONTENDS

Most activity has been dedicated to the modification of the receiver cabin optics and the preparation for the NIKA-2 continuum camera. A new support for one of the EMIR mirrors (ME5) and its electrical actuator were installed. A new bridge crane will allow to lift and reposition HERA. The attachment where NIKA-2 will be clamped to the telescope structure has been designed and the reinforcement of the cabin floor has been prepared. Furthermore, space for the electronic racks and cables has been prepared.

Another part of the activity was dedicated to further improve the performance of the heterodyne system.

The EMIR local oscillators (LOs) do create harmonics of its Gunn oscillators, which are mixed in the sideband separating mixers, and then down-converted into the intermediate frequency (IF) band. The LOs do, however, also create additional, unwanted harmonics which may not be sufficiently suppressed, leak through, and pump the mixers, leading to the detection of lines above the nominal frequency ranges. Addressing such ghost lines becomes important when conducting e.g. deep frequency surveys towards bright Galactic star forming regions like Orion or towards evolved stars like IRC+10216. There exist efficient techniques to identify them. Few ghost lines stemming from frequencies lying slightly above the nominal frequency range have been detected with the new sideband separating mixers of the 2mm band of EMIR. To suppress the unwanted harmonics, a waveguide filter was built and inserted in the LO path in December 2014.

The image-band rejection of the dual-sideband (2SB) mixers of EMIR is on average -13 dB, as shown by exhaustive test measurements conducted in the laboratory at IRAM/Grenoble. However, these tests show that the gain ratio varies with LO frequency and within the IF band, reaching values of slightly less than -10dB in isolated areas of the parameter space. An investigation was started to measure the gain ratios at the telescope, on the sky, by using the observed celestial lines detected simultaneously in the signal and image bands.

A method of transporting the larger number of IF signals produced by the future multibeam receivers is under investigation. An intermediate solution, using thinner coaxial cables, with a wider bandwidth has been proposed. A prototype, capable of transporting the full 4-12GHz IF band with almost flat frequency transmission, has been built and successfully measured in the lab. Tests at the telescope, with real astronomical signals, are planned.

The amplifiers chosen for the rack of the BBC and the IF switches are rapidly ageing - their gain drops. It was therefore decided to start an in-house development of two new types of warm amplifiers. One low-power amplifier was developed for the BBC and the IF switches, and a prototype has been successfully installed and used. In addition, a high-power amplifier was developed to compensate the losses of future long, thin IF cables and equalizers from the receiver cabin to the backend room.

COMPUTERS & SOFTWARE

Owing to the large bandwidths of EMIR covered by the Fast Fourier Transform Spectrometer (FTS), the internal data archive is currently growing at a rate of about 30TB of data per year. A new Network Attached Storage (NAS) system has been installed. The tape backup system at the observatory now can hold up to 250 TeraBytes of data (2x48 LTO-6 tapes). The software to backup the data has been improved to reduce the impact on running observations. A migration of the filesystems from RAID-5 to RAID-6 has been started in order to allow for up to two simultaneous disk failures. All Linux computers have been upgraded to the Debian 7 operating system, including our critical servers.

A new 100 Mbit/sec radiolink was installed connecting the 30-meter telescope to the RedIRIS NOVA node of the Instituto de Astrofisica de Andalucia (IAA) in Granada, increasing the access to the internet from the 30-meter telescope, and

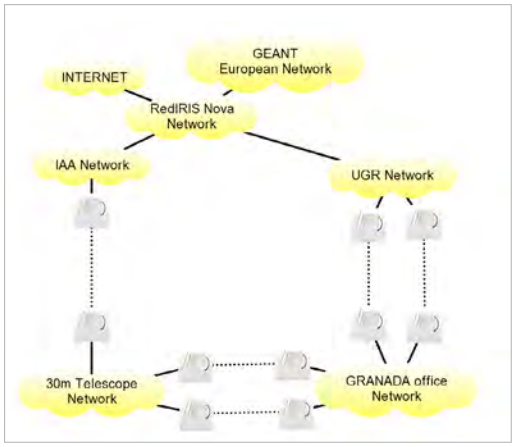

IRAM/Granada network architecture with the new, fast radiolink between the 30-meter telescope and the Instituto de Astrofisica de Andalucia (IAA).

also from IRAM/Granada, by a factor of 10. At the end of 2014, Telefonica has installed a fiber optics link to Pradollano in the Sierra Nevada, which is complemented by the local fiber optics network of the company running the ski resort, Cetursa. Once these fiber optics connections become available to IRAM, large bandwidths of 1Gbit/sec, or even of up to 10 Gbit/sec offered by the European GEANT network which IAA is a member of, will become available.

The creation of a new IP network for the office in Granada, offering a new range of IP addresses, allows to keep the network at the observatory more isolated from the network of IRAM in Granada. The Granada mail server, the DNS service, and other workstations now follow the IPv6 protocol. Two new firewalls were deployed to add better security to the network at the 30-meter telescope, and in Granada. Dynamic routing to access the internet was set up which better assures the connection to the network, allowing the firewalls to better route the traffic using alternative paths.

In the NCS and its user interface software paKo several features were added to support NIKA. As a novel way to determine focus corrections, a single scan is done with several Lissajous subscans, each at a user-specified focus offset. Several variations of Lissajous scans for different purposes like pointing, focus and mapping are now distinguished in the NCS messages and XML files. At the start of the observing modes Lissajous, Otfmap, Pointing and Focus, it is possible to command a special "tune" subscan. Measured Nasmyth offsets for each NIKA pixel may be specified in a file and retrieved according to the identifying number of the pixel.

Tracking earth-bound satellites is now possible by the antennaMountDrive program and is used to do holography measurements. Holography observations also require special flavors of the receiver and source commands, and very relaxed limits on pointing and focus corrections. Lateral focus corrections can now be specified directly from paKo; for special applications, track scans now allow subscans of 24 hours.

MISCELLANEOUS

The IRAM 30-meter telescope is listed in a newly created short-list of singular scientific and technical infrastructures (ICTS) in Spain, which are dedicated to cutting-edge and high-quality research and technological development. On October 7, the Spanish "Consejo de Política Científica, Tecnológica y de Innovación" has established a list of 29 ICTS, six in astronomy, one of them the IRAM 30-meter telescope.

Photo Sabine König

NOEMA interferometer

Sunset view of the NOEMA antennas in the winter landscape of the French Alps.

The operation of the NOEMA interferometer has been as exciting as in previous years, characterized by outstanding scientific results and a number of major technical achievements. The highlight this year was the September 22 formal inauguration ceremony to celebrate the arrival of antenna 7 and the opening of the NOEMA interferometer. The ceremony was held simultaneously at the Observatory and IRAM headquarters and involved delegates of the IRAM member states, representatives of the IRAM funding agencies, and authorities of the local governments.

As in previous years, the interferometer continued to operate efficiently with almost no downtime due to hardware upgrades, maintenance operations, construction work on the cable car, and work on antennas 7 and 8. Antennas, receivers and digital correlators all worked well throughout the year. A magnitude 5.3 earthquake struck the province around the observatory on April 7, the strongest earthquake ever recorded in the French Alps causing heavy damages in the region, but it did affect neither the observatory nor the interferometer.

Observations were performed in periods of good to excellent phase stability and atmospheric transparency during most of March. Observing conditions were correct during much of April and allowing for useful observations in the high-frequency bands during short periods until the mid of May. Typical summer conditions were observed from June to September. While conditions were good at the end of October, they were poor again till the year's end. All in all, the observatory faced the poorest weather conditions of the last ten years.

The extended configurations (A and B) were scheduled from January 13 to March 29. The scheduling of the A configuration was readjusted shortly after the beginning of the winter scheduling period to optimize the observing of A-rated projects with respect to Sun avoidance limitations and weather constraints. All interferometer observations were performed exclusively in service mode.

The percentage of contiguous array-correlation time scheduled for observing programs was on average 45% of the total time. This year 160 days and nights were scheduled for science operations.

Distribution of sources in equatorial coordinates as observed with the Plateau de Bure Interferometer and NOEMA over the years 1990 to 2014. The density of sources is weighted by the requested observing time and represented by a distinctive color tint. The distribution shows much of the emphasis is on high-redshift science (HDF-N, GOODS-N, COSMOS) and star formation in the Auriga/Taurus/Orion complex.

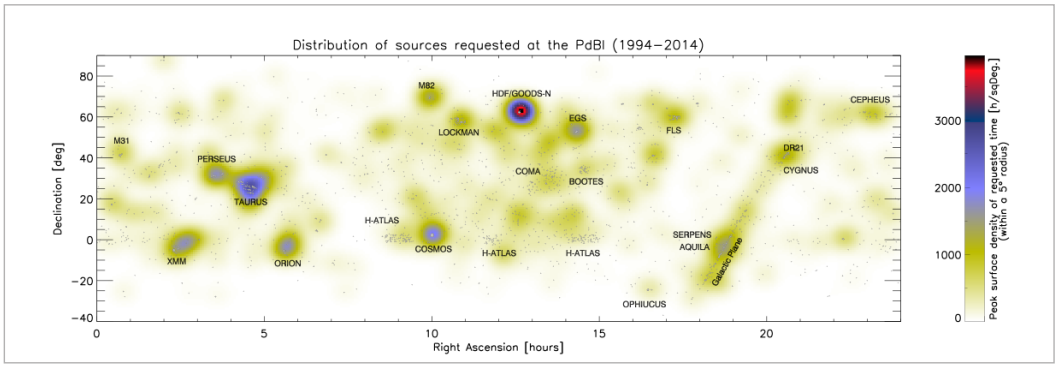

Additional 20% have to be accounted for receiver tuning, array configuration changes, engineering and commissioning activities. The remaining 35% were lost because of precipitation, wind and poor atmospheric phase stability.

The Program Committee (PC) met twice during the year, around four weeks after the deadlines for submission of proposals, and reviewed 243 regular proposals (+10%), including 3 proposals for observations in the Global 3mm VLBI array (GMVA) and 43 RadioNet eligible proposals. With 150 proposals received for the winter deadline, a new record was set in 2014, raising the pressure level on the observing time by 20%. In the same year, 6 proposals were received for Director's Discretionary Time (DDT). The program committee recommended the approval of 95 proposals, and of 2 VLBI projects in the frame of the GMVA sessions. Counting the backlog of projects from 2013, 90 proposals were scheduled in 2014, including 3 Large Programs and 10 DDT proposals. This corresponds to 241 individual projects that received time on the interferometer. All proposals were submitted and evaluated through PMS, the new web-based Proposal Management System. The online submission system was extensively tested internally and externally before being released for the proposal deadline in March 2014.

The NOEMA observatory continued to provide unique and exciting scientific results in 2014. The weight on extragalactic high-redshift research dropped significantly in 2014 but remains considerable; the requested observing time corresponds roughly to the time requested for each, nearby galaxies and young stellar objects. Also, a fairly large amount of observing time was invested in the D-configuration between spring and fall in the detection of line emission from molecular and atomic transitions in galaxies at high redshift. Annex I details all the proposals to which time was granted in the course of the year. The scientific section of the annual report presents some of the most relevant results obtained with the interferometer in 2014.

To explore the possibility of using NOEMA in the extended configurations during summer to perform observations in conditions of poor atmospheric phase stability, it was decided to allocate one week of science demonstration time to assess the effectiveness of self-calibration for high-resolution, high-dynamic range imaging of astronomical sources. To achieve this objective, projects were observed that were expected to generate a better understanding of the limitations and the requirements associated with observations in extended configurations in summer weather conditions. According to the results obtained in the frame of the campaign, observations in the extended configurations under typical summer conditions are feasible provided sources are bright and relatively compact. Based on this feasibility study, the observatory is currently considering the possibility of scheduling a long baseline observing campaign in the summer of 2015.

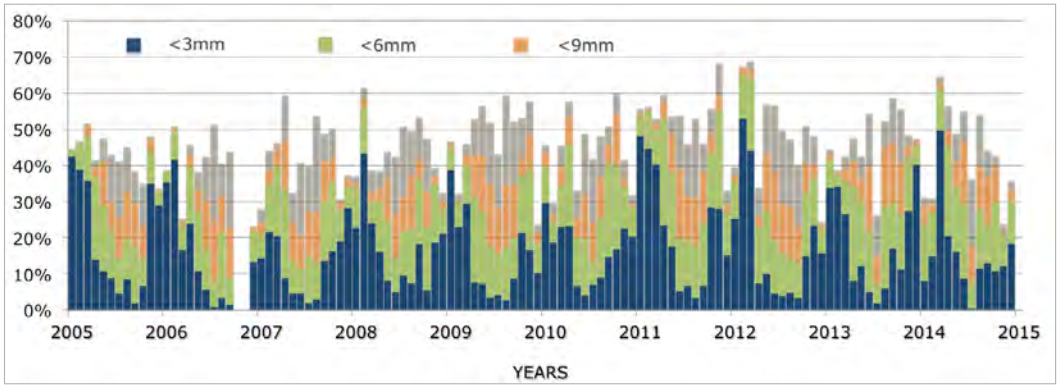

NOEMA observing time and atmospheric water vapor statistics over the last ten years. The overall correlation time accounts for 44% of the total time in 2014. Band 3 (200 – 268 GHz) and band 4 (275 – 373 GHz) programs and observations in the most extended (AB) configurations are for the most part carried out in the winter months when the atmospheric stability is highest. Science operations were suspended in the autumn of 2006 for the installation of new receivers.

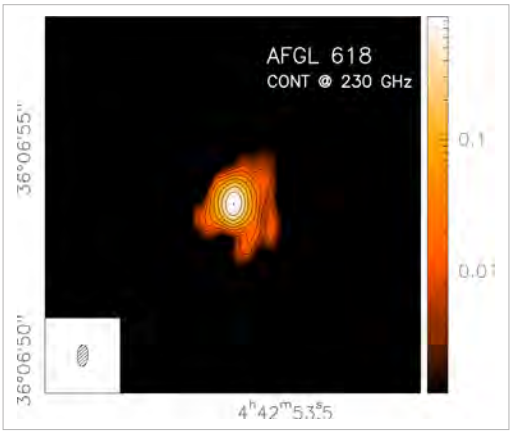

Continuum brightness map of AFGL 618 at 230 GHz obtained on Aug 28, 2014 in the most extended configuration of the array. The contour scale is logarithmically spaced by 0.3 dex and shows the proto-planetary nebula over a dynamic range of ~1000:1. The synthesized beam is 0.52"×0.26".

ONGOING WORK AND ACTIVITIES

Major developments, initiatives and infrastructure improvements were taking place during the year, that deserve a special mention.

While much of the focus at the NOEMA observatory has been on completing the construction of antenna 7 and on preparing work for the building of antenna 8, much time and effort has also been put into the regular maintenance program of the six antennas. A sound coordination and integration of the technical departments and external suppliers was required to achieve the necessary level of efficiency in both planning and execution, and a sustainable balance between science production, construction activities and maintenance work. To ensure that antenna maintenance work is made to match the antenna construction schedule, it was necessary to extend the 18-week annual maintenance period to 23 weeks. As in previous years, the surface quality of all of the antennas was verified at the end of the maintenance period of each antenna by means of holographic measurements. Surface panels were readjusted when deemed necessary, verified and iteratively improved by holographic means. All in all, the primary surfaces of all six antennas show excellent stability and an accuracy of 40μm RMS.

In the framework of the NOEMA upgrade project, we report the installation and commissioning of an extension board to the IF processor. The new board is designed to handle the down-conversion of the horizontal and vertical components of the linearly polarized signals for the NOEMA antennas 7 and 8. The extension board is also fed with a broadband noise reference source to correct the astronomical signal for the downstream baseband response. The data acquisition software was largely rewritten to provide the capability to handle the retrofitted IF system and the double-array mode. The performance of the new system was evaluated through a series of technical verifications, found to perform as expected, and validated by the end of 2014. At the same time a more efficient cooling system was installed to keep the temperature of the wideband correlator within the specifications when operating NOEMA with more than 6 antennas.

In December 2013, the Status Generator (SG), a Python-based system, was definitively implemented to automatize to a higher degree the administration surrounding the progress of observing projects at the observatory. It has been a huge success and helped decrease the day-to-day workload on the NOEMA scientific coordinator. In 2014, initial connections to other tools, like the NOEMA Dynamical Scheduling System (NDSS), to translate the scientific proposals to OBS-ready observing procedures, and last but not least our publicly accessible web pages reporting observational progress with NOEMA, have been made. Discussions are under way to start integrating the SG in the further development of PMS into OMS, the Observatory Management System. Some progress was also made in testing the NDSS, a project-ranking algorithm designed to maximize the effective observing time at the interferometer. The NDSS selects the most appropriate project for scheduling based on a number of parameters like ranking of proposals, schedule pressure, observing frequency and weather. A meeting was held on examining ways to improve the short-range weather forecasting for the observatory.

Following up on the antenna surface refurbishment plan 2007-2010, the possibility was investigated of relaxing the Sun avoidance constraints. The results of these investigations led to the design of a new Sun sensor with the aim of performing observations down to a Sun distance of 25°. By relaxing the Sun avoidance constraints from 45° to 25°, the region of the sky inaccessible to observations on any given date will become less than 5%, and will make many more objects of the sky accessible to observations in the extended configurations of the array. Due to the heavy schedule of activities at the observatory in 2014, the decision was made to limit work by reducing the Sun avoidance cone to 32° and defer further work to reducing it more to the summer of 2015.

Coupled to the development of the NOEMA project and hence the need to handle an increased volume of data, work was going on to expand the data storage capacity, to renovate the existing computer facilities and improve the communication bandwidth. While broadband communication with the observatory using fiber optics will not be operational before 2015, the first steps in moving to a high-performance computer infrastructure were completed by the end of 2014. Further activity to equip the observatory with even more powerful data servers and work-stations is planned to continue in 2015. In parallel work continued to adjust the network structure and topology of the observatory, and projects related to improving and migrating the network time protocol to a centralized server were completed.

In the framework of the NOEMA project, we investigated the possibility of having a common LO reference signal for the band 2 (129 GHz to 174 GHz) and band 3 (200 GHz to 268 GHz) receivers.

Following up on the successful testing of a waveguide system on antenna 1 in 2012, switching systems were installed on all the NOEMA antennas. They were evaluated over a period of several months and found to perform according to expectations.

The radiometer system performed well. The unit on antenna 4 showed a minor stability problem and was replaced by a spare. The temperature regulation in the receiver cabins remains an issue: on two antennas the water vapor radiometer performance is limited by the temperature variations of the receiver cabins; this problem is under study. Work on an extension of the phase correction beyond the one-scan range continues and is expected to enter the standard CLIC distribution in early 2015. The design of the next generation multi-channel radiometer for the NOEMA antennas is proceeding according to plan.

USER SUPPORT

The NOEMA Science Operations Group (SOG) is part of the Astronomy and Science Support Group, a group of astronomers and engineers with a wide range of expertise and technical knowledge in millimetre wave astronomy and associated techniques. The SOG is staffed with astronomers that regularly act as astronomers on duty (AoD) to optimize the scientific return of the instrument, directly on the site or remotely from Grenoble. The group also provides technical support and expertise on the interferometer to investigators and visiting astronomers for questions related to instrumental performance, observing procedures, data reduction and calibration, pipeline-processing and archiving of NOEMA data. The SOG interacts with the scientific software development group for developments related to the long-term future of the interferometer, performs the technical reviewing of the science proposals, collaborates with technical groups to ensure that operational requirements are being met, and keeps documentation up to date. Despite a temporarily reduced manpower and a turnover in the personnel, the SOG astronomers managed to meet their objectives in 2014 and overcome organizational and technical development challenges in the NOEMA project.
The IRAM headquarters hosts a regular stream of visiting astronomers from all around the world that stay at the institute for periods between a few days and a few months. Some of the visiting astronomers come to calibrate and analyze data from the interferometer, others are part of our Visiting Astronomers Program (VAP). The program aims at training research scientists and postgraduate students in interferometry concepts, instrumentation and data reduction, and at strengthening science collaborations. In 2014, IRAM welcomed a researcher from the University of São Paolo/Brazil on a 6-month stay to support work to prepare for the commissioning of the first NOEMA antenna. Advice and assistance was also given to 42 investigators from Europe, and overseas, visiting IRAM Grenoble for a total of 124 days to reduce and analyze data from the interferometer. Further support was provided to 10 experienced astronomers from DPAS/Dalhousie, ICC/Durham, MPIA/Heidelberg, Ithaca College/New York, OSO/Chalmers and DFA/Padova for a total of 46 days to calibrate and analyze interferometer data remotely from their home institutes. In total 49 science projects received support and advice. Compared to 2013, the overall level of user support remained manageable despite an increase in support activity by 10-20%. IRAM astronomers collaborated on more than 50 projects in which they were directly involved. The computer data storage servers were upgraded to meet user requirements and support the work of visiting astronomers on mission at IRAM headquarters. While work was being continued to improve the accuracy of the interferometer's absolute flux calibration scheme, efforts were made in parallel to start preparing the NOEMA data calibration pipeline for the arrival of antenna 7.

In a continuing and successful joint effort with the Centre de Données astronomiques de Strasbourg (CDS), data headers of observations carried out with the NOEMA interferometer are conjointly archived at the CDS, and are available for viewing via the CDS search tools. In 2014, the archive contained coordinates, on-source integration time, frequencies, observing modes, array configurations, project identification codes, etc. for observations carried out in the period from January 1990 to September 2013.

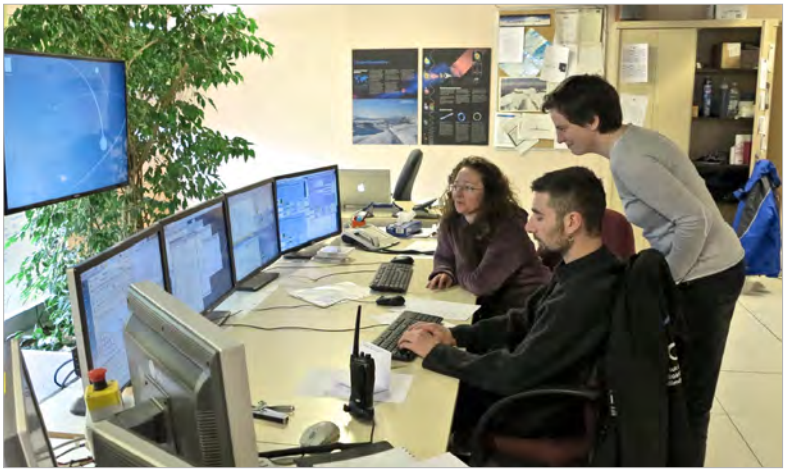

Observatory operators reviewing and consulting with astronomers on the NOEMA daily science operations plan.

The archive is updated at the CDS every 6 months (May and October) and with a delay of 12 months from the end of a scheduling semester in which a project was observed in order to keep some pieces of information confidential until that time.

NOEMA Site

The organization of NOEMA antenna construction, maintenance of existing antennas, maintenance and development of existing infrastructure as well as the continuation of normal operation of the observatory made the Plateau de Bure once more an extremely busy place throughout the year. Coordination of these parallel activities has been a major challenge.

ANTENNA MAINTENANCE

As for the previous years, the maintenance has been organized during the summer period (from the 19th of May till the 21st of September) on a 3 weeks basis per antenna.

However, for 2014 it has been decided to lighten these tasks as much as possible, so the technical staff could be essentially dedicated to the construction of antenna 7. As a consequence, some less critical work has been postponed to the next year. Analysis work on how to reconcile the requirement to bring antennas into the assembly hall for maintenance and the space requirements within the hall for the construction of new antennas has been started.

SITE DEVELOPMENT AND MAINTENANCE

NOEMA requires a dedicated evolution of the infrastructure at the Plateau de Bure, and at the same time normal maintenance of the existing infrastructure must be continued. Among the very numerous preparations for NOEMA the following points are worth mentioning:

The electrical network

Already at its maximum capacity, the electrical distribution network of the observatory had to be prepared for the arrival of the new NOEMA antennas. To avoid a global change of the system, it was decided to divide the network into 2 distinct parts for the time being. Each of them being supplied by its own 20kV power transformer. On this extended scheme, the new transformer (630 kW) feeds the outer parts of the interferometer, while the inner parts and the buildings are still on the old, slightly more powerful one (800 kW).

New high voltage transformer and cell of the extended power supply system of NOEMA.

The new Snowcat garage

With the PdB assembly and maintenance hall being largely occupied with antennas it is not possible anymore to park rolling equipment such as the snowcats inside the hall as was done during the last years. The construction of a dedicated new garage for this equipment has been started, and the construction is foreseen to be finished in spring 2015.

The control room

In order to decouple the work place of operators and astronomers from the noisy antenna assembly work the acoustic isolation and air conditioning of the control room was improved, and the working places within have been rearranged to support the parallel work on regular observations and antenna commissioning.

Fuel tank

For safety and regulation reasons the fuel tank for the backup diesel generators which previously was located inside the building has been replaced by a new tank buried underground, outside of the buildings.

CABLE CAR

During 2014, technical work on the cable car progressed considerably and at the end of the year the cable car and the stations have been almost completed. Testing and commissioning work is foreseen for early 2015, the start of operations is foreseen for summer 2015.

After the winter stop 2013/14, work resumed in early April 2014 with the construction of the boarding platforms on the lower station. Meanwhile, all electrical devices were installed (safety power generators, electrical cabinets, control panels, pylon equipment, etc.) and tested progressively throughout the entire year.

From beginning of May 2014, during a period of 3 months, a total of 32 km (~ 260 tons) of steel cables have been hauled and put under tension on the pylons between the upper and lower stations. The jumpers have then been put in place on the two tracks, and by the beginning of August the trolleys, the hangers, the lifting beam and the cabin were ready for the very first tests.

The building to protect the upper station of the cable car was constructed in parallel to the work on the cable car itself in order to make optimal use of the summer season. This required special coordination and organization within the project. The new station building is connected to the rest of the site by a gallery about twenty meters long which opens on the East wall of the main hall. This gallery, where passengers and standard loads will travel to/from the cable car, has also been designed to host wastes and garbage containers, scheduled to be transported down by the cable car (currently stored in the main hall), in a dedicated room.

Right: Upper cable car station with the building, including sliding doors to close the station building under adverse weather conditions. Left: Lower cable car station during preliminary tests.

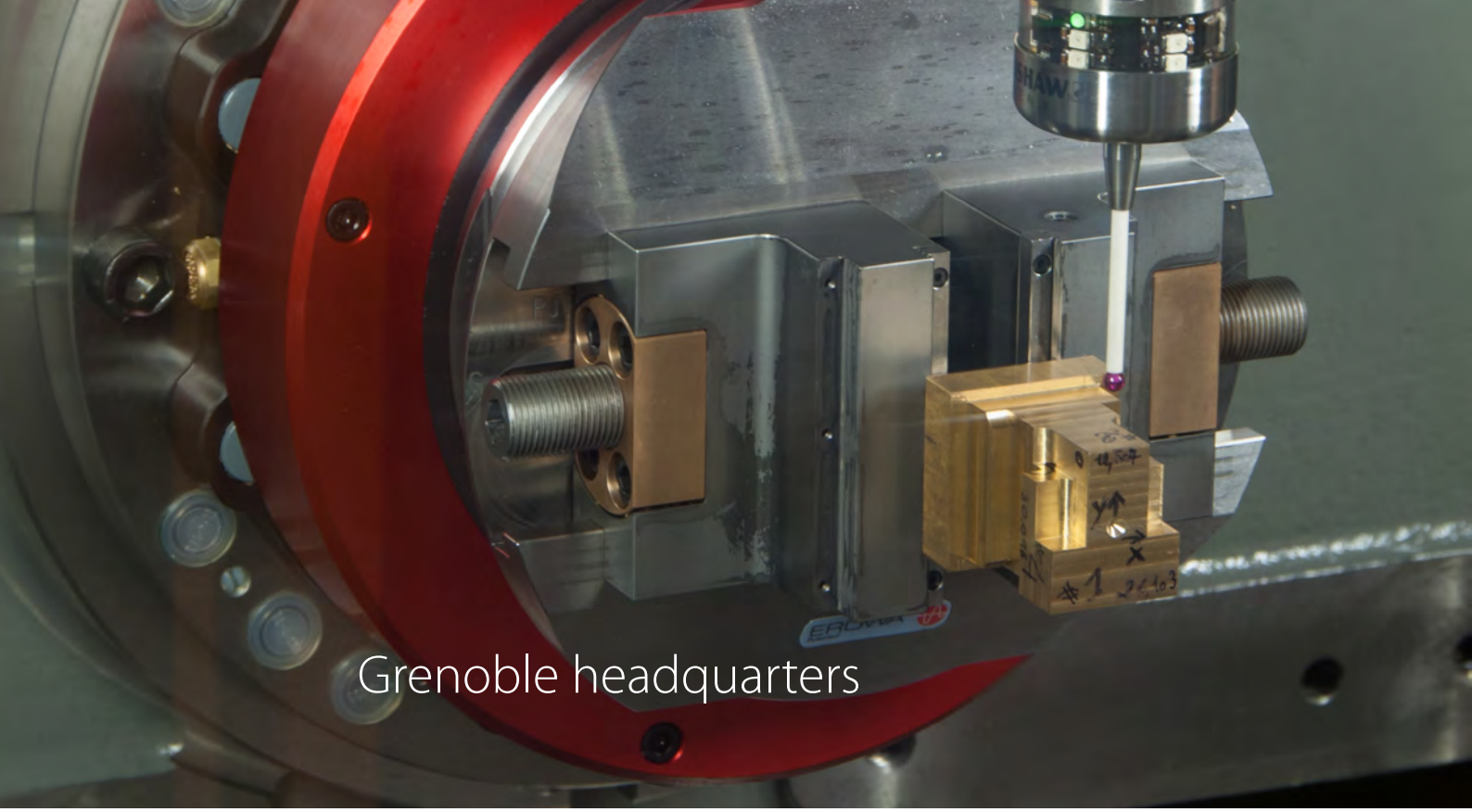

Grenoble headquarters

Frontend group

The IRAM Frontend Group had a busy year in 2014 with the construction and installation of the first NOEMA frontend on Ant. 7, the maintenance of instrumentation at the two IRAM observatories, the design of the receiver cabin optics and bolometers for the 30-meter telescope, the maintenance of ALMA Band 7 cartridges and construction of two receiver units for the Greenland Telescope, the design of the dual-band receiver for the Max Planck Institute for Solar System Research, the prototyping of components for the ALMA Band 2+3 cartridges, the design of the EMIR Band 1 receiver upgrade, and the AETHER Task 1 and 2 activities.

NOEMA FRONTEND

The first NOEMA receiver was successfully constructed and tested; it was installed in Ant. 7 in December 2014. The instrument has state-of-the-art performance and sets a new standard in the post-ALMA generation technology.

The NOEMA frontend specifications required re-designing the existing PdBI frontends, which have been in continuous operation since their installation in 2006. In particular, the backshort tuned Single Side Band (SSB) Superconductor-Insulator-Superconductor (SIS) mixers delivering 4 GHz IF bandwidth per polarization channel, currently adopted for PdBI Bands 1, 2, and 3, have been upgraded to the NOEMA sideband separating (2SB) mixers providing two ~7.6 GHz wide IF bands (LSB and USB) per polarization channel. This will increase the total IF band delivered to the correlator from 2 x 4 GHz (8 GHz) to 4 x ~7.6 GHz (~31 GHz). Also, the four RF bands of the NOEMA receivers are larger than the ones of the current receiver generation. In particular, the Band 1 lower frequency edge is extended to 72 GHz, thus allowing to cover important molecular lines not yet accessible to ALMA.

The NOEMA frontend features many novelties and improvements, the most important ones being: improved optics, state-of-the-art performance 2SB SIS mixers, new IF sections at cryogenic and room temperatures, a novel optical-fiber laser rack to

Left: NOEMA Frontend for antenna 7; view of the cold section.
Right: installed in the receiver cabin.

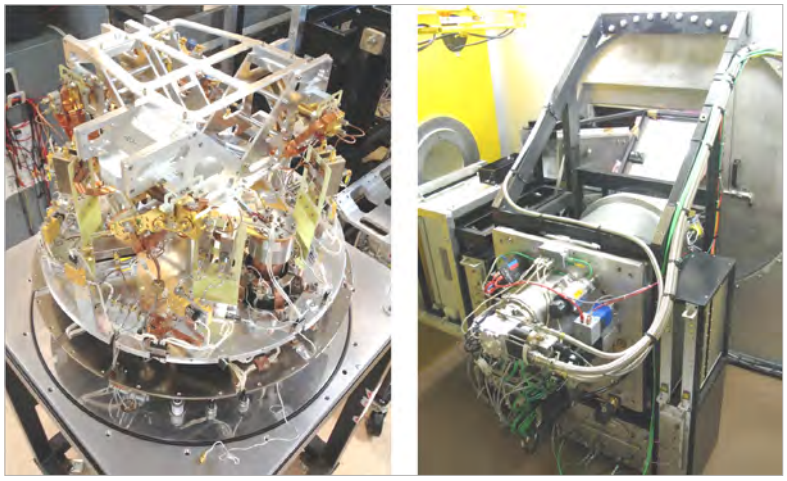

transport the IF signals, new local oscillator systems for Band 1, improved calibration loads, new control electronics, and an improved thermalization of the cryogenic stages leading to quicker warm up/cooling down cycles.

Following the successful development of the NOEMA receiver for Ant. 7, the goal of the frontend group is to upgrade all the frontends currently installed on the six existing antennas to the new NOEMA standard and to build four additional ones (three plus one spare) for the new NOEMA antennas (Ants. 8, 9 and 10). The internal production and supply from external companies of the sub-assemblies necessary to equip all NOEMA receivers (SIS mixers, waveguide couplers, optical modules, cryogenic and room temperature amplifiers, etc.) has continued all throughout 2014.

E-band Gunn module (rather than two independent ones) cascaded with an E-band waveguide switch that diverts the signal to either the doubler (Band 2) or the tripler (Band 3). Following successful laboratory and on-site tests, waveguide switches were installed in all six antennas (as well as in Ant. 7), thus freeing one E-band Gunn module per receiver for future use in the new NOEMA antennas.

Although the Gunn-based solution (plus switch and frequency multipliers) is adopted for the NOEMA LO Band 2&3, an electronically tuned E-band LO module prototype is being developed for future replacement of the Gunn modules. The development of the electronically tuned E-band oscillator started in 2014.

Inside the NOEMA frontend, a waveguide LO injection scheme is used for the four independent RF modules. Waveguide splitters divide equally the LO power coming from the LO modules placed outside the dewar, and distribute it to the two orthogonal polarization channels. New LO waveguide splitters were successfully designed, fabricated, and tested for Bands 1, 2 and 3 and their production was completed in 2014.

Definition of bands and SIS mixer technologies of the current generation PdBI receivers and of the new NOEMA receivers.

	PdBI Frontend			NOEMA Frontend		
Band	RF [GHz]	IF [GHz]	Mixer scheme	RF [GHz]	IF [GHz]	Mixer scheme
1	83-116	4-8	SSB	72-116	3.8-11.7	2SB
2	129-174	4-8	SSB	127-179	3.8-11.7	2SB
3	200-268	4-8	SSB	200-276	3.8-11.7	2SB
4	277-371	4-8	2SB	275-373	3.8-11.7	2SB

Local Oscillators

Following the successful development and installation of the prototype of an electronically tuned YIG-based Local Oscillator (LO) for NOEMA Band 1 in Ant. 7, four additional units (three plus one spare) were produced within specifications in 2014 for the new NOEMA antennas.

The LO signal necessary to drive the Band 2 and the Band 3 SIS mixers at each of the PdBI antennas was generated by two independent LO units: one Band 2 LO module (135-168 GHz) and one Band 3 LO module (206-262 GHz), both based on similar 67-91 GHz E-band Gunn oscillators cascaded respectively with a frequency doubler and a frequency tripler. The LO system for NOEMA Band 2&3 is based on a unique

IF section

The NOEMA SIS mixers are connected to cryogenic IF isolators and low noise amplifiers (LNAs) operating across the non-standard 3.872-11.616 GHz IF band (~7.6 GHz wide). The production of the 132 (plus spares) LNAs, subcontracted to CAY&TTI, and of the 132 (plus spares) isolators, subcontracted to Quinstar/Pamtech, has continued all through 2014

Left: Four electronically tuned LO modules for NOEMA Band 1 and their power supplies. Right: Measured LO power at the WR10 waveguide outputs of the four modules.

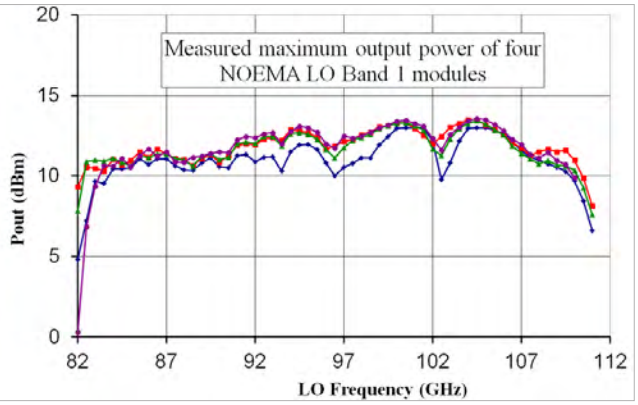

(132 units will equip 4 sidebands x 3 bands x 11 frontends).

A new room temperature IF amplification module connected to the NOEMA cryostat backplate was developed. Four such modules are used for each cryostat. Each module selects one of the four possible IFs from each of the four possible mm-wave bands. Cascaded with the IF switch are amplifiers, filters and step attenuators that deliver an IF signal in a suitable power range (of the order of -20 dBm).

Laser rack

A new laser rack was developed to convert the 4x~3.8-11.6 GHz IF signals from the four warm IF modules of each frontend into optical signals. The signals are transported through optical fibers to the correlator. The fiber-optic links are fabricated by Miteq. Two transfer switches located inside the laser rack allow to change the polarization states by reversing the signals of the horizontal and vertical polarization.

Left: NOEMA warm IF amplification module with integrated switch and digital attenuator. Right: NOEMA laser emitter rack.

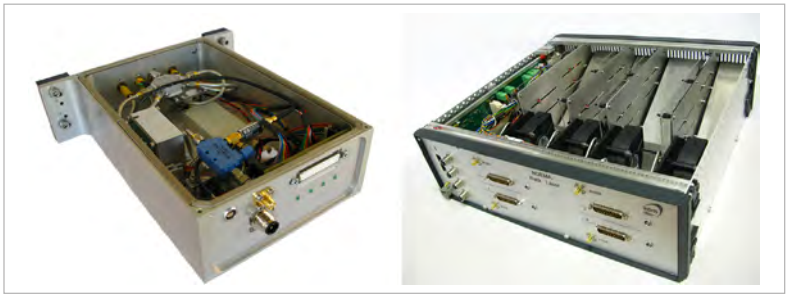

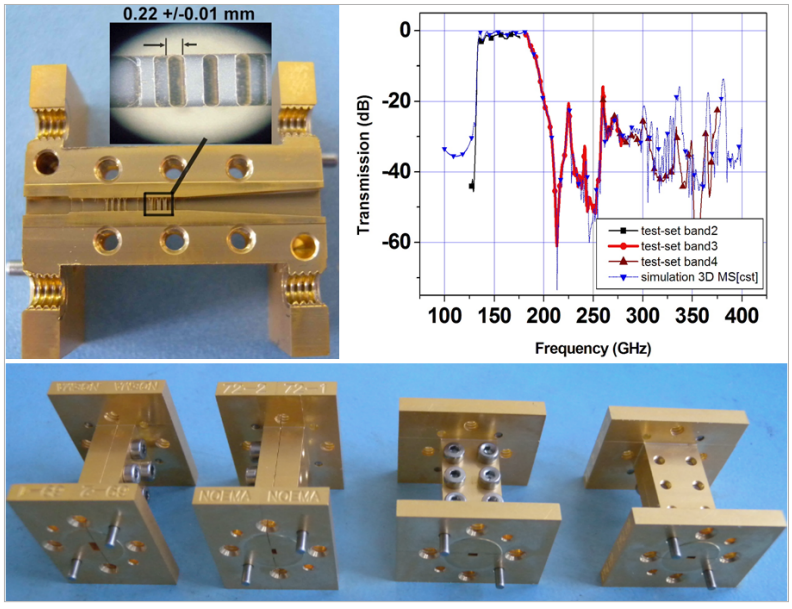

EtherCAT receiver control electronics

New bias modules for the LNAs and the SIS mixers, controlled by EtherCat, are under development. They will replace the current control electronics based on I^2C and CAN in all frontends. Each frontend will use two bias modules to monitor the 16 LNAs and one single SIS junction bias module to control the 8x2SB mixers (16 SIS junction chips). The warm IF and laser rack modules as well as a new cryogenic temperature monitoring system are also controlled by EtherCAT modules. The NOEMA frontend for Ant. 7 employs current PdBI receiver control electronics.

Vacuum windows, IR filters and calibration

The mm-wave signals of the four bands enter the frontend through four independent wideband low-loss HDPE vacuum windows and PTFE infrared filters of improved design. The dual-polarization receiver beams can be coupled to either an ambient temperature load or a cold load thermalized inside the cryostat at 15 K. The cold load is coupled through pairs of mirrors located on a carousel (two carousels are employed, one for the Band 1&2 beams, the other for the Band 3&4 beams). An improved wideband cryogenic calibration load based on pyramidal shaped sections made of Eccosorb MF-114 material from Emerson&Cuming was successfully developed for the NOEMA frontends.

Waveguide band pass filter for suppression of NOEMA Band 2 LO spurious harmonics

A 135-184 GHz waveguide band pass filter was designed, fabricated, and tested to suppress the spurious harmonics of the NOEMA Band 2 local oscillator. The filter response was measured using the IRAM MVNA test sets across the NOEMA bands 2, 3 and 4. The measurements match very well the electromagnetic filter model down to very low amplitude levels. When the filter is placed at the LO doubler output, it reduces the harmonics level of the LO below 132 GHz, and between 200 and 400 GHz by more than 20 dB. In addition, it reduces the noise temperature of the NOEMA Band 2 receiver at 136 GHz by 16 K in LSB and by 11 K in USB (measured receiver noise reduced from 53 K to 37 K in LSB). The receiver noise improvement is explained by the reduction of the excess noise contributions from the sidebands of the spurious harmonics. Filters of this type were installed in the LO paths of the NOEMA Band 2 receiver of Ant. 7 and in the E1 EMIR receiver on the 30-meter telescope.

Top left: Band pass filters for rejection of Band 2 LO harmonics. View of a split block showing internal details. Below: Four identical units were fabricated and tested. Top right: Comparison between simulation and measurement of one unit.

NOEMA OBSERVATORY MAINTENANCE

During the summer of 2014, the frontend group carried out maintenance and repair work of the Sumitomo cryogenic generators. Two compressors failed, one due to a problem with the air fan (in antenna 4), which was repaired on site, the other due to an electrical problem of the compressor capsule (in antenna 1), which was sent to Sumitomo Germany for repair. Three cold heads (antennas 1, 3 and 6) were replaced following the now established "hot-swap" procedure and shipped to Sumitomo Germany for revision. The Band 3 local oscillator of Ant. 5 failed in September 2014 due to a short-circuit problem of the Gunn oscillator (H235). Some variable attenuators were replaced during the summer maintenance period, as well.

The 22 GHz water vapor radiometer of Ant. 4 was replaced with the spare radiometer because of a problem of instability of one of the three RF channels.

30-METER TELESCOPE INSTRUMENTATION MAINTENANCE

The local oscillator system of one of the two polarization channels (Pol 1) of the HERA 230 GHz multibeam receiver was repaired after failures of the backshort mechanism of the Gunn oscillator (from RPG) that tunes the LO frequency, and of the amplifier of the phase-locked loop of the XL Microwave module. The RPG Gunn was replaced with a Carlstrom Inc. Gunn and the XL Microwave module was repaired.

The Daikin compressor of the HERA receiver was damaged during transportation. It was repaired and sent back to the 30-meter telescope, together with the cold head which was serviced at the IRAM headquarters.

The Band 4 YIG local oscillator of the EMIR receiver was repaired by Micro Lambda following a problem of lack of LO power delivered by the YIG at some frequencies.

NEW OPTICS AND BOLOMETRIC DETECTORS FOR THE 30-METER TELESCOPE

30-meter cabin mirrors refurbishment

The design of the large field-of-view (FOV) receiver cabin optics for the 30-meter telescope was finalised in 2014. At the beginning of the year, decisions on the main specifications were taken. It was decided to keep a M3 Nasmyth system with one axis of rotation combined with the telescope elevation axis. The FOV will be limited by the physical size of the cabin to a 7-arcminutes diameter, which fits the specifications of the foreseen future instruments. The M3 mount will be attached to the metallic beam on the cabin ceiling, whereas the M4 mount will be attached to the elevation bearing of the telescope.

The rest of the year was dedicated to the finalization of the project, the main part being the detailed drawing of the parts of the mounts, including the M5 and M6 for NIKA-2, which was carried out in collaboration with the ERIA design office as subcontractor. The manufacturers are SATIL Concept for the mounts and Media Lario for the mirrors. The installation of the new optics is foreseen in April 2015.

The NIKA-2 instrument

2014 was also the year of the completion of the NIKA-2 instrument. The fabrication started at the end of 2013; the assembly of the main parts at the Néel Institut (cryostat, dilution system, cryogenic cooler, optical chamber, base electronics) took place during the first part of the year. The first cool down to 4 K was carried out in spring, the first cool down to 100 mK with a 1000 pixels test array took place in the summer (electrical tests), while the first cool down with HDPE lenses and a 2000 pixels test array took place in autumn. The Néel Institut is in charge of the design and assembly of the main parts of the instrument, while IRAM participates in the design and development of the optics, KID detector arrays and external calibrator. The other institutes contributing to the development of the NIKA-2 instrument are LPSC, Cardiff University, IPAG and CEA.

Other bolometric instruments

Four observing runs were carried out with the NIKA prototype in 2014, the first two open pool runs in February and November, and the 7th and 9th test runs in January and October, respectively. Despite some problems encountered, in particular with missing telescope data which had to be solved, the runs were mostly successful. The pool runs yielded several publications, in particular the Performance and calibration of the NIKA camera at the IRAM 30-meter telescope (Catalano et al. 2014, A&A 569, A9) and the First observation of the thermal Sunyaev-Zeldovich effect with Kinetic Inductance Detectors (Adam et al. 2014, A&A 569, A66). The test runs allowed the validation of acquisition and pipeline improvements, the first tests of a polarization setup and a diode calibrator, and a test of the new PaKo observation procedures.

The GISMO open pool runs continued on the regular basis of two runs per year, with the 5th pool in April, and the 6th in October. The GISMO-2 instrument was delivered at the end of 2014.

Simulations and test on KIDs array optimisation

The IRAM frontend group carried out investigations to improve the array performance and have a better understanding of the interaction of the KID detectors with their electromagnetic environment. Different resonator topologies were proposed to reduce the pixel-to-pixel coupling. Electromagnetic simulations and experimental tests were performed to find a new array configuration with improved physical characteristics allowing a more homogenous frequency comb repartition and resonance quality factors. Such studies highlight the effects of the feed line, the ground plane, the designed frequency distribution of the pixels array, and the variation of the thickness of the superconducting metal.

ALMA BAND 7

Two IRAM frontend group members visited the ALMA Operations Support Facility (OSF) in Chile to perform a set of tests on ALMA Band 7 cartridges to verify their installation and perform commissioning, as well as to train local engineers and technicians for future maintenance purposes.

In 2014, two cartridges were returned to IRAM from the OSF to be fixed under a 12 months maintenance contract signed with ESO.

GREENLAND TELESCOPE CARTRIDGES

Two ALMA-like Band 7 cartridges were assembled, tested, and shipped to Taiwan for the future Greenland Telescope.

Design of the Dual Band Receiver showing the 3D view of the cryogenic section.

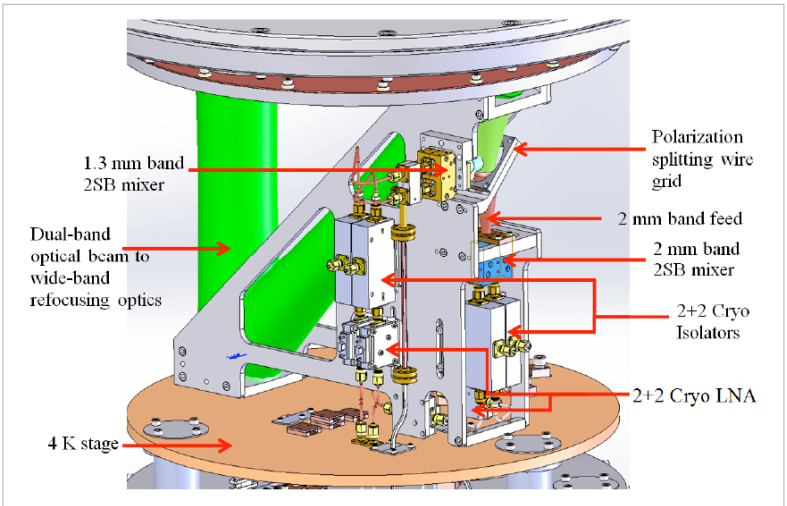

DUAL BAND RECEIVER FOR THE MPS

IRAM is studying and developing a complete dual-band (2 mm and 1.3 mm wavelengths) single-polarization SIS receiver for the Max Planck Institute for Solar System Research (MPS) which will be used to carry out atmospheric physics research. The frontend will be based on the state-of-the-art NOEMA Band 2 and Band 3 2SB mixers, accommodate four 3.8-11.7 GHz IF outputs channels, and will meet the NOEMA specifications.

ALMA BAND 2+3

IRAM collaborated with other European institutes on a 16-month feasibility study funded by ESO. The aim was to develop an ALMA Band 2 receiver system and a combined Band 2 and 3 receiver system based on W-band cryogenic LNAs. The results of the successful IRAM development, i.e., feed-horns, orthomode transducers (OMTs), vacuum windows and IR filters for the 67-116 GHz band (ALMA Band 2+3), were presented at the final review meeting in March 2014. IRAM submitted two additional proposals for studies of ALMA Band 2+3 cartridges to ESO, one based on LNAs (to be intended as a continuation of the 16-month funded study), the other based on SIS mixers. The SIS cartridge proposal was submitted in June 2014.

DESIGN OF EMIR BAND 1 RECEIVER UPGRADE

An OMT plus feed-horn combination, of the type developed within the framework of the ALMA Band 2+3 ESO-funded study, was designed for future installation in the EMIR receiver at the IRAM 30-meter telescope. The dual polarization waveguide module will be coupled to two 2SB SIS mixers covering 70-116 GHz and will deliver 4 x 4-12GHz IF bands.

AETHER ACTIVITIES

Task 1: A compact cryogenic packaging (3rd version) for new W-band mHEMT (metamorphic High-Electron-Mobility Transistor) MMIC (Monolithic Microwave Integrated Circuit) low noise amplifiers, first developed by IAF, was designed and fabricated at IRAM for AETHER Task 1 (67-116 GHz band). The packaging includes new broadband waveguide-to-microstrip probes and cryogenic Titanium thin-film resistors (fabricated by the IRAM clean-room facilities), and new compact mechanical blocks. Batches of new generation IAF MMICs were received and tested with the IRAM room-temperature W-band probe station. Several W-band LNAs were assembled and tested at room and cryogenic temperatures using the IRAM broadband test equipment. Very promising LNA performances were obtained in terms of bandwidth and noise.

Task 2: Progress was made on the design of a seven-pixel linear array of 2SB SIS receivers for the 200-280 GHz band. Two types of 4-12 GHz superconducting 90 deg hybrids, one designed at IRAM, the other at OSO (Sweden), were tested cascaded with a 2SB mixer. Each pixel of the cryogenic module will integrate a smooth walled potter-horn developed at the Oxford University (UK), which was tested on the antenna range at IRAM, and two 4-12 GHz IAF MMIC LNAs developed at the Yebes Observatory (Spain). The array of mixers is pumped by a local oscillator under development at RAL (UK).

Progress on packaging of 3 mm band MMIC low noise amplifiers carried out at IRAM in the past years. The third LNA packaging version was developed in 2014.

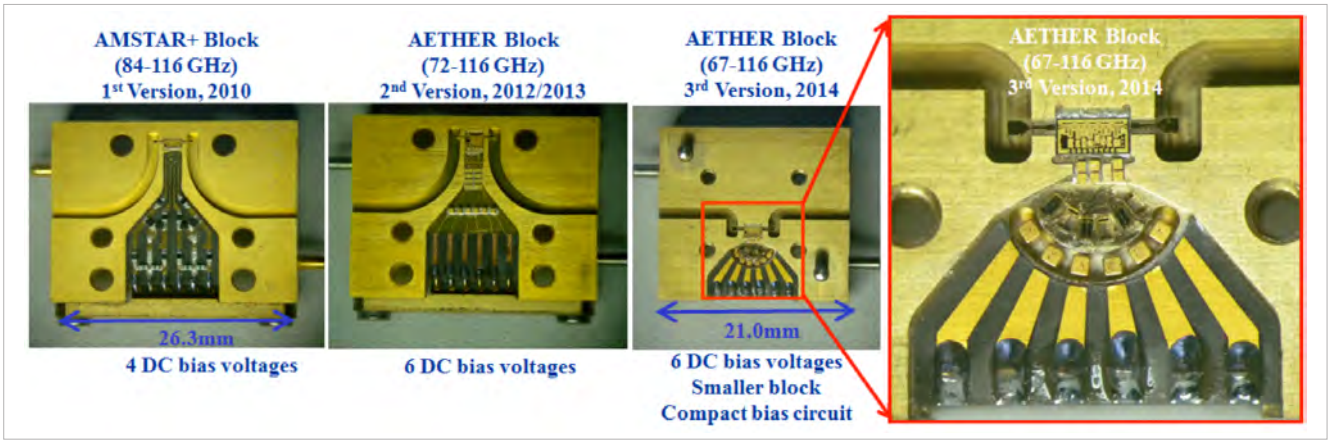

SIS Group

The work in the IRAM superconducting device group during 2014 did progress well. However, increased efforts had to be made to compensate the reduction in investments for equipment renewal.

The production of SIS junctions for various frequency bands was mainly driven by the NOEMA project. Normal-conducting passive circuits for the integration of millimeter wave MMICs and IF frequency components turn out to be of increasing importance and the micro-fabrication capability of IRAM is well matched and now frequently used. The cause of reduced device fabrication yield due to short circuits could clearly be traced back to pinhole problems with the sputtered SiO_2 layers and investigations of possible improvements are ongoing.

The development of KID detector arrays for the NIKA-2 instrument was the second main activity in the group. The work covered production of prototype arrays with several thousand pixels on 4 inch wafers as well as dedicated test structures for electromagnetic and material research. Deep silicon micro-machining for improved radiation coupling to detector arrays has been employed.

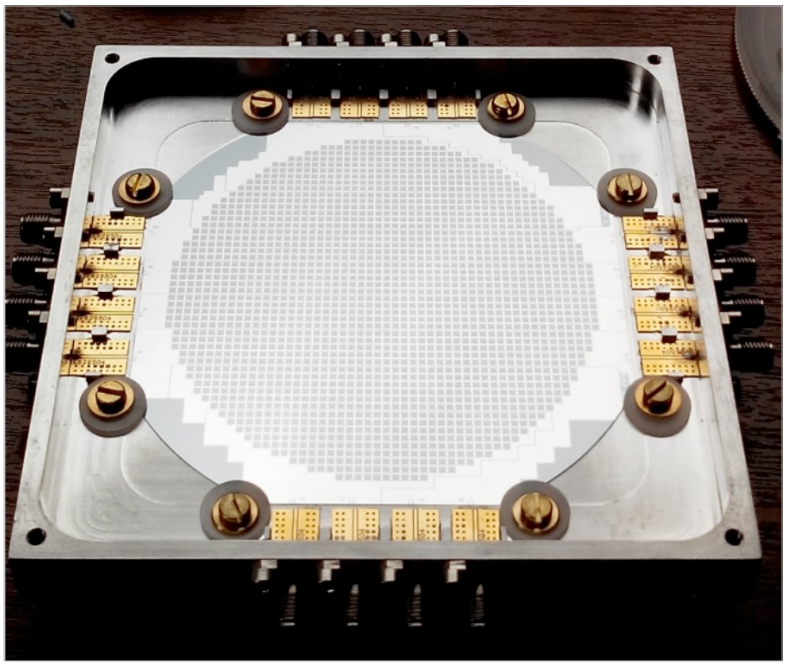

A mounted 2000 pixel prototype array for the 1mm frequency band as foreseen for the NIKA-2 instrument. The detectors are fabricated on a single 4-inch wafer. 8 readout lines for frequency multiplexed readout are employed.

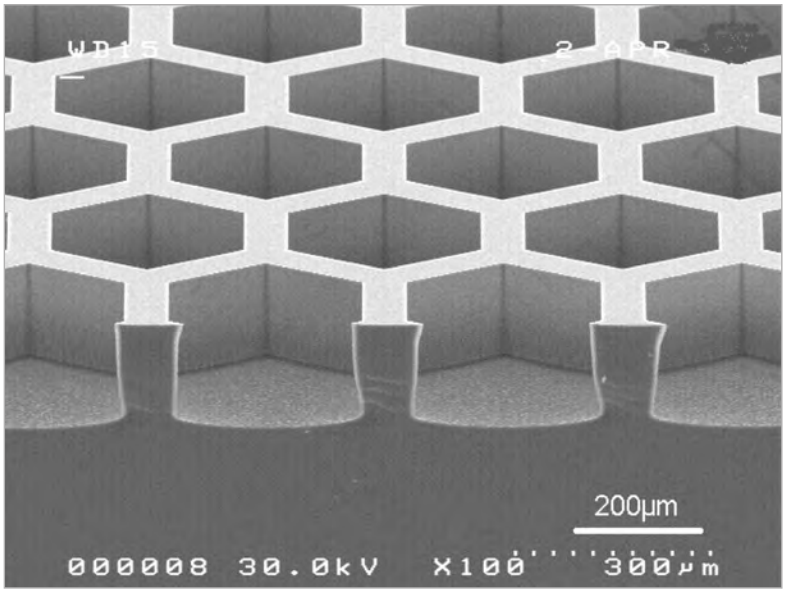

Deep silicon micro-machining of the backside of a detector array. The mixed air/silicon structure acts as an effective dielectric matching layer for optimum wideband coupling of the milimeter wave radiation to the detectors on the front side of the wafer.

Backend Group

INSTALLATION OF THE IF PROCESSOR EXTENSION: LE STRAPONTIN

In order to operate the WideX correlator with up to 8 antennas, the add-on equipment called "Le Strapontin" (jumpseat) has been finalized and installed at the NOEMA observatory during summer 2014. As in the already existing 6-Antenna IF processor, its local oscillators (LOs) are phase-steerable so that it can support sub-arraying which is a very valuable feature, especially for the commissioning of the forthcoming new antennas.

Since its installation in 2010, WideX was operating at 50% of its capacity (6-Antenna vs. 8-Antenna baseline processing) in order to save power . The arrival of antenna 7 has triggered the transition into the 8-antenna processing mode. To ensure temperatures at which the correlator can operate safely, the WideX cooling has been upgraded with more powerful blowers that enhance the range of temperatures in which the system can function, leading to a more reliable operation.

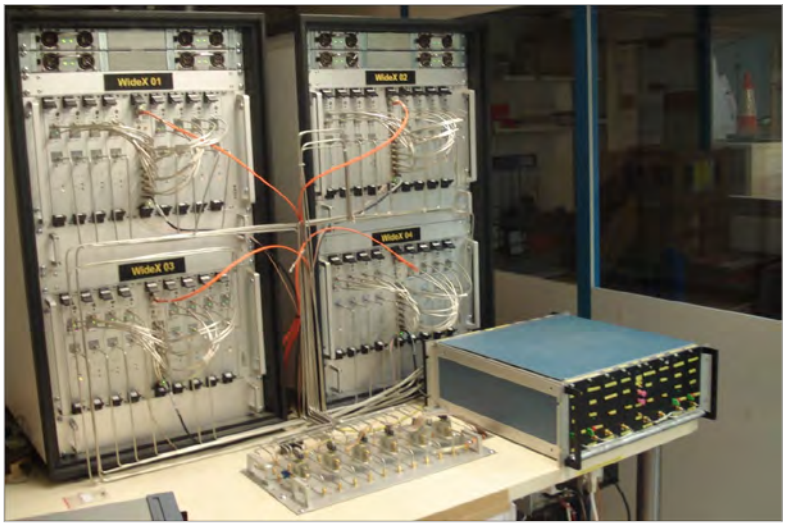

View of the "Strapontin" (black and blue rack) right beside WideX in the correlator room of the NOEMA observatory.

DEVELOPMENT OF THE NEXT CORRELATOR FOR NOEMA: POLYFIX

Analog preprocessing

The frequency plan defined for NOEMA has been translated into a hardware prototype.

For each of the 12 NOEMA antennas, the incoming light from the laser transmitters, is first converted back to a 4-12GHz RF bandwidth then split into two halves and finally down-converted to 0-4GHz basebands to feed the digitizers located into the PolyFix correlator units.

Four such signal chains have been prototyped together with a built-in noise generator which can be activated independently for each antenna when a test or calibration of the backend antenna signal path is required.

First measurements have shown a good flatness of both basebands, to less than +/- 2dB over the entire band, and the EtherCAT monitoring and control has been successfully tested.

Digital correlator

The PolyFix correlator is an FFX-Architecture machine. The "X-Engine" (baseline processing) of a correlation unit will be made up of 8 cards, each capable to process 2x 4 sub-bands of 64MHz, resulting in a total bandwidth of 4096MHz per correlation unit.

A prototype board, nicknamed "Combo", has been designed and built by end of September 2014. This board will be used to deserialize and synchronise the incoming Gigabit serial links from the 12 antennas. It will also be able to perform a high-resolution fast Fourier transform (FFT) and will determine the cross-spectrum for each of the 66 baselines. "Combo" will

View of the NOEMA IF Processor Prototype housed in a "like full-tower PC" rack.

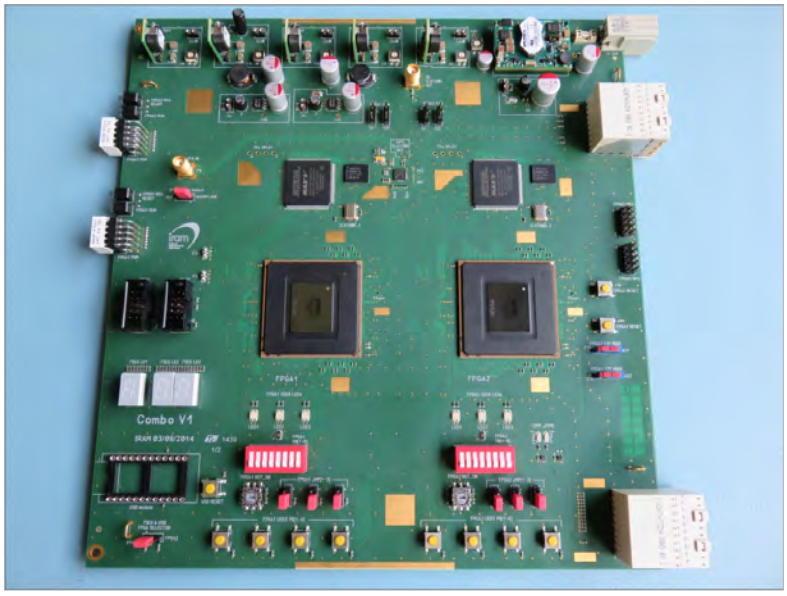

View of the "Combo" board.

also transmit the accumulated spectral data to the readout board.

The hardware is mainly composed of two FPGA (field-programmable gate array) devices (Altera Arria V GX family) which have been implemented onto a 14-layer printed circuit board (PCB). Preliminary tests have shown that the hardware is fully functional and able to support the forthcoming gateware.

The VHDL code, a hardware description language code, for each functional block is in its development phase.

Readout board prototype

In early 2014, the "D_READOUT" card which interfaces the correlator units to the real-time and data acquisition computer (RTDA PC) has been designed and built.

The incoming spectral data from all correlator boards are first collected by a FPGA (Altera Cyclone IV family) then reformatted and transmitted to a high-speed optical serial data link (a Cerntech daughter board) which transmits the high data volume of a PolyFix unit to the RTDA PC.

Data transmission rates up to 1.413Gbps have been successfully achieved, providing thus some margin with respect to the required output data rate of 1.359 Gbps.

View of the "D_READOUT" board.

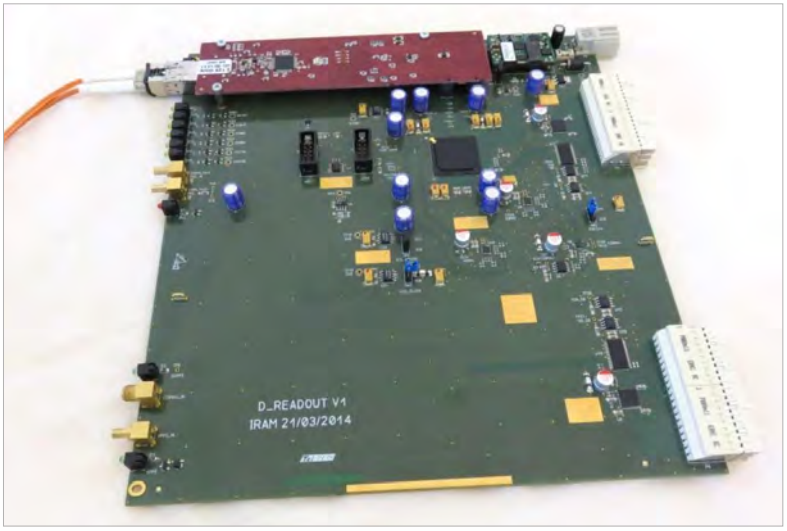

Mechanical group

In 2014, most of the work done by the mechanical group was focused on the assembly of the reflector of the first NOEMA antenna (antenna 7). This was started in April 2014. Several objectives had to be achieved for this first new reflector:

- ensure a constant high manufacturing quality of all components,
- optimize the design of numerous components in order to reduce the mass of the reflector, and
- ensure that the reflector assembly adheres to the same schedule as that of antenna 6, even though a completely new mechanical team and new suppliers are now involved.

DETAILS OF THE OPTIMIZATION OF A SUBSET OF PARTS OF THE REFLECTOR

As part of the goal of reducing the mass of the reflector, many possible optimizations have been investigated:

Carbon tubes

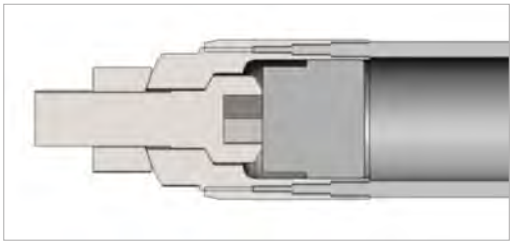

Reference tip for antennas 1 to 6

New tips

The outcome of a long period of several years (cf. 2012 IRAM Annual Report) of studies and work in collaboration with our subcontractor, Epsilon composite, allowed for a mass reduction of 60 kg. In order to meet performance goals, many qualification tests were conducted with our partner.

Upper reflector nodes

The outcome of a long period of several years (cf. 2012 IRAM Annual Report) of studies and work in collaboration with our founder subcontractors Safe, and machining company, allowed us to reduce from 20% to 30% the weight of a node, depending on its type.

Panel actuators

In cooperation with our supplier Böhm the design of the actuators was optimized and their mass was decreased by 50%.

ASSEMBLING OF THE REFLECTOR OF ANTENNA 7

The major improvement of this reflector assembly compared to the previous IRAM antennas is the use of an AT 402 laser tracker during the mounting of the support structure, the main mirror panels and the hexapod. The whole measurement part was led by an expert from the company SETIS. This device allowed to save time and brought an increased accuracy in the position of the nodes and panels.

The use of the laser tracker also allowed additional information to be obtained during the assembly of the reflector. For example, it allowed an evaluation of the observed deviations of the nodes from their theoretical positions, after the assembly. The laser tracker also allowed the accurate measurement of the position of the quadrupod legs and subreflector with respect to the parabolic dish of the main reflector.

Calculations using the finite element method have shown that the fastening of the four quadrupod legs in the upper section could be simplified. Instead of joining the legs via a dynamic cross, with incorporated ball bearings, a fixed cross, stiff in its behavior, has been installed.

The last three rings of panels, ring 4, 5 and 6, are too inclined with respect to horizontal to ensure a correct alignment of the respective panels. Therefore a new technique was used to allow for faster panel adjustment.

The major improvement brought by the laser tracker for the alignment of the panels, is to improve the accuracy on the position of support point 5. This technique was used for the panels of the 5th ring only, but after holography tests, this method was validated by the commissioning team, and it will be used for antenna 8 assembling.

The final measurement of the alignment of all panels of the primary reflector surface resulted in surface errors below 80 micron rms, a value that would have been even better if the 5th support point of all the panels had been aligned.

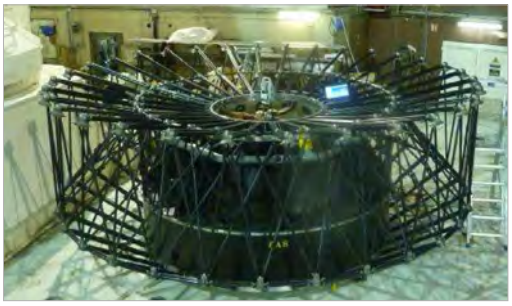

Assembly of the inner rings of the reflector. These first two rings were assembled on the ground and then installed on the antenna mount, before the assembly of the remaining support structure. During the whole mounting of the reflector, the laser tracker is installed in the middle of the central hub.

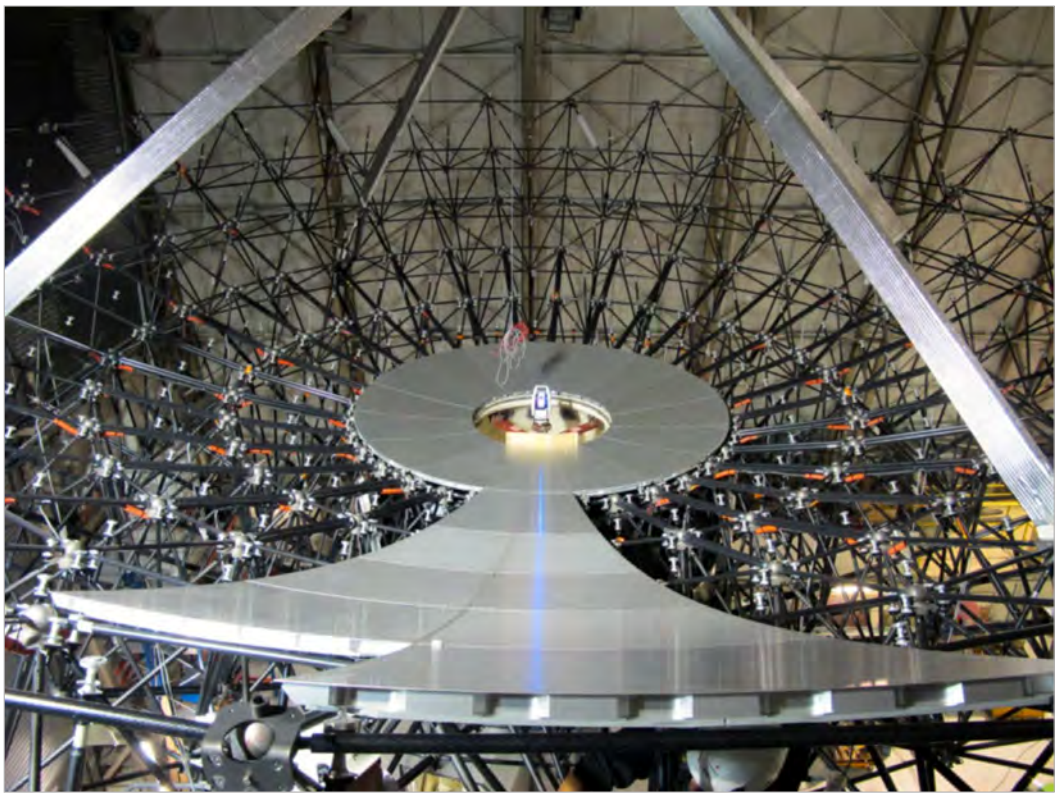

Assembly of a first sector of panels after having mounted and aligned the first ring of panels. This operation is necessary to ensure that the position of each ring of panels remains within the tolerances of movement of the actuators carrying the panels.

NEW HEXAPOD

One of the main technical challenges of the NOEMA project is the integration of a new hexapod for the secondary mirror. Numerous qualification tests of the hexapod were performed in-house and together with our partner Symetrie.

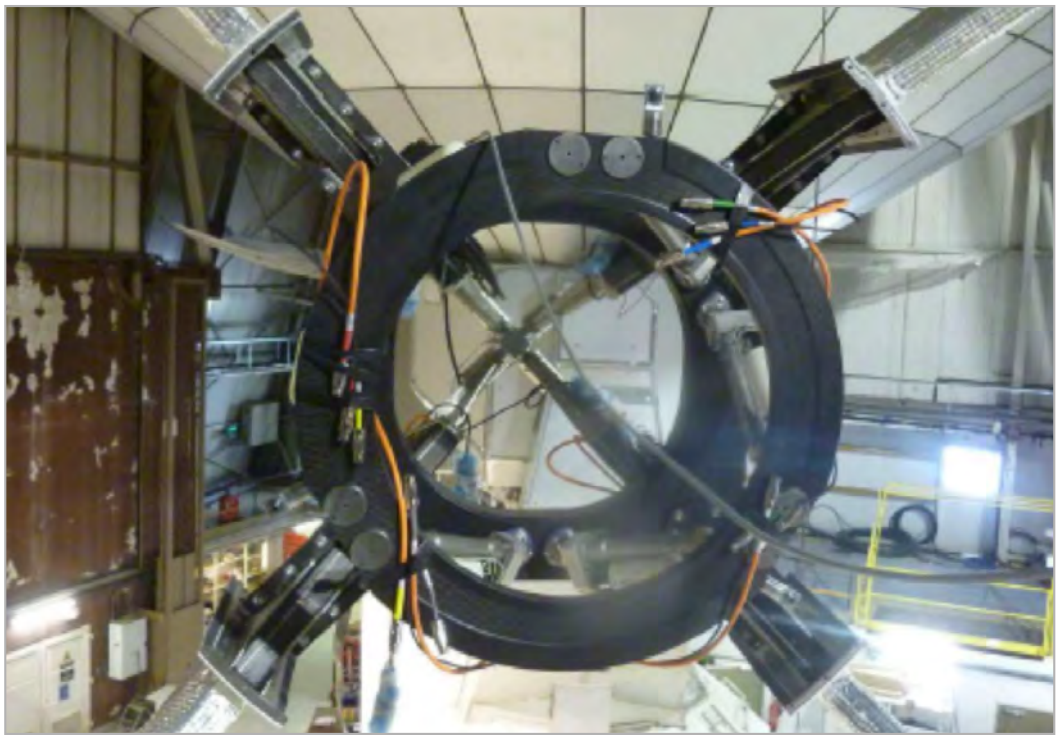

Installation of the hexapod.

BEGINNING OF THE CONSTRUCTION OF ANTENNA 8

Despite delays in the delivery of antenna 7, the construction of the mechanical mount for antenna 8 was started, according to the schedule of the NOEMA project. At the end of 2014, the assembly of the pedestal and the chariot of antenna 8 was complete.

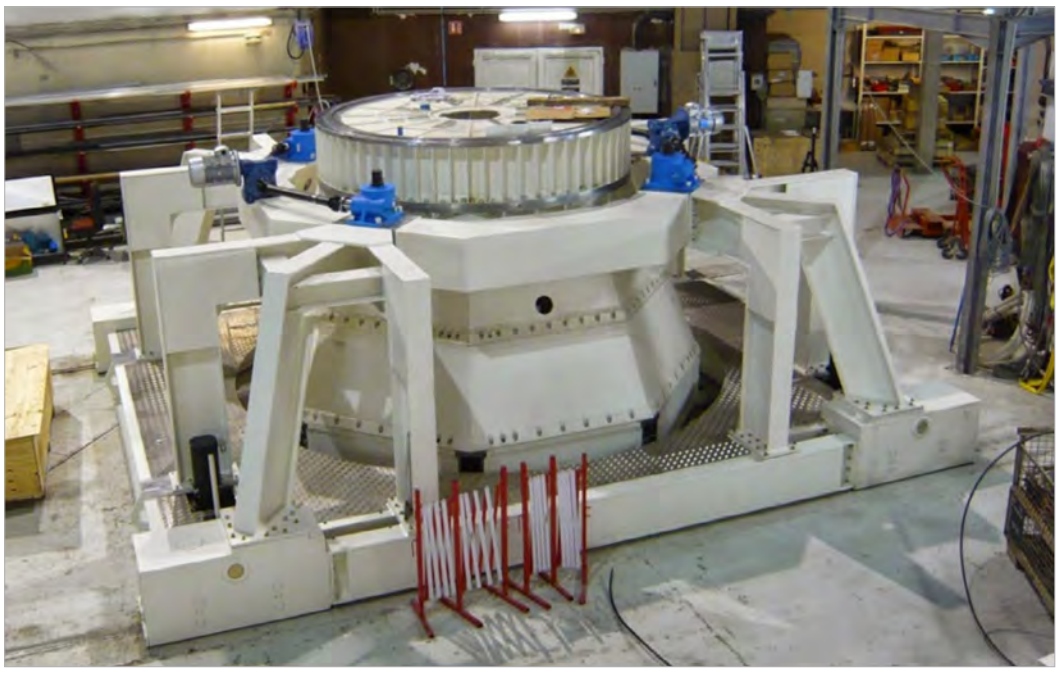

Antenna 8 at the end of 2014.

STUDY, DEVELOPMENT AND PRE-ASSEMBLY OF NOEMA RECEIVER PARTS

As part of the NOEMA project, the drawing office has conducted the complete design of the receiver using the SolidWorks software package; in total several hundreds of different references have been integrated.

The workshop mainly worked on the manufacture of NOEMA high added value components; in particular, 28 mixers each for bands 1, 2 and 3, i.e. a total of 84 mixers were produced. The horns and the complete optical modules were machined in the workshop as well.

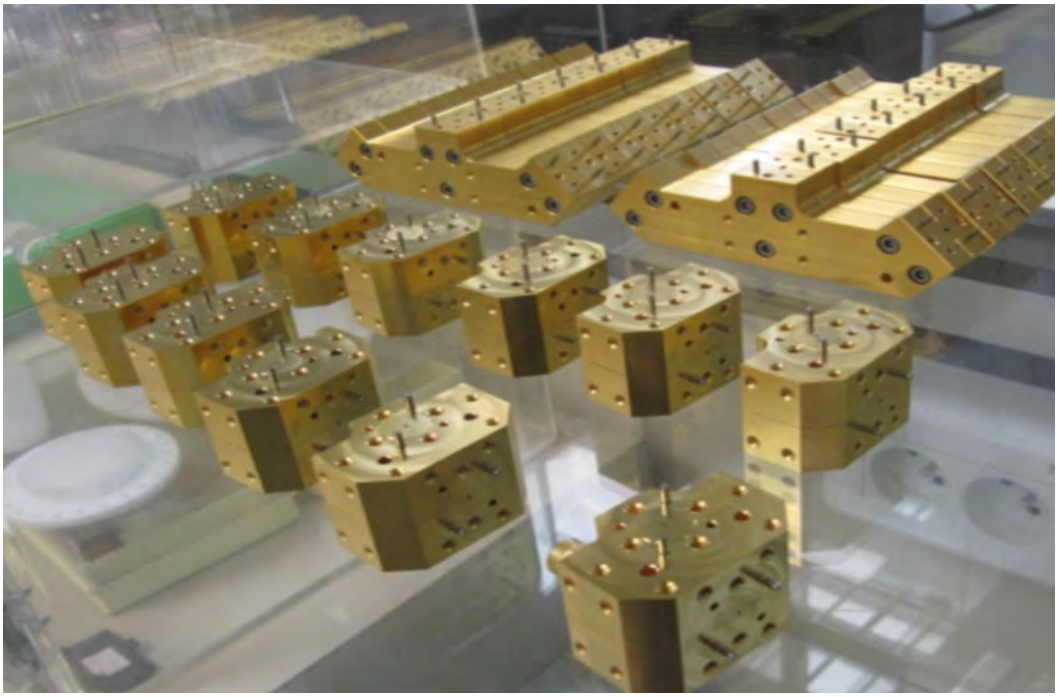

Mass production of a batch of mixers and band 1 splitters.

Computer group

UPGRADES

In 2014, some IRAM file servers needed to be replaced (two Netapp FAS 270, installed in 2004 and in 2007 respectively). Also maintenance was not available for them anymore. Nevertheless, these storage systems are very crucial for IRAM operations because they host all users data and application databases. Therefore, the Computer Group has decided to replace these file servers with newer ones. The new models are two Netapp FAS2240 with 10 GbE interfaces and redundant controllers. The first one has been installed with a 40 TB initial capacity at IRAM headquarters, the second has been installed with a 20 TB initial capacity at the NOEMA observatory.

In the same spirit, the main computers of the NOEMA observatory have been upgraded to two DELL PowerEdge R620 servers with 64 GB of RAM and 10-core Intel Xeon processors. These new computers will host the observation and the commissioning operations for the next coming years. At the headquarters, the migration to newer operating systems (Windows 7 and Scientific Linux 6.4) has been completed, and important software packages have been upgraded to their latest versions, including Solidworks (mechanical CAD software) and LabVIEW. All the Windows servers have been migrated to Windows Server 2012. The new servers are virtual and are hosted by the Citrix XenServer 6.2 platform which was introduced in 2013.

NOEMA

At the NOEMA observatory, a new 150 Mbps wireless network link has been established between the upper and lower cable car stations during the summer period. This new network link will be in commissioning during the next winter to check if it withstands extreme weather conditions. When the results are satisfactory, the wireless link will be used for communication between the cable car stations, being independent on external networks.

The new WIFI antenna near the NOEMA lower cable car station.

The Computer Group has delivered a new alarm monitoring system to replace the old one which has become obsolete. Unlike the old system, which used many proprietary programs (in particular LabVIEW for Windows), the new system uses only open-source software (C++/Qt) and runs on Linux.

The group has also delivered a new control software for the NOEMA receiver. This is a major improvement of the current receiver control software. In particular, a hardware abstract layer (HAL) was implemented to make t evolution of the receiver control software easier

The computer group has also delivered the antenna control software for antenna 7 that regulates the antenna's motions. The software has some new features like an EtherCAT field bus and digital-only servo loops.

SCIENCE SOFTWARE ACTIVITIES

The main goal of the science software activities at IRAM is to support the preparation, the acquisition and the reduction of observational data both at the 30-meter telescope and NOEMA. This includes the delivery of 1) software to the community for proposing and setting up observations, 2) software to the IRAM staff for use in the online acquisition system, and 3) offline software to end users for the final reduction and analysis of their data. However, the GILDAS suite of software is freely available to, and used by other radio telescopes, like Herschel/HIFI, APEX, SOFIA/GREAT, and the YEBES 45m telescope. Specific efforts are also made to include imaging and deconvolution capabilities for ALMA data inside GILDAS.

Work continued to pave the way towards a full integration of NIKA-2 in the control system of the 30-meter telescope. The new dual-band bolometer camera is planned to become operational at the end of 2015. To facilitate easier handling of spectroscopic observations, work continued on MRTCAL, the new calibration software that will progressively replace MIRA. In 2014, efforts were mainly devoted to ensure the robustness of the software in the quasi real time use at the telescope. In addition to testing new calibration methods, this software was designed to ensure efficient data processing in preparation of the future 3mm and 1mm multibeam receivers. CLASS will still handle the offline spectroscopic data reduction and analysis (e.g., baselining, gridding). Many minor but useful improvements, like the possibility to add comments to observations, were thus implemented in CLASS. Moreover, support for third-party telescopes was continued in CLASS. In particular, following a request from the Herschel community, CNES funded an IRAM project to support the archival science data format of the HIFI instrument. This development, made in collaboration with the ESA Herschel Science Center in Madrid and with IRAP in Toulouse, was started in autumn 2014 and is scheduled for delivery in mid-2015. Finally, to take advantage of the 39.4 GHz beacon of the ESA Alphasat communication satellite launched in July 2013, efforts were also made to reinstate the software for the acquisition and analysis of holographic data at the 30-meter telescope.

In the NOEMA project, the 7th antenna of the interferometer was inaugurated end of September 2014. The advent of a new antenna, 13 years after the last one was built, implied the adjustment of many hardware and software components. The hardware changes that required software modifications included, among others, the new drive control system of the subreflector, a full new set of receivers at 3, 2, 1, and 0.8 mm, and the replacement of the online computers, including new versions of their operating systems. While the WIDEX correlator was already able to process up to 8 antennas simultaneously, the possibility to correlate the signals of more than 6 antennas was first tested in 2014. In the same line of work, it also became necessary to adjust the code to match the processor performance and define a new set of Walsh switching functions for the correlator. In addition, new control commands were added to facilitate the commissioning of the new antenna, e.g., to test the antenna tracking performance. With the advent of the 7th antenna, the PdBI observatory officially became the NOEMA observatory, implying many small changes in the software and its documentation. In order to obtain a minimum of backward compatibility, it was decided to keep the PdBI name in memos older than 2014, and in the software to handle and keep trace of the pre-NOEMA hardware configurations. Finally, software development work started for POLYFIX, NOEMA's wide bandwidth correlator with flexible high-spectral resolution capabilities, with the programming of the data-readout card designed at IRAM. This card controls the high-speed optical link between the POLYFIX digital unit and its associated computer. The required data transfer rate of 1.4 Gbit per second was successfully achieved.

At the same time, support for standard science operations continued at the interferometer. For instance, the nomenclature for project names, which changed in spring 2014, implied many changes in the acquisition and data reduction software. Standard science operations also implied several improvements in the calibration pipeline: 1) the flux monitoring, using LkHa101 as a primary flux calibrator in addition to MWC349, was fine-tuned, 2) the detection of parasites in the bandpass calibration was further improved, and 3) the bandpass solution was optimized for the current high spectral resolution narrow-band correlator. Developments in the pipeline had to be stepped up, and regular pipeline maintenance work to meet users' needs and keep the pipeline running was found to be quite time consuming. The tuning of the calibration algorithms being extremely instrument specific, the instrument team recommended to calibrate the interferometer data using the software specifically developed for the instrument. On the other hand, imaging and deconvolution of interferometric data is mostly independent of the instrument. In this frame, ALMA broadband (8 GHz per polarization) high-spectral resolution data triggered a series of

changes in MAPPING, the GILDAS imaging and deconvolution software. In particular, a project was started in 2014 to refurbish the way the software deals with 1) the Doppler corrections due to Earths daily and yearly movements and 2) the variation of the dirty beam (and other quantities) with frequency. This work, which is conducted in collaboration with the Observatoire de Bordeaux, paves the path to the unprecedented wide bandwidth (16 GHz per polarization) high-spectral resolution capabilities of the future NOEMA correlator.

In the years to come, the observation of IRAM projects with both the interferometer and the 30-meter telescope will lead to an increase of data rates by one to two orders of magnitudes. This implied a review of the different limitations of the raw data formats. These data formats, i.e., the CLASS and CLIC data formats, share the same data binary container (the way the bits are ordered, independent of their scientific value), even though the semantics of both data formats are very different due to the specific characteristics of the single-dish and interferometry observing techniques. It was thus decided at the end of 2012 to create a new library, named CLASSIC, which factorizes the code, as this will decrease maintenance efforts in the medium term. As part of this work, all known limitations (e.g., the size of the dataset was limited to 1TB) were waived in 2013. Fine tuning and implementation of these new formats took place in mid-2014.

All software developments are based on the common GILDAS services, e.g., a set of common low-level libraries, collectively named GILDAS kernel, which handle the scripting and plotting capabilities of GILDAS. After many efforts to comply with the newest standards, e.g., the version 3.0 of the Python language and extensive tests of recent versions of the free GFORTRAN compiler, software code associated to obsolete standards or computer systems was cleaned. In particular, HPUX, OSF, Solaris, SunOS, Alpha, VMS, ULTRIX are officially not supported anymore. A new language, named LINEDB, generalized the interface to the JPL and CDMS online databases, previously introduced in the WEEDS extension of CLASS. This is the first step to facilitate line assignations everywhere in GILDAS.

Finally, PMS (Proposal Management System) fully replaced the old proposal submission and processing facility for the IRAM 30-meter telescope and the NOEMA interferometer starting with the summer deadline of 2014 (i.e., mid-March 2014). In the course of this action, the online time estimators for both observatories were upgraded to follow the latest hardware changes.

IRAM ARC node

Photo: Masaaki Hiramatsu, National Astronomical Observatory of Japan

IRAM is a node of the European ALMA Regional Center (ARC), the structure responsible for the ALMA science operations in Europe. The nodes are more specifically in charge of providing user support to the community. IRAM's involvement in the ARC is part of a long-term, global involvement in the design, construction, and operation of ALMA. One of the goals of the IRAM ARC node is to provide to the astronomical community a common support for the IRAM and ALMA facilities, hence maximizing the scientific synergies between the observatories.

ALMA USERS SUPPORT

The main tasks of the IRAM ARC node in 2014 were:

- Cycle 1 & Cycle 2 contact scientists: the ARC node staff act as "Contact Scientists" for the accepted ALMA projects, providing help and expertise to check and validate the Scheduling Blocks that are created from the initial proposals. The IRAM ARC node supported more than 35% of all accepted+filler projects in Europe.
- Data quality assurance: IRAM is providing help to assess the quality of the datasets observed by ALMA. This implies calibration and imaging of the data, in order to check that the final data quality (in particular the noise rms) matches the initial requests from the proposal.
- Face-to-face support for data reduction: users can obtain direct help for the data reduction, in a way similar to the support provided for the Plateau de Bure (and now NOEMA) projects. Data fillers to transfer calibrated data from/to CASA to/from GILDAS were developed, allowing the data to be imaged in both software environments.

TELESCOPE CALIBRATION SOFTWARE

IRAM is responsible for the development and maintenance of one of the key software for the real-time operations of ALMA, the Telescope Calibration (TelCal) software. TelCal is performing all real-time calibrations necessary to run the array. 2014 showed a continuous improvement of the TelCal capabilities, culminating with the long-baselines campaign during the fall. Observations with >10 km baselines were performed during that campaign, giving spectacular results that were widely advertised. The IRAM TelCal team was directly involved in these observations in Chile, as several of the TelCal processing tools (e.g. atmospheric phase correction) are instrumental to allow the longest baselines to be used.

Administration

ADMINISTRATION 2014

During 2014 the administration management system was updated to standardize the tools at the french and spanish IRAM locations. The multitude of software packages was replaced by one single tool from SAGE, which meets European management standards. By 2015/2016, a real mini ERP (Enterprise Resource Planning) will be at IRAM's disposal – at a reasonable and manageable investment cost. This tool will enable a better and more coherent collaboration between the French and Spanish administrative teams from 2015 on. The treatment of information will therefore be possible almost in real time, regardless of the management site.

FINANCIAL RESULTS

IRAM's budget for 2014 are close to balanced. The overall operating budget of 11.5M€ was only exceeded by 25k€. This is remarkable in the context of the very intense activity around NOEMA and also a result of the very tight cost controlling put in place during the last years.

K€	Operations	Investment
Total Income	12 099	22 863
Total Expense	12 124	10 411
2014 Result	-25	12 452

HUMAN RESOURCES

In 2014, total number of employees, staff positions of the equivalent of 116 full-time employees (FTE) were filled by IRAM, 88 FTE in France and 28 in Spain. The age distribution among the staff improved. Two thirds of the employees are between 35 years and 55 years of age, whereas the employees below 35 years of age represent roughly 20% of the staff. This balance of ages allows to conserve the expertise IRAM is known for and to ensure the transfer of knowledge among the generations of employees at IRAM.

IRAM STAFF LIST 2014

Group	NAME Surname	Position
IRAM Headquarter, Grenoble, France		
DIRECTION	SCHUSTER Karl-Friedrich	Director
	GUETH Frédéric	Deputy Director
	DELLA BOSCA Paolo	
	GUELIN Michel	
	ZACHER Karin	
ADMINISTRATION FRANCE	DELAUNAY Isabelle	Head of Administration
	BACHET Claude	
	COHEN BOULAKIA Sandrine	
	DAMPNE Maryline	
	FERREIRA Dina	
	INDIGO Brigitte	
	MAIRE Béatrice	
	MARCOUX Stéphane	
	PALARIC Laurent	
	SIMONE Jeannine	
	ZERROUKHI Akila	
MECHANICAL WORKSHOP AND DRAWING OFFICE	LEFRANC Bastien	Head of the Mechanical Group
	COPE Florence	
	COUTANSON Laurent	
	DANNEEL Jean-Marc	
	JUBARD Vincent	
	ORECCHIA Jean-Louis	
BACKEND GROUP	GENTAZ Olivier	Head of the Backend Group
	TORRES Marc	Head of the Backend Group until January 31, 2014
	BALDINO Maryse	
	CHAVATTE Philippe	
	GARCIA GARCIA Roberto	
	GEOFFROY Daniel	
	MAYVIAL Jean-Yves	
COMPUTER GROUP	BLANCHET Sébastien	Head of the Computer Group
	CHALAIN Julien	
	DUMONTROTY Patrick	
	REYGAZA Mickaël	
FRONTEND GROUP	NAVARRINI Alessandro	Head of the Frontend Group
	ADANE Amar	
	BERTON Marylène	
	BORTOLOTTI Yves	
	BUTIN Gilles	
	CHENU Jean-Yves	
	COQ Fabrice	
	FONTANA Anne-Laure	
	GARNIER Olivier	
	LECLERCQ Samuel	
	MAHIEU Sylvain	
	MAIER Doris	
	MATTIOCCO François	
	MOUTOTE Quentin	
	PARIOLEAU Magali	
	PERRIN Guillaume	
	PISSARD Bruno	
	REVERDY Julien	
	SERRES Patrice	
ASTRONOMY & SCIENCE SUPPORT GROUP	NERI Roberto	Head of the Astronomy & Science Support Group
	BARDEAU Sébastien	
	BERJAUD Catherine	
	BOISSIER Jérémie	
	BREMER Michael	
	BROGUIERE Dominique	
	CASTRO CARRIZO Aranzazu	
	CHAPILLON Edwige	
	DOWNES Wilfriede	
	DUMAS Gaëlle	
	FERUGLIO Chiara	
	KRIPS Melanie	
	KÖNIG Sabine	
	MARTIN RUIZ Sergio	
	MONTARGES Miguel	
	PETY Jérôme	
	PIETU Vincent	
	REYNIER Emmanuel	
	ROCHE Jean-Christophe	
	VAN DER LAAN Tessel	
	WINTERS Jan-Martin	
	ZYLKA Robert	

Group	NAME Surname	Position
SIS GROUP	SCHUSTER Karl-Friedrich	Interim Head of the SIS Group
	BARBIER Arnaud	
	BILLON-PIERRON Dominique	
	COIFFARD Grégoire	
	HALLEGUEN Sylvie	
	HAMELIN Catherine	
NOEMA Plateau de Bure, France		
NOEMA, PLATEAU DE BURE	GAUTIER Bertrand	Station Manager
	AZPEITIA Jean-Jacques	
	BARD Florentin	
	CASALI Julien	
	CAYOL Alain	
	CHAUDET Patrick	
	CONVERS Bruno	
	DAN Michel	
	DI LEONE SANTULLO Cécile	
	GROSZ Alain	
	KINTZ Philippe	
	LAPEYRE Laurent	
	LEONARDON Sophie	
	MASNADA Lilian	
	MOURIER Yvan	
	RAMBAUD André	
	SALGADO Emmanuel	
IRAM 30-meter telescope, Granada, Spain		
IRAM 30-meter telescope, GRANADA	KRAMER Carsten	Station Manager
	PENALVER Juan	Deputy Station Manager
	BILLOT Nicolas	
	BRUNSWIG Walter	
	DAMOUR Frederic	
	ESPANA Gloria	
	FRANZIN Esther	
	GALVEZ Gregorio	
	GARCIA José	
	GONZALEZ Manuel	
	HERMELO Israel	
	JOHN David	
	LARA Maria	
	LOBATO Enrique	
	LOBATO Javier	
	MELLADO Pablo	
	MENDEZ Isabel	
	MORENO Maria	
	MUNOZ GONZALEZ Miguel	
	NAVARRO Santiago	
	PAUBERT Gabriel	
	PEULA Victor	
	RUIZ Carmen	
	RUIZ Ignacio	
	RUIZ Manuel	
	SANCHEZ Salvador	
	SANCHEZ Rosa	
	SANTAREN Juan Luis	
	SANTIAGO Joaquin	
	SERRANO David	
	SIEVERS Albrecht	
	THUM Clemens	
	TREVINO Sandra	
	UNGERECHTS Hans	

Annex I – Telescope schedules

30-METER TELESCOPE

Ident.	Title of investigations	Authors
114-13	Fire and Ice in comet C/2012 S1 (ISON): phase 3	Biver, Bockelée-Morvan, Moreno, Debout, Colom, Crovisier, Yvart, Lis, Boissier, Paubert, Weaver, Russo, Vervack, Kawakita
115-13	The (sub)millimeter energy distribution of Comet C/2012 S1 (ISON)	Sievers, Altenhoff, Menten, Thum
117-13	Observation of an equatorial jet in the atmosphere of Jupiter	Cavalié, Hue, Billebaud, Dobrijevic, Hersant, Spiga, Guerlet
118-13	Pluto's thermal emission at radio-wavelengths	Lellouch, Moreno
120-13	Measuring the deuterium fractionation of water in a WCCC source	Coutens, Rgensen, Kristensen, Persson, Sakai, Vastel, Yamamoto
121-13	A Study of the Deuterated Ammonium ion in Prototypical Cold Cores	Cernicharo, Roueff, Marcelino, Tercero, Fuente, Gerin, Tanarro, Domenech, Herrero, Cueto
122-13	Deuterium chemistry in dark clouds: detection of l-C_3HD in TMC-1C	Spezzano, Schlemmer, Brünken, Caselli, Mccarthy, Müller, Schilke, Menten, Gottlieb, Bizzocchi
126-13	H_2CO and CH_3OH depletion in prestellar and protostellar cores	Guzmán, Øberg, Pety, Gerin, Goicoechea, Kønyves, André, Palmeirim, Roueff, Le Petit
128-13	Mapping complex organic molecules in pre-stellar cores	Bacmann, Taquet, Faure
129-13	Formation of COMs during the early stages of high-mass star formation	Vasyunina, Herbst, Øberg, Hincelin, Commerçon, Beuther, Linz
130-13	Sulphur-bearing interstellar hydrides: a probe of warm chemistry in diffuse clouds	Neufeld, Gerin, Falgarone, Godard
132-13	Monitoring the Encounter of a Gas Cloud with Sgr A*	Agudo, Thum, Wiesemeyer, Sievers, Gómez, Casadio, Molina
133-13	Non-Zeeman Circular Polarization of CO lines in rho Ophiuchus A	Houde, Hezareh, Jones, Chapman, Novak, Paubert
134-13	Non-Zeeman Circular Polarization of CO Spectral lines in W44	Hezareh, Wiesemeyer, Houde, Gusdorf
136-13	Is the Dust in OMC 2/3 Anomalous?	Sadavoy, Schnee, di Francesco, Friesen, Mason, Stanke
137-13	A high angular resolution view of the Orion Bar PDR at 0.9 mm	Goicoechea, Cuadrado, Dumas, Pety, Cernicharo, Fuente
138-13	The IRAM 30-m line survey of Orion KL: 2 and 0.9 mm	Tercero, Cernicharo, López, Bañó, Bell, Carvajal, Margulès, Haykal, Motiyenko, Huet, Kleiner, Coudert, Guillemin, Alonso, Cabezas, Kolesniková, Marcelino
140-13	Large scale mapping of the ionized gas content of Sagittarius B2	Schmiedeke, Schilke, Lis, Jimenez-Serra, Martín, Mills
142-13	Measuring the gas-phase C/O abundance ratio in dark clouds	Le Gal, Hily-Blant, Faure, Pineau des Forêts, Walmsley
143-13	Converging flows in the Infrared Dark Cloud G14.225-0.506	Busquet, Palau, Zhang, Frau, Estalella, de Gregorio-Monsalvo, Girart, Ho, Liu, Pillai, Sánchez-Monge, Wyrowski, Franco, Santos
144-13	Using kinematics to disentangle the structure of the «simplest» IRDC	Frau, Tafalla, Hacar
145-13	Observing Orion's Ferment: HEFE (Heterodyne Exploration of Filament Evolution)	Megeath, Stutz, Wyrowski, Billot, Fischer, Furlan, Heitsch, Henning, Menten, Osorio, Smith, Stanke, Tobin
146-13	Probing the inner structure of the Taurus main filament (NIKA guaranteed time proposal)	André, Palmeirim, Roy, Peretto, Désert, Hily-Blant, Bacmann, Billot, Adam, Adane, Ade, Beelen, Belier, Benoit, Bideaud, Bourrion, Calvo, Catalano, Coiffard, Comis, D'addabbo, Doyle, Goupy, Kramer, Leclercq, Martino, Mauskopf, Mayet, Monfardini, Pajot, Pascale, Perotto, Pointecouteau, Ponthieu, Revéret, Rodriguez, Savini, Sievers, Tucker, Zylka
147-13	Probing the formation of filamentary and clumpy structures in the Polaris flare	Arzoumanian, Boulanger, Falgarone, Alves, Hennebelle, Bracco
149-13	Unbiased spectral survey of CygX-N63 a unique pre-hot core source	Bontemps, Fechtenbaum, Csengeri, Lefloch, Herpin, Duarte-Cabral, Hennemann, Schneider, Motte, Gusdorf, Wakelam, Hersant
150-13	Are chains the natural environment of dense cores?	Tafalla, Hacar, Frau
151-13	Unveiling dust evolution and deuteration across pre-stellar cores	Bizzocchi, Caselli
152-13	CO and N2 depletion and the age of dark cloud cores	Pagani, Cuillandre, Dulieu, Lesaffre, Lefèvre, Parise
156-13	Searching for pre-brown dwarfs in the rho Oph protocluster	André, Greaves, Ward-Thompson, Kønyves, Palmeirim, Billot
157-13	A turbulent shock origin for the pre-brown dwarf core Oph B-11?	André, Greaves, Ward-Thompson, Kønyves, Palmeirim, Lesaffre

Ident.	Title of investigations	Authors
160-13	Mapping protostellar outflows in NGC 1333 - the overlooked ones	Weiss, Stecklum, Beuther, Caratti O Garatti
161-13	Probing converging flows with SiO emission: the W43-MM1 ridge	Louvet, Gusdorf, Lesaffre, Schilke, Carlhoff, Motte, Nguyen-Luong
162-13	Searching for hidden outflow jets with SiO	Tafalla, Bachiller, Lefloch, Rodríguez-Fernández, Codella, López-Sepulcre, Gomez-Ruiz
163-13	Short spacing CO data for SMA observations of the S255 outflow	Zinchenko, Liu, Su, Trofimova, Zemlyanukha
164-13	A search of the methoxy radical (CH3O) in low-mass star forming regions	Marcelino, Cernicharo, Roueff, Gerin, Fuente, Muñoz-Caro, Jiménez-Escobar
165-13	Investigating the triggered sequential star formation in S235 complex	Wang, Beuther, Gong, Audard, Fontani
166-13	A new Class 0 object in IC1396A: Multi-episodic star formation?	Sicilia-Aguilar, Roccatagliata, Fang, Getman, Eiroa
167-13	Molecular clumps triggered by the infrared dust bubble N131	Zhang, Wang
170-13	Characterizing the first O-type `swollen star' candidate	Palau, Sánchez-Monge, Girart
171-13	Chemical study of the flat disk around the B0 star R Mon	Fuente, Trevi No, González-García, Bachiller, Cernicharo
172-13	Search for molecular gas in young debris disks	Moór, Ábrahám, Csengeri, Kóspál
173-13	Modeling the azimuthal structures of the debris disk around epsilon Eri	Lestrade, Etienne, Jean-Charles, S, David, C
174-13	An atypical case for planetesimal stirring?	Moór, Ábrahám, Csengeri, Kóspál
175-13	A Line Survey of the Supergiant O-rich star VY CMa. III	Quintana-Lacaci, Cernicharo, Contreras, Velilla, Bujarrabal, Marcelino, Alcolea, Santander, Pearson, Teyssier
176-13	Unveiling the rich chemistry of yellow hypergiant stars: IRC +10420	Quintana-Lacaci, Cernicharo, Bujarrabal, Castro-Carrizo, Contreras, Alcolea
182-13	Dense Molecular Gas in the Wind of NGC 253	Bolatto, Walter, Leroy, Warren, Zschaechner
183-13	Dense Gas in the HerCULES Sample	Weiss, van der Werf, Rosenberg, Greve, Downes, Papadopoulos, Walter, Aalto
185-13	Calibrating molecular metallicity diagnostics with CS/HCN in M101	Davis, Bayet, Martín
186-13	Water in nearby active galaxies: thermal or maser emission?	Krips, Aladro, Dumas, Feruglio, Koenig, Van Der Laan, Martín, Neri
189-13	Molecular abundances in GMCs across the galaxy M 31	Dumas, Martín, Hily-Blant, Lefloch, Ceccarelli, López-Sepulcre, Aladro
190-13	Determining the Resolved Star Formation Rate in NGC 6946	Eufrasio, Arendt, Dwek, Staguhn
191-13	Determining the Resolved Star Formation Rate in Messier 51	Eufrasio, Arendt, Dwek, Staguhn
192-13	Constraining the dust excess emission in Herschel dwarf galaxies with GISMO	Albrecht, Rémy-Ruyer, Madden, Bertoldi
193-13	The dust SED of dwarf galaxies: NGC1569 and NGC4449	Hermelo, Verley
194-13	CO-dark H_2 gas in the southern spiral arm of M33	Kramer, Buchbender, Gratier, Braine, García-Burillo, Israel, Mookerjea, Nikola, Stacey, Røllig, Stutzki, Combes
195-13	Star formation traced by CO in ram pressure tails: the Virgo cluster.	Verdugo, Combes, Dasyra, Salomé
196-13	HERA CO Mapping of Virgo Spiral Galaxies	Schruba, Walter, Leroy, Sandstrom, Kramer, Usero, Hughes, Zschaechner
197-13	The molecular gas mass in the dwarf elliptical NGC 205	Israel, Buchbender, Meijerink
198-13	A Complete and Deep CO Map of the Nearest Dwarf Starburst	Leroy, Walter, Schruba, Sandstrom, Krips, Kramer, Hughes, Gratier, Meyer, Bolatto
200-13	Search for extra planar cold molecular gas in nearby edge-on galaxies	Dumas, Pety, Schuster, García-Burillo, Usero, Gratier, Kramer, Schinnerer, Meidt, Hugues, Zschaechner, Lisenfeld, Leroy
205-13	The Role of Molecular Gas in Galaxy Disk Growth and Evolution	Cormier, Bigiel, Usero, Pety, Kauffmann, González-García, Saintonge, Huang, Wang, Józsa, Carton, Brinchmann
208-13	What causes the sSFR in local galaxies: Is it only gas content?	Lehnert, Driel
210-13	Probing the conditions for star formation in nearby luminous QSOs	Husemann, Davis, Dannerbauer, Jahnke, Hodge, Urrutia, Wisotzki
211-13	Positive feedback II: A pilot search of CO in 3C 285	Salomé, Combes, Salomé
214-13	Molecular gas in nuclear dust lanes; target selection for black-hole mass measurements	Davis, Bureau, Cappellari, Sarzi, Blitz
220-13	MAPI: Monitoring AGN with Polarimetry at the IRAM-30 m	Agudo, Thum, Gómez, Casadio, Molina, Marscher, Jorstad, Wiesemeyer
221-13	Coordinated cm to mm monitoring of variability and spectral evolution of a selected Fermi blazar sample	Fuhrmann, Zensus, Karamanavis, Myserlis, Angelakis, Krichbaum, Ungerechts, Sievers, Readhead

Ident.	Title of investigations	Authors
222-13	Molecular Gas Observations of Luminous Infrared Galaxies in the Great Observatories All-sky LIRG Survey (GOALS)	Iwasawa, Evans, Aalto, Frayer, Perez-Torres, Herrero-Illana, Surace, Privon, Kim, Mazzarella, Armus
223-13	An EMIR line survey of Planck/Herschel lenses	Nesvadba, Canameras, Boone, Boulanger, Beelen, Dicken, Dole, Flores-Cacho, Frye, Guery, Guillard, Koenig, Krips, Le Floc'h, Lehnert, Mackenzie, Malhotra, Montier, Omont, Rhoads, Scott
224-13	μ-variation from methanol in PKS1830-211; systematic effects	Ubachs, Bagdonaite, Dapra, Bethlem
226-13	Searching for the bright reverse shock emission in GRBs	Castro-Tirado, Kramer, Bremer, Winters, Gorosabel, Jeong, Pérez-Ramírez, Castro Cerón, Jelinek, Tello
227-13	Candidate Lensed Sub-millimeter Galaxies from ACT	Gralla, Staguhn, Marriage, Su, Baker, Marsden
230-13	Star Formation in High Redshift Lensed Quasar Host Galaxies	Wang, Bertoldi, Fan, Carilli, Walter, Strauss, Riechers
231-13	Identifying high-*z* single-halo proto-clusters of H-ATLAS submm galaxies	Omont, Clements, Ivison, Lehnert, Bremer, Dannerbauer, Beelen, van der Werf, Yang, Bertoldi, Bussmann, Dunne, Eales, Ibar, Michalowski, Smith, Serjeant, Temi, Verma, Adam, Adane, Ade, André, Belier, Benoit, Bideaud, Billot, Bourrion, Calvo, Catalano, Coiffard, Comis, D'addabbo, Désert, Doyle, Goupy, Kramer, Leclercq, Martino, Mauskopf, Mayet, Monfardini, Pajot, Pascale, Perotto, Pointecouteau, Ponthieu, Revéret, Rodriguez, Savini, Sievers, Tucker, Zylka
232-13	Confirming $z \geq 2$ cluster candidates observed by Planck and Herschel (NIKA guaranteed time proposal)	Macías-Pérez, Dole, Adam, Adane, Ade, André, Beelen, Belier, Benoit, Bideaud, Billot, Bourrion, Calvo, Catalano, Coiffard, Comis, D'addabbo, Désert, Doyle, Goupy, Kramer, Leclercq, Martino, Mauskopf, Mayet, Monfardini, Pajot, Pascale, Perotto, Pointecouteau, Ponthieu, Revéret, Rodriguez, Savini, Schuster, Sievers, Tucker, Zylka, Nesvadba, Kønig, Chary, Flores-Cacho, Frye, Giard, (phd), Kneissl, Lagache, Le Floc'h, (phd), Montier, Puget, Scott, Yan
233-13	Unveiling the most distant star forming galaxies behind clusters with GISMO	Aravena, Gonzalez, Staguhn, Anguita, Infante, Postman, Bauer
234-13	Dust content in a merger of two very-high-mass galaxies at z~3.2	Béthermin, Ciesla, Heinis, Sargent, Burgarella, Ponthieu, Désert
235-13	A Rogue's Gallery of Massive Merging High Redshift Clusters	Mroczkowski, Kovács, Weeren, Clarke, Benford, Staguhn
237-13	Thermal Sunyaev-Zel'dovich mapping of high redshift galaxy clusters (NIKA guaranteed time proposal)	Comis, Adam, Adane, Ade, André, Beelen, Belier, Benoit, Bideaud, Billot, Bourrion, Calvo, Catalano, Coiffard, D'addabbo, Désert, Doyle, Goupy, Kramer, Leclercq, Macías-Pérez, Martino, Mauskopf, Mayet, Monfardini, Pajot, Pascale, Perotto, Pointecouteau, Ponthieu, Revéret, Rodriguez, Savini, Schuster, Sievers, Tucker, Zylka
239-13	Dust Continuum Emission in the Most Luminous Z~3 Lyman Break Galaxy	Bian, Fan, Wang, Walter, Mcgreer, Green
240-13	The space density and environments of z>4 ultra-red Herschel SMGs	Pérez-Fournon, Ivison, Omont, Conley, Riechers, Clements, Bertoldi, Dannerbauer, Cooray, Wardlow, Calanog, Martinez-Navalas, Streblyanska, Laporte, Eales, Valiante, Oliver
242-13	COSMO Part III: The synergetic GISMO survey in the COSMOS field	Staguhn, Karim, Schinnerer, Smolvcic, Bertoldi, Aravena, Smail, Benford, Kovács, Swinbank, Dwek, Su
246-13	A Project for the Master2 in Astrophysics in Grenoble: Probing Shocks in L1157	Lefloch
252-13	A complete homogeneous CO survey of northern FU Ori-type objects	Kóspál, Ábrahám, Hogerheijde, Brinch
D01-13	Surprisingly overluminous ^{13}CO in hot LIRGs (DDT Proposal)	Herrero-Illana, Evans, Pérez-Torres, Aalto, Alberdi, Frayer, Surace, Privon, Kim, Mazzarella, Armus, Spoon
D03-13	A study of prestellar cores in Planck cold clumps	Wu, Liu, Yuan, Meng, Belloche, Henkel, Menten
D04-13	Paris M2 AAIS survey of M82	Le Bourlot, Lefevre
D08-13	Flare of the masing water lines in W49N	Menten, Kramer, Kraus, Kaminski
003-14	A census of complex organic molecules around low-mass embedded protostars	Oberg, Graninger, Garrod
005-14	H_2CO and CH_3OH chemistry in prestellar and protostellar cores	Guzman Veloso, Oberg, Pety, Gerin, Goicoechea, Konyves, Andre, Palmeirim, Roueff, Le Petit
006-14	HCO as a precursor of glycolaldehyde	Beltran, Codella, Fontani, Woods, Viti, Cesaroni, Caselli, Vasyunin
007-14	A search for the simplest isocyanide, CH_3NC	Gerin, Cernicharo, Goicoechea, Pety, Gratier, Guzman Veloso, Roueff, Le Petit, Wiedner, Laurent, Guillemin, Cuadrado
011-14	Looking for CH_2D^+ in the PDR around the UCHII region Mon R2	Trevino-Morales, Fuente, Roueff, Gonzalez-Garcia, Pilleri, Goicoechea, Kramer, Sanchez-Monge, Gerin, Pety, Cernicharo
012-14	A 3 mm Survey of PDRs and Complex Molecular Sources for $l\text{-}C_3H^+$	McGuire, Brandon Carroll, Guzman Veloso, Gratier, Roueff, Gerin, Goicoechea, Blake, Remijan, Pety
013-14	Testing the anion time-dependent chemistry in IRC+10216: radical and anion short spacing observations	Guelin, Cernicharo, Agundez, Winters
014-14	Testing variations of the proton-to-electron mass ratio in the Milky Way	Henkel, Levshakov, Ubachs, Lapinov, Paubert, Muller, Menten, Gong, Leurini, Kozlov, Bethlem
015-14	The Origin of ^{15}N and Galactic C_2H Carbon Isotope Ratios	Henkel, Martin Ruiz, Aalto, Asiri, Harada, Aladro, Gong
016-14	Molecular gas in a high-latitude intermediate-velocity cloud	Kerp, Rohser, Schilke, Pineda
021-14	Unbiased spectral survey of NGC 7023, a mild-UV illuminated PDR	Pilleri, Joblin, Gerin, Fuente, Gonzalez-Garcia, Pety, Goicoechea, Berne

Ident.	Title of investigations	Authors
022-14	The Anatomy of the Orion B Giant Molecular Cloud	Pety, Guzman Veloso, Gratier, Tremblin, Goicoechea, Gerin, Bardeau, Sievers, Liszt, Lucas, Oberg, Peretto
024-14	Understanding molecular globules around massive young runaway stars	Gratier, Pety, Boisse, Cabrit, Gerin, Lesaffre, Pineau des Forets, Witt
026-14	Flow-driven formation of molecular cloud filaments: A kinematic study of the dense gas in IRDCs	Henshaw, Jimenez-Serra, Caselli, Fontani, Tan, Pon, Barnes
027-14	Infall and outflow in a filamentary hub	Fuente, Trevino-Morales, Cernicharo, Didelon, Gonzalez-Garcia, Kramer, Motte, Pilleri, Rayner, Sanchez-Monge, Schneider, Tremblin
029-14	Observing Orion's Ferment: HEFE (Heterodyne Exploration of Filament Evolution)	Stutz, Megeath, Billot, Wyrowski, Henning, Menten, Fischer, Heitsch, Osorio, Smith, Stanke, Tobin, Abreu-Vicente
032-14	Deuterium Fraction in the Taurus Molecular Cloud Complex	Punanova, Caselli, Pon
033-14	Understanding the L1544 cloud	Tafalla, Hacar, Frau
036-14	Chemistry in the earliest phase of high-mass star formation: SMA & 30-meter telescope in concert	Feng, Beuther, Zhang, Henning, Ragan, Linz, Smith
039-14	CO and N_2 depletion and the age of dark cloud cores	Pagani, Cuillandre, Dulieu, Lesaffre, Lefevre, Parise, Bonnin
040-14	Characterization of the hot molecular core phase	Sanchez-Monge, Schilke, Beltran, Busquet, Cesaroni, Choudhury, Comito, Kurtz, Palau, Schmiedeke, Zernickel
042-14	Following the Trail of Organic Nitrogen in Star-Formation: the Pre-Stellar Stage	Bergin, Maret, Hily-Blant, Faure, Rice
043-14	Disentangling the dominant dynamics in a contracting core	Frau, Girart, Juarez, Galli, Beltran, Alves, Franco, Tafalla, Morata, Palau
044-14	Linking velocity And Magnetic-B field Analyses from Disks to Associated clouds (LAMBADA)	Yen, Tang, Koch, Takakuwa, Guilloteau, Tomisaka, Machida
046-14	A turbulent shock origin for the pre-brown dwarf Oph B-11?	Andre, Konyves, Lesaffre, Ladjelate
051-14	Studying the Outflow (Jet) Properties in IRAS 16253-2429	Hsieh, Lai, Wyrowski, Belloche
052-14	Spatial distribution and physical properties of a low-mass protostellar outflow	Taquet, Lopez-Sepulcre, Ceccarelli, Lefloch, Charnley, Cordiner
056-14	The three ages of RDI-triggered protostars	Sicilia-Aguilar, Fang, Patel, Goldsmith, Getman
057-14	On the thermal state of a dense layer enclosing a HII region	Gong, Henkel, Mao, Li, Wyrowski, Urquhart
062-14	Studying the chemistry of the HVC stars	Quintana-Lacaci, Cernicharo, Bujarrabal, Castro-Carrizo, Velilla Prieto, Sanchez-Contreras
064-14	On the double-dust chemistry phenomenon in Planetary Nebulae: a pilot study	Garcia Hernandez, Gomez, Karakas, Lugaro, Gorny, Garcia-Rojas, Manchado
065-14	Circumstellar molecular gas in extremely young planetary nebulae	Uscanga, Rizzo, Rodriguez, Gomez, Boumis, Suarez, Miranda
066-14	Low- and high-mass protoplanetary nebulae	Bujarrabal, Santander-Garcia, Van Winckel, Alcolea, Castro-Carrizo
067-14	Chemical inventory of born-again planetary nebulae	Toala Sanz, Gonzalez-Garcia, Trevino-Morales, Guerrero, Sanchez-Monge, Tafoya, Macias, Ascaso
069-14	Magnetic field in the extended atmosphere of Red SuperGiant stars	Herpin, Auriere, Petit, Lebre, Gillet, Wiesemeyer, Josselin, Josselin
070-14	CO-dark H_2 gas in the southern arm of M33	Kramer, Buchbender, Gratier, Garcia-Burillo, Israel, Mookerjea, Nikola, Stacey, Roellig, Stutzki, Combes, Braine, Henkel, Wiedner
071-14	Searching for CO J 1-0 emission in an extremely metal poor galaxy	Shi, Zhang, Wang
073-14	Gas compression and star formation efficiency. Tidal and ram pressure interactions	Nehlig, Vollmer, Braine
075-14	Star formation traced by CO in ram pressure tails: the Virgo cluster	Verdugo, Combes, Salome, Braine, Dasyra
077-14	A new population of dust-rich galaxies with extreme H_2/dust ratios?	Dunne, Gomez, Eales, Ivison, Maddox, Papadopoulos, de Vis, Smith, clark, Bourne
078-14	Towards a Complete Census of Molecular Gas in a Key Local Galaxy Reference Sample	Schruba, Walter, Leroy, Sandstrom, Kramer, Usero, Hughes, Zschaechner
083-14	The molecular gas of local Lyman-alpha emitters	Oteo, Cepa, Bongiovanni, Perez Garcia
085-14	The gas-to-dust ratio in dust-lane early-type galaxies	Allaert, Baes, Gentile
089-14	Comparison of Chemical Compositions between Two Regions in NGC 3627	Watanabe, Sakai, Sorai, Kuno, Yamamoto
091-14	Cool Gas Physics in Abell 1068	Oonk, Edge, Frayer
092-14	Water in nearby active galaxies: thermal or maser emission?	Krips, Martin Ruiz, Dumas, Konig, Aladro, van der Laan, Feruglio
101-14	Hunting for high velocity molecular gas outflows in BAL QSOs	Dasyra, Combes, Salome, Andreani
102-14	Testing the connection between nuclear activity and galaxy quenching with CO observations of AGN in the SDSS/Stripe82	Rosario, Saintonge, Lutz, Tacconi, Genzel, Davies, Ellison, Mendel

Ident.	Title of investigations	Authors
103-14	Extragalactic radio recombination lines from ionized gas in the central nuclear regions of nearby AGNs	Fuhrmann, Henkel, Eckart, Vitale, Komossa, Zensus
106-14	CO Redshift Search for an Exceptionally Bright Submillimeter Galaxy Lensed by a Massive Galaxy Cluster at *z*=0.9	Egami, Dessauges-Zavadsky, Altieri, Clement, Richard, Rawle, Perez-Gonzalez, Chapman, Smail, Kneib, Boone, Combes, Omont, Swinbank, Schaerer, van der Werf, Jauzac
107-14	Spectroscopic redshifts of bright sources within high-*z* proto-cluster candidates discovered with Planck and Herschel	Dole, Nesvadba, Beelen, Chary, Dicken, Flores-Cacho, Frye, Giard, (phd), Kneissl, Konig, Krips, Lagache, Le Floc'h, MacKenzie, Puget, Scott, Martinache
108-14	Probing dense gas in the brightest gravitationally lensed galaxies in the Planck all-sky survey with EMIR	Nesvadba, Canameras, Boone, Beelen, Dicken, Dole, Flores-Cacho, Frye, Konig, Krips, Le Floc'h, MacKenzie, Malhotra, Montier, Scott, Chary, Yan, Lagache, Soucail
118-14	Imaging spatial variations of the nitrogen isotope composition in a nascent solar system	Wampfler, Jorgensen, Bisschop, Bizzaro
D01-14	Dense gas vs. intense star formation in the circumnuclear ring of NGC4736	Van Der Laan, Koenig

NOEMA INTERFEROMETER

Ident	Title of Investigation	Authors
T0CC	IRAM Lensing Survey: Probing Galaxy Formation in the Early Universe	Kneib, Clément, Cuby, Peroux, Ilbert, Jablonka, Boone, Combes, Neri, Krips, Lagache, Beelen, Pello, Courbin, Meylan, Schaerer, Dessauges, Knudsen, van der Werf, Richard, Smail, Swinbank, Chapman, Ivison, Egami, Altieri, Valtchanov
W07D	Keplerian disks and expanding bipolar flows in post-AGB stars	Bujarrabal, Castro-Carrizo, Winckel, Alcolea, Santander-García
W0AA	Testing the evolutionary link between QSOs and submm galaxies	Simpson, Swinbank, Smail, Cox, Danielson, Bonfield, van der Werf, Jarvis, Coppin, Ivison, Hughes, Vaccari, Dunlop, Verma, Clements, Leeuw, Smith, Benford, Owski, Omont
X002	Understanding small and bright CO clumps exposed to far-UV illumination from the runaway O star HD34078	Gratier, Boissé, Cabrit, Gerin, Lesaffre, Pety, Pineau des Forêts
X00C	Filament fragmentation in high-mass star formation	Beuther, Tackenberg, Johnston, Ragan, Henning
X01A	The Anatomy of a Spiral Arm: From Molecular Gas to Stellar Clusters	Schinnerer, Meier, Meidt, Garcia-Burillo, Bigiel, Usero, Pety, Dumas, Hughes
X033	The Molecular Gas in High-*z* Star-Forming Galaxies from HiZELS	Swinbank, Smail, Simpson, Sobral, Best, Geach, van der Werf
X04D	A census of [CI] in high-*z* galaxies with available [CII] observations	Decarli, Walter, Riechers, Weiss, Bertoldi, Carilli, Ferkinhoff, Groves, Neri
X052	Unveiling the population of highly obscured and high-*z* gamma-ray bursts (ToO)	Castro-Tirado, Bremer, Winters, Gorosabel, Guziy, Pérez-Ramírez, Castro Cerón, Pandey, Tello, Sánchez-Ramírez
X053	PHIBSS2: molecular gas at the peak epoch of galaxy formation	Combes, García-Burillo, Neri, Tacconi, Genzel, Contini, Bolatto, Lilly, Boone, Bouché, Bournaud, Burkert, Carollo, Colina, Cooper, Cox, Feruglio, Freundlich, Schreiber, Juneau, Kovac, Lippa, Lutz, Naab, Omont, Renzini, Saintonge, Salomé, Sternberg, Walter, Weiner, Weiss, Wuyts
X05A	Red-shifted absorption as a probe of infall in high-mass star forming cores	Wyrowski, Menten, Güsten, Wiesemeyer
X065	Origin of warm water emission in low-mass protostars	Persson, Jørgensen, Dishoeck, Harsono, Mottram, Visser
X067	A complete homogeneous CO survey of northern FU Ori-type objects	Kóspál, Ábrahám, Hogerheijde, Brinch
X06A	Tracing Turbulence in Proto-Planetary Disks	Guilloteau, Chapillon, Di Folco, Dutrey, Gueth, Henning, Hersant, Launhardt, Pietu, Reboussin, Schreyer, Semenov, Wakelam
X06B	Deuteration as a Tool to investigate the physics of protoplanetary disk midplanes: the GG Tau case	Dutrey, Di Folco, Guilloteau, Hersant, Wakelam, Vastel, Piétu, Gueth, Chapillon, Beck, Bary, Simon, Boehler, Tang
X06D	Probing the planet forming regions of GV Tau N and S	Fuente, Cernicharo, Agúndez, Neri, Pilleri
X06E	V1331 Cyg - Hosting planet formation?	Choudhary, Stecklum, Schreyer, Launhardt, Stapelfeldt
X070	HD141569: disk dissipation caught in action	Pericaud, Di Folco, Dutrey, Piétu, Guilloteau, Augereau
X073	The rotating disk in 89 Her	Bujarrabal, Castro-Carrizo, Winckel, Alcolea
X074	Rotating and expanding gas around post-AGB stars	Bujarrabal, Castro-Carrizo, Winckel, Alcolea
X076	Probing ISM shock heating in the massive outflow of Markarian 231	Feruglio, Ceccarelli, Fiore, Piconcelli, Maiolino, Cicone
X078	Follow-up study: Identifying the differences between NGC 5248's two circumnuclear rings	van der Laan, Schinnerer, Meidt, Dumas, Sandstrom
X079	Quenched star formation by enhanced turbulence in the Taffy gas bridge	Vollmer, Braine, Nehlig
X081	Star formation efficiency in M31, the closest giant spiral galaxy	Guélin, Muller, Dumas, Pety, Schuster

Ident	Title of Investigation	Authors
X087	Mapping the ionisation of NGC1068: what feedback where?	Ceccarelli, Fiore, Feruglio, Neri, Antonucci, Hily-Blant, Krips, Piconcelli, Vaupré
X08F	Hot HCN in buried nuclei - probing the AGN torus	Aalto, Muller, Sakamoto, Falstad, Costagliola, Gonzales-Alfonso
X091	AGN feedback and molecular gas filaments in Abell 1795	Hamer, Salomé, Combes, Russell, McNamara
X094	The ultra-massive black hole in NGC 1277 probed via CO kinematics	Scharwächter, Salomé, Sun, Combes
X095	The nature of the unique source SWIFT J1644+57	Castro-Tirado, Agudo, Jeong, Bremer, Winters, Gorosabel, Gómez, Sánchez-Ramirez, Tello
X0A1	Molecular gas properties of resolved clumps in a strongly-lensed galaxy	Dessauges-Zavadsky, Combes, Richard, Krips, Boone, Omont, Kneib, Schaerer, Cava, Zamojski, Egami, Rawle, van der Werf
X0A2	Lensed Galaxies Extend CO Studies to Lower Stellar Masses	Wuyts, Saintonge, Tacconi, Lutz, Gladders, Rigby, Sharon
X0AD	CO Mapping of Two Strongly Lensed Galaxies at High-Redshift	Zamojski, Dessauges-Zavadsky, Rujopakarn, Egami, Rawle, Cava, Combes, Boone, Schaerer, Richard, Kneib, Cément, Walth
X0AE	Zooming in onto the brightest sub-mm lenses on the sky	Nesvadba, Canameras, Boone, Beelen, Dicken, Dole, Flores-Cacho, Frye, Guery, Koenig, Krips, Le Floc'h, Lehnert, MacKenzie, Malhotra, Montier, Omont, Rhoads, Scott
X0AF	Understanding the Nature of Herschel-Selected Submillimeter Galaxies	Riechers, Viero, Omont, Perez-Fournon, Neri, Cooray, Wardlow, Clements, Ivison, Cox, Bock, Oliver
X0B1	The Molecular Gas Content of the Most Dramatic High-*z* AGN Overdensities	Hennawi, Arrigoni-Battaia, Walter, Decarli
X0B2	A molecular scan in the Hubble Deep Field North: 2 mm follow-up observations	Decarli, Walter, Riechers, Carilli, Neri, Cox
X0B3	First Systematic Survey for CO and Dust in Lyman α Blobs	Yang, Walter, Decarli, Bertoldi, Weiss, Adescu
X0BA	The Extreme Dense Gas Excitation in the *z*=4 Galaxy APM 08279+5255	Riechers, Neri, Weiss, Walter, Downes, Cox, Wagg
X0BC	Resolving the star formation in a *z*=4 starburst	Hodge, Decarli, Walter, Riechers, Carilli
X0C6	Blind redshifts for ultra-red Herschel galaxies	Krips, Ivison, Fournon, Bertoldi, Omont, Cox, Neri, Koenig, van der Werf, Dannerbauer, Eales, Valiante
X0C8	Small-scale structure of molecular gas at *z*=5.243 (continued)	Boone, Combes, Krips, Richard, Egami, Rawle, Smail, Ivison, Omont, Dessauges-Zavadsky, Schaerer, Kneib, Zamojski, van der Werf, Pham, Pello
X0CA	A systematic search for CO and FIR emission in a flux limited sample of *z*=6 quasars: completing a pilot study	Venemans, Walter, Decarli, Banados
X0CE	Nailing down redshifts for the first galaxies	Carilli, Walter, Decarli, Cox, Riechers, Wagg, Menten, Bertoldi, Kanekar
X––3	Resolving the star-forming clumps in a lensed L* galaxy at z∼1.6	Dessauges-Zavadsky, Combes, Krips, Schaerer, Zamojski, Richard, Cava, Boone, Kneib, Egami, Omont, Rawle, van der Werf
X––4	Probing the Spatial Distribution of H_2O Emission in a Lensed Herschel Galaxy	Omont, Yang, Beelen, Neri, Gavazzi, van der Werf, Krips, Ivison, Cox, Lehnert, Bussmann, Weiss, Bertoldi, Dannerbauer, Downes, Gao, Guelin, Perez-Fournon, Menten
X––5	New History for an Old Friend: The Redshift of GN10	Riechers, Hodge, Walter, Daddi, Neri, Carilli
X––7	HD141569: disk dissipation caught in action - DDT Request ^{12}CO 2-1	Dutrey, Pericaud, Di Folco, Guilloteau, Pietu, Augereau
X––8	A spectacular outflow in a z∼1.6 QSO	Brusa, Cresci, Mainieri, Feruglio, Marconi, Maiolino, Perna
S14AE	Imaging spatial variations of the nitrogen isotope composition in a nascent solar system	Susanne Wampfler, Jes Jorgensen, Suzanne Bisschop, Martin Bizzarro
S14AO	Tracing the structure of AB Aur molecular disk in H_2CO emission	Susana Pacheco Vazquez, Asuncion Fuente, Marcelino Agundez, Tomas Alonso-Albi, Roberto Neri, Jose Cernicharo, Javier R. Goicoechea, O. Berne, Laurent Wiesenfeld, Rafael Bachiller, Bertrand Lefloch
S14AR	Grain growth in disks around brown dwarfs	Paola Pinilla, Myriam Benisty, Leonardo Testi, Antonella Natta, Thomas Henning, Luca Ricci, Tilman Birnstiel
S14AS	Dust growth in the Orion proplyds	Myriam Benisty, Paola Pinilla, Luca Ricci, Tilman Birnstiel, Thomas Henning, Antonella Natta, Leonardo Testi
S14AT	Particle growth in protoplanetary disks across the stellar/substellar transition	Gerrit van der Plas, Francois Menard, Jennifer Patience
S14AW	Clumping in the winds of OB stars	Danielle Fenech, Raman Prinja, Ronny Blomme, Luke Peck, Jack Morford
S14AX	Mapping the gaseous and dusty envelope of Betelgeuse	Miguel Montarges, Pierre Kervella, Arancha Castro-Carrizo, Jan Martin Winters, Valentin Bujarrabal, Guy Perrin, Leen Decin, Anita M. S. Richards, Eamon O'Gorman, Thibaut Le Bertre, Xavier Haubois, Stephen Ridgway, Graham Harper, Iain McDonald, Andrea Chiavassa, Sylvestre Lacour
S14BC	Tracing the impact of AGN feedback in the nucleus of M51a	Miguel Querejeta, Eva Schinnerer, Santiago Garcia-Burillo, Jerome Pety, David S. Meier, Frank Bigiel, Annie Hughes, S. Meidt, Kathryn Kreckel, Guillermo Blanc
S14BD	The dense gas fraction of inefficiently star-forming gas	Eva Schinnerer, Annie Hughes, S. Meidt, Miguel Querejeta, Dario Colombo, Santiago Garcia-Burillo, Clare Dobbs, Todd Thompson
S14BE	High Resolution Imaging of Dense Gas in the Outer Spiral Arm of M51	Hao Chen, Jonathan Braine, Yu Gao
S14BH	The connection between gas fraction and resolved properties of massive star forming clumps	David Fisher, Karl Glazebrook, Danail Obreschkow, Alberto D. Bolatto, R. Bassett, Emily Wisnioski, A. Popping, I. Damjanov, R. Abraham, E. Mentuch Cooper
S14BL	Are Starburst-Driven Molecular Superwinds Pervasive in the Local ULIRG Population?	Fabian Walter, Adam Leroy, Laura Zschaechner, Alberto D. Bolatto

Ident	Title of Investigation	Authors
S14BM	Quenched star formation by enhanced turbulence in the Taffy gas bridge	Bernd Vollmer, Francois Nehlig, Jonathan Braine
S14BR	Hydrogen millimeter recombination lines as a SFR indicator	Toma Badescu, Frank Bertoldi, Yujin Yang, Alexander Karim, Benjamin Magnelli, Kaustuv Basu
S14BS	Molecular Gas in an Unusual, Low Redshift Long GRB Host Galaxy	Elizabeth Stanway, Andrew Levan
S14BT	From Star-Forming Galaxies to Passive Spheroids: Gas Dynamics of Dusty Starbursts in Distant Galaxy Clusters	Mark Swinbank, Helen Johnson, Ian Smail, Richard Bower, James Geach, Yusei Koyama
S14BU	The fate of cold gas in galaxy clusters: probing evolution at intermediate redshift	Pascale Jablonka, Francoise Combes, Eiichi Egami, M. Jauzac, Jean-Paul Kneib, Tim Rawle
S14BV	Linking gas mass fraction with star formation history: a CO(1-0) survey of A851	James Geach, Melanie Krips, Mark Swinbank, Ian Smail, Richard Ellis, Claudia Lagos
S14BW	The nature of the unique source SWIFT J1644+57	Angela Gonzalez Rodriguez, Alberto J. Castro-Tirado, Ivan Agudo, Michael Bremer, Jan Martin Winters, Jose L. Gomez
S14BX	Strong Differential Lensing in a Distant Wet-Dry Merger: Gas Properties	Dominik A. Riechers
S14CE	Probing the Molecular Gas Resevoir of Extreme C^+ Emitters at $z\sim1.8$	Carl Ferkinhoff, Drew Brisbin, Gordon Stacey, Thomas Nikola, Fabian Walter
S14CG	First Systematic Survey for CO and Dust in Lyman α Blobs	Yujin Yang, Frank Bertoldi, Fabian Walter, Roberto Decarli, Axel Weiss, Alexander Karim, Toma Badescu
S14CH	The build-up of galaxies: PdBI view on galaxy growth at $z\sim2$	Joseph Hennawi, Fabian Walter, Roberto Decarli, Fabrizio Arrigoni-Battaia
S14CK	A S_{850}=20mJy source in the z=2.3 H1700 protocluster	Frank Bertoldi, Scott Chapman, Andrew Blain, Chuck Steidel
S14CM	Searching for the most massive and CO-bright main sequence galaxies at 1<z<3	Mark T. Sargent, Emanuele Daddi, Matthieu Bethermin, Frederic Bournaud, Eva Schinnerer, H. Aussel, Emeric Le Floc'h, Georgios Magdis, Fabian Walter, Alexander Karim, J. Trump, J. Silverman
S14CN	The Molecular Gas Reservoir of Normal Galaxies at $z\sim3$	Georgios Magdis, Dimitra Rigopoulou, Emanuele Daddi, Mark T. Sargent, Qinghua Tan, Jiasheng Huang, David Elbaz, Mark Dickinson, Matthieu Bethermin, James Geach, Chiara Feruglio
S14CO	Understanding the Nature of Herschel-Selected Distant Starbursts	Dominik A. Riechers, Marco Viero, Alain Omont, Ismael Perez-Fournon, Roberto Neri, Asantha Cooray, Julie Wardlow, David Clements, Rob Ivison, Pierre Cox, Jamie Bock, Seb Oliver
S14CS	Zooming in onto the brightest gravitationally lensed high-z galaxies in the Planck sub-mm all-sky survey	Nicole Nesvadba, R. Canameras, Frederic Boone, Alexandre Beelen, Dan Dicken, Herve Dole, I. Flores-Cacho, Brenda Frye, Sabine Konig, Melanie Krips, Emeric Le Floc'h, Guilaine Lagache, T. MacKenzie, Sangeeta Malhotra, L. Montier, Ranga-Ram Chary, Douglas Scott, G. Soucail, Lin Yan
S14CT	Probing the dense molecular gas in a $z\sim3.6$ lensed ULIRG	Chentao Yang, Alain Omont, Cecilia Ceccarelli, Alexandre Beelen, Yu Gao, Roxana Lupu, Zhiyu Zhang, Roberto Neri, R. Gavazzi, Michel Guelin, Melanie Krips
S14CY	Molecular Gas and Star Formation in the Host Galaxy of the Most Massive Quasar at z>6	Ran Wang, Xue-Bing Wu, Xiaohui Fan, Feige Wang, Frank Bertoldi, Chris L. Carilli, Fabian Walter, Roberto Neri, Michael A. Strauss, Linhua Jiang, Fuyan Bian, Ian McGreer
S14DB	Characterizing the molecular content in a volume-limited sample of high-z galaxies	Roberto Decarli, Fabian Walter, Chris L. Carilli, Dominik A. Riechers, Roberto Neri
S14DD	The physics of highly obscured and high-z gamma-ray bursts	Alberto J. Castro-Tirado, Jan Martin Winters, Michael Bremer, Javier Gorosabel, Sergei Guziy, Soomin Jeong, Dolores Perez-Ramirez, Jose Maria Castro Ceron, Shashi B. Pandey, Juan Carlos Tello, Ruben Sanchez-Ramirez
L14AB	Fragmentation and disk formation during high-mass star formation	Henrik Beuther, Thomas Henning, Hendrik Linz, Siyi Feng, Katharine Johnston, Rolf Kuiper, Sarah Ragan, Dmitry Semenov, Frederic Gueth, Jan Martin Winters, Karl M. Menten, James Urquhart, Timea Csengeri, Pamela Klaassen, Joseph C. Mottram, Peter Schilke, Melvin Hoare, Luke Maud, Stuart Lumsden, Maria Teresa Beltran, Riccardo Cesaroni, Malcolm Walmsley, Alvaro Sanchez-Monge, Qizhou Zhang, Cornelis Dullemond, Frederique Motte, Philippe Andre, Gary Fuller, Nicolas Peretto, Roberto Galvan-Madrid, S. Longmore, Sylvain Bontemps, Th. Peters, Aina Palau, R. Pudritz, Hans Zinnecker
D14AA	A test case for dense giant outflows in ULIRGs	Chiara Feruglio, Roberto Maiolino, Susanne Aalto, Eckhard Sturm
D14AB	Identification of a $z\geq9$ candidate submillimeter galaxy	Itziar Aretxaga, Roberto Neri, Alain Omont, Olga Vega, David Hughes, Grant Wilson, Min Yun, James Dunlop, James Geach
D14AC	NGC5044 - an extremely self-absorbed, low power AGN?	Alastair Edge, Michael Hogan, James Geach, Philippe Salome, Francoise Combes, Jeremy Lim
D14AD	Confirming the redshift of a hyper-luminous SMG at z>2.3	Scott Chapman
D14AE	Spectroscopic confirmation of a novel, possibly fundamental stage of structure formation at $z\sim2.5$	David Elbaz, Tao Wang, Emanuele Daddi, Xinwen Shu, Daizhong Liu, Chiara Feruglio, Sergio Martin Ruiz, Qinghua Tan, Francesco Valentino, Raphael Gobat
W14AA	The L1157-B1 astrochemical laboratory: testing the origin of DCN	Francesco Fontani, Claudio Codella, Cecilia Ceccarelli, Bertrand Lefloch, Serena Viti, Milena Benedettini, Gemma Busquet
W14AF	Molecule Formation in Protostellar Jets: a study of CepE	Bertrand Lefloch, Antoine Gusdorf, Claudio Codella, Cecilia Ceccarelli
W14AJ	Infall Signatures in the Youngest Protostars	Amelia Stutz, John Tobin, Thomas Henning, Philip C. Myers, Thomas L. Wilson, James di Francesco, S. Thomas Megeath, Dan Watson, Thomas Stanke, Friedrich Wyrowski, Hendrik Linz
W14BC	Origin of the CF^+ emission in a young and massive protostar	Sarah Fechtenbaum, Sylvain Bontemps, Timea Csengeri, Nicola Schneider
W14BQ	Behind the wall: planet formation in a giant «dead zone» around GG Tau A?	Anne Dutrey, Emmanuel Di Folco, Vincent Pietu, Frederic Gueth, Edwige Chapillon, Stephane Guilloteau, Ya-Wen Tang, Jeffrey Bary, Jean-Marc Hure, Michal Simon, Arnaud Pierens, Herve Beust, Franck Hersant, Yann Boehler
W14BT	Additional compact-configuration observations of ^{13}CO emission in 89 Her	Valentin Bujarrabal, Arancha Castro-Carrizo, Hans Van Winckel, Javier Alcolea

Ident	Title of Investigation	Authors
W14BU	The remarkable disk orbiting AC Her	Valentin Bujarrabal, Arancha Castro-Carrizo, Hans Van Winckel, Javier Alcolea
W14DB	The ultra-massive black hole in NGC 1277 probed via CO kinematics: follow-up observations	Julia Scharwächter, Francoise Combes, Philippe Salome, Melanie Krips, Ming Sun
W14DG	Hiding in Plain Sight - self-absorbed, low power AGN in massive galaxies	Alastair Edge, Michael Hogan, Philippe Salome, Francoise Combes, Helen Russell, Keith Grainge
W14DS	Evolution of CO and Star Formation as Probed by Herschel-Selected Pure Starbursts at $z\sim1.5$	Emanuele Daddi, Daizhong Liu, J. Silverman, Giulia Rodighiero, Frederic Bournaud, Dieter Lutz, Mark T. Sargent, Georgios Magdis, Matthieu Bethermin, Yu Gao, Stephanie Juneau, Daichi Kashino
W14EB	A complete study of the ISM properties of a z=2 main sequence galaxy	Manuel Aravena, Emanuele Daddi, Dominik A. Riechers, Fabian Walter, Chris L. Carilli, Jeff Wagg, Jacqueline Hodge
W14FB	Extreme CO and HCN Excitation in APM08279+5255 (z=3.91): The Final Chapter	Dominik A. Riechers, Roberto Neri, Axel Weiss, Fabian Walter, Dennis Downes, Pierre Cox, Jeff Wagg
W14FP	The Youngest Dust Forming Galaxy in the Universe?	Johannes Staguhn, Eli Dwek, Richard G. Arendt, Jorge Gonzalez, Fabian Walter, Ting Su, Sune Toft, Thomas R. Greve, Michal J. Michalowski
GH011	High-resolution 220 Rs imaging of the jet nozzle in 3C84	Jeffrey Hodgson, Monica Orienti, Filippo D'Ammando, Thomas Krichbaum, Lars Fuhrmann, Hiroshi Nagai, Rocco Lico, Elisabetta Liuzzo, Kazuhiro Hada, Marcello Giroletti, Michael Bremer
GM071	Continued 3mm Imaging of Gamma-ray Blazars	Alan Marscher, Thomas Krichbaum, Svetlana Jorstad, Jeffrey Hodgson, Bindu Rani, Nicholas MacDonald, Mason Keck, Jose L. Gomez, Ivan Agudo, Michael Bremer
GB078	Ultra-high resolution imaging of Cygnus A: where do the two jets start?	Biagina Boccardi, Thomas Krichbaum, Uwe Bach, Walter Alef, Anton Zensus
GS034	Probing the symmetry of jet and counter-jet production in NGC1052	Robert Schulz, Anne-Kathrin Baczko, Matthias Kadler, Thomas Krichbaum, Moritz Bock, Eduardo Ros, Cornelia Mueller, Christoph Grossberger, Lars Fuhrmann, Karl Mannheim, Joern Wilms, Heino Falcke
MA002	Revealing the polarized fine structure of AGN Relativistic Jets with the GMVA	Antonio Alberdi Odriozola, Eduardo Ros, Thomas Krichbaum, Miguel Angel Perez-Torres, Juan-Maria Marcaide, Ivan Marti-Vidal, Jose Guirado
MB002	SiO maser missed flux in AGB envelopes: extended component or weak maser clumps?	Alain Baudry, Valentin Bujarrabal, Francisco Colomer, Antonio Diaz
GB078	Ultra-high resolution imaging of Cygnus A: where do the two jets start?	Biagina Boccardi, Thomas Krichbaum, Uwe Bach, Walter Alef, Anton Zensus

Annex II – Publications in 2014

The list of refereed publications, conferences and workshop papers as well as thesis based upon data obtained using the IRAM instruments are provided in the following two tables : the first table gives the publications with the IRAM staff members as co-author (including technical publications by the IRAM staff), and the second table those with results from the user's community.

The running number is the cumulative number since the first annual report was published for the year 1987.

2014 PUBLICATION LIST: IRAM COMMUNITY:

1901	First detection of rotational CO line emission in a red giant branch star	Groenewegen M. A. T.	2014, A&A 561, LL11
1902	Rotationally-supported disks around Class I sources in Taurus: disk formation constraints	Harsono D., Jørgensen J. K., van Dishoeck E. F., Hogerheijde M. R., Bruderer S., Persson M. V., Mottram J. C.	2014, A&A 562, AA77
1903	The deuterium fractionation of water on solar-system scales in deeply-embedded low-mass protostars	Persson M. V., Jørgensen J. K., van Dishoeck E. F., Harsono D.	2014, A&A 563, AA74
1904	Chemical evolution in the early phases of massive star formation. I	Gerner T., Beuther H., Semenov D., Linz H., Vasyunina T., Bihr S., Shirley Y. L., Henning T.	2014, A&A 563, AA97
1905	Millimetre spectral indices of transition disks and their relation to the cavity radius	Pinilla P., Benisty M., Birnstiel T., Ricci L., Isella A., Natta A., Dullemond C. P., Quiroga-Nuñez L. H., Henning T., Testi L.	2014, A&A 564, AA51
1906	Cold gas properties of the Herschel Reference Survey. I. ^{12}CO(1-0) and HI data	Boselli A., Cortese L., Boquien M.	2014, A&A 564, AA65
1907	Extended warm gas in Orion KL as probed by methyl cyanide	Bell T. A., Cernicharo J., Viti S., Marcelino N., Palau A., Esplugues G. B., Tercero B.	2014, A&A 564, AA114
1908	The molecular gas reservoir of 6 low-metallicity galaxies from the Herschel Dwarf Galaxy Survey. A ground-based follow-up survey of CO(1-0), CO(2-1), and CO(3-2)	Cormier D., Madden S. C., Lebouteiller V., Hony S., Aalto S., Costagliola F., Hughes A., Rémy-Ruyer A., Abel N., Bayet E., Bigiel F., Cannon J. M., Cumming R. J., Galametz M., Galliano F., Viti S., Wu R.	2014, A&A 564, AA121
1909	Molecular observations of comets C/2012 S1 (ISON) and C/2013 R1 (Lovejoy): HNC/HCN ratios and upper limits to PH_3	Agúndez M., Biver N., Santos-Sanz P., Bockelée-Morvan D., Moreno R.	2014, A&A 564, LL2
1910	The molecular gas content of ULIRG type 2 quasars at $z<1$	Rodríguez M. I., Villar-Martín M., Emonts B., Humphrey A., Drouart G., García Burillo S., Pérez Torres M.	2014, A&A 565, AA19
1911	Molecular ions in the protostellar shock L1157-B1	Podio L., Lefloch B., Ceccarelli C., Codella C., Bachiller R.	2014, A&A 565, AA64
1912	Evidence of internal rotation and a helical magnetic field in the jet of the quasar NRAO 150	Molina S. N., Agudo I., Gómez J. L., Krichbaum T. P., Martí-Vidal I., Roy A. L.	2014, A&A 566, AA26
1913	The ^{12}C/^{13} ratio in AGB stars of different chemical type. Connection to the C/C ratio and the evolution along the AGB	Ramstedt S., Olofsson H.	2014, A&A 566, AA145
1914	CO map and steep Kennicutt-Schmidt relation in the extended UV disk of M 63	Dessauges-Zavadsky M., Verdugo C., Combes F., Pfenniger D.	2014, A&A 566, AA147
1915	Cosmic ray induced ionisation of a molecular cloud shocked by the W28 supernova remnant	Vaupré S., Hily-Blant P., Ceccarelli C., Dubus G., Gabici S., Montmerle T.	2014, A&A 568, AA50
1916	The dynamics and star-forming potential of the massive Galactic centre cloud G0.253+0.016	Johnston K. G., Beuther H., Linz H., Schmiedeke A., Ragan S. E., Henning T.	2014, A&A 568, AA56
1917	THz spectroscopy and first ISM detection of excited torsional states of ^{13}C-methyl formate	Haykal I., Carvajal M., Tercero B., Kleiner I., López A., Cernicharo J., Motiyenko R. A., Huet T. R., Guillemin J. C., Margulès L.	2014, A&A 568, AA58
1918	The hot core towards the intermediate-mass protostar NGC 7129 FIRS 2. Chemical similarities with Orion KL	Fuente A., Cernicharo J., Caselli P., McCoey C., Johnstone D., Fich M., van Kempen T., Palau A., Yıldız U. A., Tercero B., López A.	2014, A&A 568, AA65
1919	Molecular gas heating in Arp 299	Rosenberg M. J. F., Meijerink R., Israel F. P., van der Werf P. P., Xilouris E. M., Weiß A.	2014, A&A 568, AA90
1920	Herschel-ATLAS and ALMA. HATLAS J142935.3-002836, a lensed major merger at redshift 1.027	Messias H., Dye S., Nagar N., Orellana G., Bussmann R. S., Calanog J., Dannerbauer H., Fu H., Ibar E., Inohara A., Ivison R. J., Negrello M., Riechers D. A., Sheen Y.-K., Aguirre J. E., Amber S., Birkinshaw M., Bourne N., Bradford C. M., Clements D. L., Cooray A., De Zotti G., Demarco R., Dunne L., Eales S., Fleuren S., Kamenetzky J., Lupu R. E., Maddox S. J., Marrone D. P., MichaŃowski M. J., Murphy E. J., Nguyen H. T., Omont A., Rowlands K., Smith D., Smith M., Valiante E., Vieira J. D.	2014, A&A 568, AA92
1921	The Earliest Phases of Star formation (EPoS). Temperature, density, and kinematic structure of the star-forming core CB 17	Schmalzl M., Launhardt R., Stutz A. M., Linz H., Bourke T. L., Beuther H., Henning T., Krause O., Nielbock M., Schmiedeke A.	2014, A&A 569, AA7
1922	Deuterated methanol in the pre-stellar core L1544	Bizzocchi L., Caselli P., Spezzano S., Leonardo E.	2014, A&A 569, AA27
1923	Dust and gas in luminous proto-cluster galaxies at z = 4.05: the case for different cosmic dust evolution in normal and starburst galaxies	Tan Q., Daddi E., Magdis G., Pannella M., Sargent M., Riechers D., Béthermin M., Bournaud F., Carilli C., da Cunha E., Dannerbauer H., Dickinson M., Elbaz D., Gao Y., Hodge J., Owen F., Walter F.	2014, A&A 569, AA98
1924	Physical structure of the photodissociation regions in NGC 7023. Observations of gas and dust emission with Herschel	Köhler M., Habart E., Arab H., Bernard-Salas J., Ayasso H., Abergel A., Zavagno A., Polehampton E., van der Wiel M. H. D., Naylor D. A., Makiwa G., Dassas K., Joblin C., Pilleri P., Berné O., Fuente A., Gerin M., Goicoechea J. R., Teyssier D.	2014, A&A 569, AA109

1925	SiO emission from low- and high-velocity shocks in Cygnus-X massive dense clumps	Duarte-Cabral A., Bontemps S., Motte F., Gusdorf A., Csengeri T., Schneider N., Louvet F.	2014, A&A 570, AA1
1926	CO in Hickson compact group galaxies with enhanced warm H_2 emission: Evidence for galaxy evolution?	Lisenfeld U., Appleton P. N., Cluver M. E., Guillard P., Alatalo K., Ogle P.	2014, A&A 570, AA24
1927	ATLASGAL-selected massive clumps in the inner Galaxy. I. CO depletion and isotopic ratios	Giannetti A., Wyrowski F., Brand J., Csengeri T., Fontani F., Walmsley C. M., Nguyen Luong Q., Beuther H., Schuller F., Güsten R., Menten K. M.	2014, A&A 570, AA65
1928	Carbon in different phases ([CII], [CI], and CO) in infrared dark clouds: Cloud formation signatures and carbon gas fractions	Beuther H., Ragan S. E., Ossenkopf V., Glover S., Henning T., Linz H., Nielbock M., Krause O., Stutzki J., Schilke P., Güsten R.	2014, A&A 571, AA53
1929	Jet outflow and gamma-ray emission correlations in S5 0716+714	Rani B., Krichbaum T. P., Marscher A. P., Jorstad S. G., Hodgson J. A., Fuhrmann L., Zensus J. A.	2014, A&A 571, LL2
1930	Laboratory characterization and astrophysical detection of vibrationally excited states of vinyl cyanide in Orion-KL	López A., Tercero B., Kisiel Z., Daly A. M., Bermúdez C., Calcutt H., Marcelino N., Viti S., Drouin B. J., Medvedev I. R., Neese C. F., PszczóŃkowski L., Alonso J. L., Cernicharo J.	2014, A&A 572, AA44
1931	Diversity of chemistry and excitation conditions in the high-mass star forming complex W33	Immer K., Galván-Madrid R., König C., Liu H. B., Menten K. M.	2014, A&A 572, AA63
1932	HerMES: Candidate High-redshift Galaxies Discovered with Herschel/SPIRE	Dowell C. D., Conley A., Glenn J., Arumugam V., Asboth V., Aussel H., Bertoldi F., Béthermin M., Bock J., Boselli A., Bridge C., Buat V., Burgarella D., Cabrera-Lavers A., Casey C. M., Chapman S. C., Clements D. L., Conversi L., Cooray A., Dannerbauer H., De Bernardis F., Ellsworth-Bowers T. P., Farrah D., Franceschini A., Griffin M., Gurwell M. A., Halpern M., Hatziminaoglou E., Heinis S., Ibar E., Ivison R. J., Laporte N., Marchetti L., Martínez-Navajas P., Marsden G., Morrison G. E., Nguyen H. T., O'Halloran B., Oliver S. J., Omont A., Page M. J., Papageorgiou A., Pearson C. P., Petitpas G., Pérez-Fournon I., Pohlen M., Riechers D., Rigopoulou D., Roseboom I. G., Rowan-Robinson M., Sayers J., Schulz B., Scott D., Seymour N., Shupe D. L., Smith A. J., Streblyanska A., Symeonidis M., Vaccari M., Valtchanov I., Vieira J. D., Viero M., Wang L., Wardlow J., Xu C. K., Zemcov M.	2014, ApJ 780, 75
1933	Organic Species in Infrared Dark Clouds	Vasyunina T., Vasyunin A. I., Herbst E., Linz H., Voronkov M., Britton T., Zinchenko I., Schuller F.	2014, ApJ 780, 85
1934	HOPS 136: An Edge-on Orion Protostar near the End of Envelope Infall	Fischer W. J., Megeath S. T., Tobin J. J., Hartmann L., Stutz A. M., Kounkel M., Poteet C. A., Ali B., Osorio M., Manoj P., Remming I., Stanke T., Watson D. M.	2014, ApJ 781, 123
1935	Herschel Observations of Far-infrared Cooling Lines in Intermediate Redshift (Ultra)-luminous Infrared Galaxies	Rigopoulou D., Hopwood R., Magdis G. E., Thatte N., Swinyard B. M., Farrah D., Huang J.-S., Alonso-Herrero A., Bock J. J., Clements D., Cooray A., Griffin M. J., Oliver S., Pearson C., Riechers D., Scott D., Smith A., Vaccari M., Valtchanov I., Wang L.	2014, ApJ 781, LL15
1936	[CII] and ^{12}CO(1-0) Emission Maps in HLSJ091828.6+514223: A Strongly Lensed Interacting System at $z = 5.24$	Rawle T. D., Egami E., Bussmann R. S., Gurwell M., Ivison R. J., Boone F., Combes F., Danielson A. L. R., Rex M., Richard J., Smail I., Swinbank A. M., Altieri B., Blain A. W., Clement B., Dessauges-Zavadsky M., Edge A. C., Fazio G. G., Jones T., Kneib J.-P., Omont A., Pérez-González P. G., Schaerer D., Valtchanov I., van der Werf P. P., Walth G., Zamojski M., Zemcov M.	2014, ApJ 783, 59
1937	Observational Results of a Multi-telescope Campaign in Search of Interstellar Urea $[(NH_2)_2CO]$	Remijan A. J., Snyder L. E., McGuire B. A., Kuo H.-L., Looney L. W., Friedel D. N., Golubiatnikov G. Y., Lovas F. J., Ilyushin V. V., Alekseev E. A., Dyubko S. F., McCall B. J., Hollis J. M.	2014, ApJ 783, 77
1938	Pinpointing the Molecular Gas within an Lyα Blob at $z \sim 2.7$	Yang Y., Walter F., Decarli R., Bertoldi F., Weiss A., Dey A., Prescott M. K. M., Bădescu T.	2014, ApJ 784, 171
1939	Spectroscopic Characterization and Detection of Ethyl Mercaptan in Orion	Kolesniková L., Tercero B., Cernicharo J., Alonso J. L., Daly A. M., Gordon B. P., Shipman S. T.	2014, ApJ 784, LL7
1940	Fragmentation of Massive Dense Cores Down to < ~1000 AU: Relation between Fragmentation and Density Structure	Palau A., Estalella R., Girart J. M., Fuente A., Fontani F., Commerçon B., Busquet G., Bontemps S., Sánchez-Monge Á., Zapata L. A., Zhang Q., Hennebelle P., di Francesco J.	2014, ApJ 785, 42
1941	The DiskMass Survey. VIII. On the Relationship between Disk Stability and Star Formation	Westfall K. B., Andersen D. R., Bershady M. A., Martinsson T. P. K., Swaters R. A., Verheijen M. A. W.	2014, ApJ 785, 43

1942	Multifrequency Studies of the Peculiar Quasar 4C +21.35 during the 2010 Flaring Activity	Ackermann M., Ajello M., Allafort A., Antolini E., Barbiellini G., Bastieri D., Bellazzini R., Bissaldi E., Bonamente E., Bregeon J., Brigida M., Bruel P., Buehler R., Buson S., Caliandro G. A., Cameron R. A., Caraveo P. A., Cavazzuti E., Cecchi C., Chaves R. C. G., Chekhtman A., Chiang J., Chiaro G., Ciprini S., Claus R., Cohen-Tanugi J., Conrad J., Cutini S., D'Ammando F., de Palma F., Dermer C. D., Silva E. d. C. e., Donato D., Drell P. S., Favuzzi C., Finke J., Focke W. B., Franckowiak A., Fukazawa Y., Fusco P., Gargano F., Gasparrini D., Gehrels N., Giglietto N., Giordano F., Giroletti M., Godfrey G., Grenier I. A., Guiriec S., Hayashida M., Hewitt J. W., Horan D., Hughes R. E., Iafrate G., Johnson A. S., Knödlseder J., Kuss M., Lande J., Larsson S., Latronico L., Longo F., Loparco F., Lovellette M. N., Lubrano P., Mayer M., Mazziotta M. N., McEnery J. E., Michelson P. F., Mizuno T., Monzani M. E., Morselli A., Moskalenko I. V., Murgia S., Nemmen R., Nuss E., Ohsugi T., Orienti M., Orlando E., Perkins J. S., Pesce-Rollins M., Piron F., Pivato G., Porter T. A., Rainò S., Razzano M., Reimer A., Reimer O., Sanchez D. A., Schulz A., Sgrò C., Siskind E. J., Spandre G., Spinelli P., Stawarz Ł., Takahashi H., Takahashi T., Thayer J. G., Thayer J. B., Thompson D. J., Tinivella M., Torres D. F., Tosti G., Troja E., Usher T. L., Vandenbroucke J., Vasileiou V., Vianello G., Vitale V., Werner M., Winer B. L., Wood D. L., Wood K. S., Fermi Large Area Telescope Collaboration, Aleksić J., Ansoldi S., Antonelli L. A., Antoranz P., Babic A., Bangale P., Barres de Almeida U., Barrio J. A., Becerra González J., Bednarek W., Berger K., Bernardini E., Biland A., Blanch O., Bock R. K., Bonnefoy S., Bonnoli G., Borracci F., Bretz T., Carmona E., Carosi A., Carreto Fidalgo D., Colin P., Colombo E., Contreras J. L., Cortina J., Covino S., Da Vela P., Dazzi F., De Angelis A., De Caneva G., De Lotto B., Delgado Mendez C., Doert M., Domínguez A., Dominis Prester D., Dorner D., Doro M., Einecke S., Eisenacher D., Elsaesser D., Farina E., Ferenc D., Fonseca M. V., Font L., Frantzen K., Fruck C., García López R. J., Garczarczyk M., Garrido Terrats D., Gaug M., Giavitto G., Godinović N., González Muñoz A., Gozzini S. R., Hadasch D., Herrero A., Hildebrand D., Hose J., Hrupec D., Idec W., Kadenius V., Kellermann H., Knoetig M. L., Kodani K., Konno Y., Krause J., Kubo H., Kushida J., La Barbera A., Lelas D., Lewandowska N., Lindfors E., Lombardi S., López M., López-Coto R., López-Oramas A., Lorenz E., Lozano I., Makariev M., Mallot K., Maneva G., Mankuzhiyil N., Mannheim K., Maraschi L., Marcote B., Mariotti M., Martínez M., Mazin D., Menzel U., Meucci M., Miranda J. M., Mirzoyan R., Moralejo A., Munar-Adrover P., Nakajima D., Niedzwiecki A., Nishijima K., Nilsson K., Nowak N., Orito R., Overkemping A., Paiano S., Palatiello M., Paneque D., Paoletti R., Paredes J. M., Paredes-Fortuny X., Partini S., Persic M., Prada F., Prada Moroni P. G., Prandini E., Preziuso S., Puljak I., Reinthal R., Rhode W., Ribó M., Rico J., Rodriguez Garcia J., Rügamer S., Saggion A., Saito T., Saito K., Salvati M., Satalecka K., Scalzotto V., Scapin V., Schultz C., Schweizer T., Shore S. N., Sillanpää A., Sitarek J., Snidaric I., Sobczynska D., Spanier F., Stamatescu V., Stamerra A., Steinbring T., Storz J., Sun S., Surić T., Takalo L., Takami H., Tavecchio F., Temnikov P., Terzić T., Tescaro D., Teshima M., Thaele J., Tibolla O., Toyama T., Treves A., Vogler P., Wagner R. M., Zandanel F., Zanin R., MAGIC Collaboration, Aller M. F., Angelakis E., Blinov D. A., Djorgovski S. G., Drake A. J., Efimova N. V., Gurwell M. A., Homan D. C., Jordan B., Kopatskaya E. N., Kovalev Y. Y., Kurtanidze O. M., Lähteenmäki A., Larionov V. M., Lister M. L., Nieppola E., Nikolashvili M. G., Ros E., Savolainen T., Sigua L. A., Tornikoski M.	2014, ApJ 786, 157
1943	Herschel Observations of Extraordinary Sources: Analysis of the HIFI 1.2 THz Wide Spectral Survey toward Orion KL. I. Methods	Crockett N. R., Bergin E. A., Neill J. L., Favre C., Schilke P., Lis D. C., Bell T. A., Blake G., Cernicharo J., Emprechtinger M., Esplugues G. B., Gupta H., Kleshcheva M., Lord S., Marcelino N., McGuire B. A., Pearson J., Phillips T. G., Plume R., van der Tak F., Tercero B., Yu S.	2014, ApJ 787, 112
1944	Spectral Line Survey toward the Spiral Arm of M51 in the 3 and 2 mm Bands	Watanabe Y., Sakai N., Sorai K., Yamamoto S.	2014, ApJ 788, 4
1945	Complex Organic Molecules during Low-mass Star Formation: Pilot Survey Results	Öberg K. I., Lauck T., Graninger D.	2014, ApJ 788, 68
1946	Molecular Gas Heating Mechanisms, and Star Formation Feedback in Merger/Starbursts: NGC 6240 and Arp 193 as Case Studies	Papadopoulos P. P., Zhang Z.-Y., Xilouris E. M., Weiss A., van der Werf P., Israel F. P., Greve T. R., Isaak K. G., Gao Y.	2014, ApJ 788, 153
1947	Dust Formation, Evolution, and Obscuration Effects in the Very High-redshift Universe	Dwek E., Staguhn J., Arendt R. G., Kovacks A., Su T., Benford D. J.	2014, ApJ 788, LL30
1948	The L1157-B1 Astrochemical Laboratory: Measuring the True Formaldehyde Deuteration on Grain Mantles	Fontani F., Codella C., Ceccarelli C., Lefloch B., Viti S., Benedettini M.	2014, ApJ 788, LL43
1949	HerMES: The Rest-frame UV Emission and a Lensing Model for the z = 6.34 Luminous Dusty Starburst Galaxy HFLS3	Cooray A., Calanog J., Wardlow J. L., Bock J., Bridge C., Burgarella D., Bussmann R. S., Casey C. M., Clements D., Conley A., Farrah D., Fu H., Gavazzi R., Ivison R. J., La Porte N., Lo Faro B., Ma B., Magdis G., Oliver S. J., Osage W. A., Pérez-Fournon I., Riechers D., Rigopoulou D., Scott D., Viero M., Watson D.	2014, ApJ 790, 40
1950	The Shock-induced Star Formation Sequence Resulting from a Constant Spiral Pattern Speed	Martínez-García E. E., Puerari I.	2014, ApJ 790, 118
1951	A 30 kpc Chain of "Beads on a String" Star Formation between Two Merging Early Type Galaxies in the Core of a Strong-lensing Galaxy Cluster	Tremblay G. R., Gladders M. D., Baum S. A., O'Dea C. P., Bayliss M. B., Cooke K. C., Dahle H., Davis T. A., Florian M., Rigby J. R., Sharon K., Soto E., Wuyts E.	2014, ApJ 790, LL26
1952	Confirmation of Circumstellar Phosphine	Agúndez M., Cernicharo J., Decin L., Encrenaz P., Teyssier D.	2014, ApJ 790, LL27
1953	Extreme Gas Fractions in Clumpy, Turbulent Disk Galaxies at z ~ 0.1	Fisher D. B., Glazebrook K., Bolatto A., Obreschkow D., Mentuch Cooper E., Wisnioski E., Bassett R., Abraham R. G., Damjanov I., Green A., McGregor P.	2014, ApJ 790, LL30
1954	The Census of Complex Organic Molecules in the Solar-type Protostar IRAS16293-2422	Jaber A. A., Ceccarelli C., Kahane C., Caux E.	2014, ApJ 791, 29
1955	Distributed Low-mass Star Formation in the IRDC G34.43+00.24	Foster J. B., Arce H. G., Kassis M., Sanhueza P., Jackson J. M., Finn S. C., Offner S., Sakai T., Sakai N., Yamamoto S., Guzmán A. E., Rathborne J. M.	2014, ApJ 791, 108

1956	Molecular Gas in the X-Ray Bright Group NGC 5044 as Revealed by ALMA	David L. P., Lim J., Forman W., Vrtilek J., Combes F., Salome P., Edge A., Hamer S., Jones C., Sun M., O'Sullivan E., Gastaldello F., Bardelli S., Temi P., Schmitt H., Ohyama Y., Mathews W., Brighenti F., Giacintucci S., Trung D.-V.	2014, ApJ 792, 94
1957	High D_2O/HDO Ratio in the Inner Regions of the Low-mass Protostar NGC 1333 IRAS2A	Coutens A., Jørgensen J. K., Persson M. V., van Dishoeck E. F., Vastel C., Taquet V.	2014, ApJ 792, LL5
1958	Regularity Underlying Complexity: A Redshift-independent Description of the Continuous Variation of Galaxy-scale Molecular Gas Properties in the Mass-star Formation Rate Plane	Sargent M. T., Daddi E., Béthermin M., Aussel H., Magdis G., Hwang H. S., Juneau S., Elbaz D., da Cunha E.	2014, ApJ 793, 19
1959	IRAM 30 m Large Scale Survey of ^{12}CO(2-1) and ^{13}CO(2-1) Emission in the Orion Molecular Cloud	Berné O., Marcelino N., Cernicharo J.	2014, ApJ 795, 13
1960	The Origin of Complex Organic Molecules in Prestellar Cores	Vastel C., Ceccarelli C., Lefloch B., Bachiller R.	2014, ApJ 795, LL2
1961	Isotopologues of Dense Gas Tracers in NGC 1068	Wang J., Zhang Z.-Y., Qiu J., Shi Y., Zhang J., Fang M.	2014, ApJ 796, 57
1962	A Far-infrared Spectroscopic Survey of Intermediate Redshift (Ultra) Luminous Infrared Galaxies	Magdis G. E., Rigopoulou D., Hopwood R., Huang J.-S., Farrah D., Pearson C., Alonso-Herrero A., Bock J. J., Clements D., Cooray A., Griffin M. J., Oliver S., Perez Fournon I., Riechers D., Swinyard B. M., Scott D., Thatte N., Valtchanov I., Vaccari M.	2014, ApJ 796, 63
1963	Cold Molecular Gas in Merger Remnants. I. Formation of Molecular Gas Disks	Ueda J., Iono D., Yun M. S., Crocker A. F., Narayanan D., Komugi S., Espada D., Hatsukade B., Kaneko H., Matsuda Y., Tamura Y., Wilner D. J., Kawabe R., Pan H.-A.	2014, ApJS 214, 1
1964	Cold gas dynamics in Hydra-A: evidence for a rotating disc	Hamer S. L., Edge A. C., Swinbank A. M., Oonk J. B. R., Mittal R., McNamara B. R., Russell H. R., Bremer M. N., Combes F., Fabian A. C., Nesvadba N. P. H., O'Dea C. P., Baum S. A., Salomé P., Tremblay G., Donahue M., Ferland G. J., Sarazin C. L.	2014, MNRAS 437, 862
1965	Probing the turbulent ambipolar diffusion scale in molecular clouds with spectroscopy	Hezareh T., Csengeri T., Houde M., Herpin F., Bontemps S.	2014, MNRAS 438, 663
1966	Gas kinematics and excitation in the filamentary IRDC G035.39-00.33	Jiménez-Serra I., Caselli P., Fontani F., Tan J. C., Henshaw J. D., Kainulainen J., Hernandez A. K.	2014, MNRAS 439, 1996
1967	A Herschel and BIMA study of the sequential star formation near the W 48A H II region	Rygl K. L. J., Goedhart S., Polychroni D., Wyrowski F., Motte F., Elia D., Nguyen-Luong Q., Didelon P., Pestalozzi M., Benedettini M., Molinari S., André P., Fallscheer C., Gibb A., Giorgio A. M. d., Hill T., Könyves V., Marston A., Pezzuto S., Rivera-Ingraham A., Schisano E., Schneider N., Spinoglio L., Ward-Thompson D., White G. J.	2014, MNRAS 440, 427
1968	The dynamical properties of dense filaments in the infrared dark cloud G035.39-00.33	Henshaw J. D., Caselli P., Fontani F., Jiménez-Serra I., Tan J. C.	2014, MNRAS 440, 2860
1969	The variation in molecular gas depletion time among nearby galaxies: what are the main parameter dependences?	Huang M.-L., Kauffmann G.	2014, MNRAS 443, 1329
1970	A high-resolution study of complex organic molecules in hot cores	Calcutt H., Viti S., Codella C., Beltrán M. T., Fontani F., Woods P. M.	2014, MNRAS 443, 3157
1971	A Bayesian blind survey for cold molecular gas in the Universe	Lentati L., Carilli C., Alexander P., Walter F., Decarli R.	2014, MNRAS 443, 3741
1972	The ATLAS^{3D} Project - XXVIII. Dynamically driven star formation suppression in early-type galaxies	Davis T. A., Young L. M., Crocker A. F., Bureau M., Blitz L., Alatalo K., Emsellem E., Naab T., Bayet E., Bois M., Bournaud F., Cappellari M., Davies R. L., de Zeeuw P. T., Duc P.-A., Khochfar S., Krajnović D., Kuntschner H., McDermid R. M., Morganti R., Oosterloo T., Sarzi M., Scott N., Serra P., Weijmans A.-M.	2014, MNRAS 444, 3427
1973	Molecules with a peptide link in protostellar shocks: a comprehensive study of L1157	Mendoza E., Lefloch B., López-Sepulcre A., Ceccarelli C., Codella C., Boechat-Roberty H. M., Bachiller R.	2014, MNRAS 445, 151
1974	Water deuterium fractionation in the high-mass star-forming region G34.26+0.15 based on Herschel/HIFI data	Coutens A., Vastel C., Hincelin U., Herbst E., Lis D. C., Chavarría L., Gérin M., van der Tak F. F. S., Persson C. M., Goldsmith P. F., Caux E.	2014, MNRAS 445, 1299
1975	Mid-J CO observations of Perseus B1-East 5: evidence for turbulent dissipation via low-velocity shocks	Pon A., Johnstone D., Kaufman M. J., Caselli P., Plume R.	2014, MNRAS 445, 1508
1976	New insights on the recoiling/binary black hole candidate J0927+2943 via molecular gas observations	Decarli R., Dotti M., Mazzucchelli C., Montuori C., Volonteri M.	2014, MNRAS 445, 1558
1977	Uncorrelated Volatile Behavior during the 2011 Apparition of Comet C/2009 P1 Garradd	Feaga L. M., A'Hearn M. F., Farnham T. L., Bodewits D., Sunshine J. M., Gersch A. M., Protopapa S., Yang B., Drahus M., Schleicher D. G.	2014, Astron. J. 147, 24
1978	Binary orbits as the driver of γ-ray emission and mass ejection in classical novae	Chomiuk L., Linford J. D., Yang J., O'Brien T. J., Paragi Z., Mioduszewski A. J., Beswick R. J., Cheung C. C., Mukai K., Nelson T., Ribeiro V. A. R. M., Rupen M. P., Sokoloski J. L., Weston J., Zheng Y., Bode M. F., Eyres S., Roy N., Taylor G. B.	2014, Nature 514, 339
1979	Molecules in the circumnuclear disk of the Galactic center	Harada N., Riquelme D., Viti S., Menten K., Requena-Torres M., Güsten R., Hochgürtel S.	2014, Proc. of the IAU 303, 78
1980	SiO and CH_3OH mega-masers in NGC 1068	Wang J., Zhang J., Gao Y., Zhang Z.-Y., Li D., Fang M., Shi Y.	2014, Nature Communications 5, 5449
1981	Lyman alpha emitting and related star-forming galaxies at high redshift	Schaerer D.	2014, arXiv 1407.2796
1982	3C 285: a nearby galaxy with jet-induced star formation	Salomé Q., Salomé P., Combes F.	2014, SF2A, 371
1983	Understanding the state of the gas surrounding Andromeda's black hole.	Melchior A.-L., Combes F.	2014, SF2A, 351
1984	Study for Planck Cold Clumps with molecular lines	Wu Y.	2014, AAS Top. Conf Series Vol. 4, 107
1985	Detection of ethylene glycol - toward W51/e2 and G34.3+0.02	Lykke J. M., Favre C.	2014, AAS Top. Conf Series Vol. 4, 108

1986	HCO emission toward the X-ray reflexion nebula Sgr B2 in the Galactic Center	Armijos Abendaño J.	2014, 40th COSPAR Scient. Assembly, 120
1987	Probing the jet acceleration region - S5 0716+714 - a case study	Rani B., Marscher A., Jorstad S., Hodgson J., Krichbaum T., Fuhrmann L., Zensus A.	2014, 40th COSPAR Scient. Assembly, 2697
1988	Millimeter emission from "water fountain" evolved stars	Duran-Rojas M.„ Gomez J. F., Osorio M. C., Anglada G., Rizzo J. R., Suárez O., Miranda L. F., D'Alessio P., Calvet N.	2014, Asymmetrical Planet. Nebulae VI Conf, 19
1989	SHAPEMOL: Modelling molecular line emission in protoplanetary and planetary nebulae with SHAPE	Santander-García M., Bujarrabal V., Steffen W., Koning N.	2014, Asymmetrical Planet. Nebulae VI Conf, 90
1990	Probing the Earliest Stages of Massive Star Formation Through Observations of N_2D^+	Fontani F.	2014, Astrophys. and Space Science Proc. 36, 419
1991	Toward a Chemical Evolutionary Sequence in High-Mass Star Formation	Gerner T., Beuther H., Semenov D., Linz H., Vasyunina T., Henning T.	2014, Astrophys. and Space Science Proc. 36, 415
1992	Properties of Interstellar Filaments as Derived from Herschel Observations	Arzoumanian D., André P., Peretto N., Könyves V.	2014, Astrophys. and Space Science Proc. 36, 259
1993	NH_2D in Orion KL: Results from ALMA, EVLA, and IRAM	Lucy A. B., Wootten A., Marcelino N.	2014, AAS 223, #454.38
1994	Temperature, Density, and Collision Rates in the IC63 Nebula	Vaillancourt J. E., Andersson B., Polehampton E., Sanders J., Widicus-Weaver S.	2014, AAS 223, #454.37
1995	The Molecular Gas - Star Formation Connection in an Extended Ultraviolet (XUV) Disk	Watson L. C., Martini P., Lisenfeld U., Boeker T., Gil de Paz A., Schinnerer E.	2014, AAS 223, #454.22
1996	Examining the Initial Conditions of Star Formation Through Dense Gas Kinematics	Mead A. T., Tobin J. J., Smith R.	2014, AAS 223, #454.07
1997	Tracing molecular gas content through optical extinction within nearby galaxies	Avalani B. R., Groves B., Kreckel K.	2014, AAS 223, #454.02
1998	The chemical inventory of pre/proto-stellar cores	Marcelino N., Cernicharo J., Roueff E., Gerin M., Fuente A.	2014, AAS 223, #331.06
1999	The CO-to-H_2 Conversion Factor and Dust-to-Gas Ratio on Kiloparsec Scales in Nearby Galaxies	Sandstrom K., Leroy A. K., Kennicutt R., KINGFISH Team, HERACLES Team	2014, AAS 223, #312.04
2000	Infall as a Function of Position and Molecular Tracer in L1544 and L694	Keown J. A., Schnee S., Bourke T. L., Friesen R.	2014, AAS 223, #244.13
2001	Modeling the Star Formation Properties of Massive Galaxies with the COLD GASS Survey	Hopkins E., Shetty R., Bigiel F., Klessen R., Saintonge A., Willman B.	2014, AAS 223, #244.06
2002	Inferring the Evolutionary Stages of High-mass Star-forming Regions from Chemistry	Feng S., Beuther H., Henning T., Semenov D., Linz H.	2014, AAS 223, #214.02
2003	Broad-band study of selected γ-ray active Blazars	Rani, B.	2014, Thesis

2014 PUBLICATION LIST: IRAM (CO) AUTHORS

1875	Kinematics of the ionized-to-neutral interfaces in Monoceros R2	Pilleri P., Fuente A., Gerin M., Cernicharo J., Goicoechea J. R., Ossenkopf V., Joblin C., González-García M., Treviño-Morales S. P., Sánchez-Monge Á., Pety J., Berné O., Kramer C.	2014, A&A 561, AA69
1876	SDC13 infrared dark clouds: Longitudinally collapsing filaments?	Peretto N., Fuller G. A., André P., Arzoumanian D., Rivilla V. M., Bardeau S., Duarte Puertas S., Guzman Fernandez J. P., Lenfestey C., Li G.-X., Olguin F. A., Röck B. R., de Villiers H., Williams J.	2014, A&A 561, AA83
1877	Variation in the dust emissivity index across M 33 with Herschel and Spitzer (HerM 33es)	Tabatabaei F. S., Braine J., Xilouris E. M., Kramer C., Boquien M., Combes F., Henkel C., Relano M., Verley S., Gratier P., Israel F., Wiedner M. C., Röllig M., Schuster K. F., van der Werf P.	2014, A&A 561, AA95
1878	Searches for HCl and HF in comets 103P/Hartley 2 and C/2009 P1 (Garradd) with the Herschel Space Observatory	Bockelée-Morvan D., Biver N., Crovisier J., Lis D. C., Hartogh P., Moreno R., de Val-Borro M., Blake G. A., Szutowicz S., Boissier J., Cernicharo J., Charnley S. B., Combi M., Cordiner M. A., de Graauw T., Encrenaz P., Jarchow C., Kidger M., Küppers M., Milam S. N., Müller H. S. P., Phillips T. G., Rengel M.	2014, A&A 562, AA5
1879	Massive molecular outflows and evidence for AGN feedback from CO observations	Cicone C., Maiolino R., Sturm E., Graciá-Carpio J., Feruglio C., Neri R., Aalto S., Davies R., Fiore F., Fischer J., García-Burillo S., González-Alfonso E., Hailey-Dunsheath S., Piconcelli E., Veilleux S.	2014, A&A 562, AA21
1880	High-resolution C^+ imaging of HDF850.1 reveals a merging galaxy at z = 5.185	Neri R., Downes D., Cox P., Walter F.	2014, A&A 562, AA35
1881	The molecular circumnuclear disk (CND) in Centaurus A. A multi-transition CO and [CI] survey with Herschel, APEX, JCMT, and SEST	Israel F. P., Güsten R., Meijerink R., Loenen A. F., Requena-Torres M. A., Stutzki J., van der Werf P., Harris A., Kramer C., Martin-Pintado J., Weiss, A.	2014, A&A 562, AA96
1882	First results from the CALYPSO IRAM-PdBI survey. I. Kinematics of the inner envelope of NGC 1333-IRAS2A	Maret S., Belloche A., Maury A. J., Gueth F., André P., Cabrit S., Codella C., Bontemps S.	2014, A&A 563, LL1
1883	First results from the CALYPSO IRAM-PdBI survey. II. Resolving the hot corino in the Class 0 protostar NGC 1333-IRAS2A	Maury A. J., Belloche A., André P., Maret S., Gueth F., Codella C., Cabrit S., Testi L., Bontemps S.	2014, A&A 563, LL2
1884	First results from the CALYPSO IRAM-PdBI survey. III. Monopolar jets driven by a proto-binary system in NGC 1333-IRAS2A	Codella C., Maury A. J., Gueth F., Maret S., Belloche A., Cabrit S., André P.	2014, A&A 563, LL3
1885	Chemistry in isolation: High CCH/HCO^+ line ratio in the AMIGA galaxy CIG 638	Martín S., Verdes-Montenegro L., Aladro R., Espada D., Argudo-Fernández M., Kramer C., Scott T. C.	2014, A&A 563, LL6
1886	HCO, c-C_3H and CF^+: three new molecules in diffuse, translucent and "spiral-arm" clouds	Liszt H. S., Pety J., Gerin M., Lucas R.	2014, A&A 564, AA64

1887	Faint disks around classical T Tauri stars: Small but dense enough to form planets	Piétu V., Guilloteau S., Di Folco E., Dutrey A., Boehler Y.	2014, A&A 564, AA95
1888	Fueling the central engine of radio galaxies. III. Molecular gas and star formation efficiency of 3C 293	Labiano A., García-Burillo S., Combes F., Usero A., Soria-Ruiz R., Piqueras López J., Fuente A., Hunt L., Neri R.	2014, A&A 564, AA128
1889	Carbon and oxygen isotope ratios in starburst galaxies: New data from NGC 253 and Mrk 231 and their implications	Henkel C., Asiri H., Ao Y., Aalto S., Danielson A. L. R., Papadopoulos P. P., García-Burillo S., Aladro R., Impellizzeri C. M. V., Mauersberger R., Martín S., Harada N.	2014, A&A 565, AA3
1890	Two active states of the narrow-line gamma-ray-loud AGN GB 1310+487	Sokolovsky K. V., Schinzel F. K., Tanaka Y. T., Abolmasov P. K., Angelakis E., Bulgarelli A., Carrasco L., Cenko S. B., Cheung C. C., Clubb K. I., D'Ammando F., Escande L., Fegan S. J., Filippenko A. V., Finke J. D., Fuhrmann L., Fukazawa Y., Hays E., Healey S. E., Ikejiri Y., Itoh R., Kawabata K. S., Komatsu T., Kovalev Y. A., Kovalev Y. Y., Krichbaum T. P., Larsson S., Lister M. L., Lott B., Max-Moerbeck W., Nestoras I., Pittori C., Pursimo T., Pushkarev A. B., Readhead A. C. S., Recillas E., Richards J. L., Riquelme D., Romani R. W., Sakimoto K., Sasada M., Schmidt R., Shaw M. S., Sievers A., Thompson D. J., Uemura M., Ungerechts H., Vercellone S., Verrecchia F., Yamanaka M., Yoshida M., Zensus J. A.	2014, A&A 565, AA26
1891	Heating of the molecular gas in the massive outflow of the local ultraluminous-infrared and radio-loud galaxy 4C12.50	Dasyra K. M., Combes F., Novak G. S., Bremer M., Spinoglio L., Pereira Santaella M., Salomé P., Falgarone E.	2014, A&A 565, AA46
1892	The multi-scale environment of RS Cancri from CO and H I observations	Hoai D. T., Matthews L. D., Winters J. M., Nhung P. T., Gérard E., Libert Y., Le Bertre T.	2014, A&A 565, AA54
1893	Gas reservoir of a hyper-luminous quasar at z = 2.6	Feruglio C., Bongiorno A., Fiore F., Krips M., Brusa M., Daddi E., Gavignaud I., Maiolino R., Piconcelli E., Sargent M., Vignali C., Zappacosta L.	2014, A&A 565, AA91
1894	ALMA reveals the feeding of the Seyfert 1 nucleus in NGC 1566	Combes F., García-Burillo S., Casasola V., Hunt L. K., Krips M., Baker A. J., Boone F., Eckart A., Marquez I., Neri R., Schinnerer E., Tacconi L. J.	2014, A&A 565, AA97
1895	GG Tauri: the fifth element	Di Folco E., Dutrey A., Le Bouquin J.-B., Lacour S., Berger J.-P., Köhler R., Guilloteau S., Piétu V., Bary J., Beck T., Beust H., Pantin E.	2014, A&A 565, LL2
1896	A simultaneous 3.5 and 1.3 mm polarimetric survey of active galactic nuclei in the northern sky	Agudo I., Thum C., Gómez J. L., Wiesemeyer H.	2014, A&A 566, AA59
1897	Detection of a dense clump in a filament interacting with W51e2	Mookerjea B., Vastel C., Hassel G. E., Gerin M., Pety J., Goldsmith P. F., Black J. H., Giesen T., Harrison T., Persson C. M., Stutzki J.	2014, A&A 566, AA61
1898	Imaging the disk around IRAS 20126+4104 at subarcsecond resolution	Cesaroni R., Galli D., Neri R., Walmsley C. M.	2014, A&A 566, AA73
1899	GRB 120422A/SN 2012bz: Bridging the gap between low- and high-luminosity gamma-ray bursts	Schulze S., Malesani D., Cucchiara A., Tanvir N. R., Krühler T., de Ugarte Postigo A., Leloudas G., Lyman J., Bersier D., Wiersema K., Perley D. A., Schady P., Gorosabel J., Anderson J. P., Castro-Tirado A. J., Cenko S. B., De Cia A., Ellerbroek L. E., Fynbo J. P. U., Greiner J., Hjorth J., Kann D. A., Kaper L., Klose S., Levan A. J., Martín S., O'Brien P. T., Page K. L., Pignata G., Rapaport S., Sánchez-Ramírez R., Sollerman J., Smith I. A., Sparre M., Thöne C. C., Watson D. J., Xu D., Bauer F. E., Bayliss M., Björnsson G., Bremer M., Cano Z., Covino S., D'Elia V., Frail D. A., Geier S., Goldoni P., Hartoog O. E., Jakobsson P., Korhonen H., Lee K. Y., Milvang-Jensen B., Nardini M., Nicuesa Guelbenzu A., Oguri M., Pandey S. B., Petitpas G., Rossi A., Sandberg A., Schmidl S., Tagliaferri G., Tilanus R. P. J., Winters J. M., Wright D., Wuyts E.	2014, A&A 566, AA102
1900	An ALMA Early Science survey of molecular absorption lines toward PKS 1830-211. Analysis of the absorption profiles	Muller S., Combes F., Guélin M., Gérin M., Aalto S., Beelen A., Black J. H., Curran S. J., Darling J., V-Trung D., García-Burillo S., Henkel C., Horellou C., Martín S., Martí-Vidal I., Menten K. M., Murphy M. T., Ott J., Wiklind T., Zwaan M. A.	2014, A&A 566, AA112
1901	Complex organic molecules in comets C/2012 F6 (Lemmon) and C/2013 R1 (Lovejoy): detection of ethylene glycol and formamide	Biver N., Bockelée-Morvan D., Debout V., Crovisier J., Boissier J., Lis D. C., Dello Russo N., Moreno R., Colom P., Paubert G., Vervack R., Weaver H. A.	2014, A&A 566, LL5
1902	Detection of chloronium and measurement of the $^{35}Cl/^{37}Cl$ isotopic ratio at z = 0.89 toward PKS 1830-211	Muller S., Black J. H., Guélin M., Henkel C., Combes F., Gérin M., Aalto S., Beelen A., Darling J., Horellou C., Martín S., Menten K. M., V-Trung D., Zwaan M. A.	2014, A&A 566, LL6
1903	The masses of young stars: CN as a probe of dynamical masses	Guilloteau S., Simon M., Piétu V., Di Folco E., Dutrey A., Prato L., Chapillon E.	2014, A&A 567, AA117
1904	The IRAM M 33 CO(2-1) survey. A complete census of molecular gas out to 7 kpc	Druard C., Braine J., Schuster K. F., Schneider N., Gratier P., Bontemps S., Boquien M., Combes F., Corbelli E., Henkel C., Herpin F., Kramer C., van der Tak F., van der Werf P.	2014, A&A 567, AA118
1905	Molecular line emission in NGC 1068 imaged with ALMA. I. An AGN-driven outflow in the dense molecular gas	García-Burillo S., Combes F., Usero A., Aalto S., Krips M., Viti S., Alonso-Herrero A., Hunt L. K., Schinnerer E., Baker A. J., Boone F., Casasola V., Colina L., Costagliola F., Eckart A., Fuente A., Henkel C., Labiano A., Martín S., Márquez I., Muller S., Planesas P., Ramos Almeida C., Spaans M., Tacconi L. J., van der Werf P. P.	2014, A&A 567, AA125
1906	First detection of [N II] 205 μm absorption in interstellar gas. Herschel-HIFI observations towards W 31C, W 49N, W 51, and G34.3+0.1	Persson C. M., Gerin M., Mookerjea B., Black J. H., Olberg M., Goicoechea J. R., Hassel G. E., Falgarone E., Levrier F., Menten K. M., Pety J.	2014, A&A 568, AA37
1907	The ALMA view of the protostellar system HH212. The wind, the cavity, and the disk	Codella C., Cabrit S., Gueth F., Podio L., Leurini S., Bachiller R., Gusdorf A., Lefloch B., Nisini B., Tafalla M., Yvart W.	2014, A&A 568, LL5
1908	Molecular tendrils feeding star formation in the Eye of the Medusa. The Medusa merger in high resolution ^{12}CO 2-1 maps	König S., Aalto S., Lindroos L., Muller S., Gallagher J. S., Beswick R. J., Petitpas G., Jütte E.	2014, A&A 569, AA6
1909	Performance and calibration of the NIKA camera at the IRAM 30-meter telescope	Catalano A., Calvo M., Ponthieu N., Adam R., Adane A., Ade P., André P., Beelen A., Belier B., Benoît A., Bideaud A., Billot N., Boudou N., Bourrion O., Coiffard G., Comis B., D'Addabbo A., Désert F.-X., Doyle S., Goupy J., Kramer C., Leclercq S., Macías-Pérez J. F., Martino J., Mauskopf P., Mayet F., Monfardini A., Pajot F., Pascale E., Perotto L., Revéret V., Rodriguez L., Savini G., Schuster K., Sievers A., Tucker C., Zylka R.	2014, A&A 569, AA9

1910	Deuteration around the ultracompact HII region Monoceros R2	Treviño-Morales S. P., Pilleri P., Fuente A., Kramer C., Roueff E., González-García M., Cernicharo J., Gerin M., Goicoechea J. R., Pety J., Berné O., Ossenkopf V., Ginard D., García-Burillo S., Rizzo J. R., Viti S.	2014, A&A 569, AA19
1911	MAGIC gamma-ray and multi-frequency observations of flat spectrum radio quasar PKS 1510-089 in early 2012	Aleksić J., Ansoldi S., Antonelli L. A., Antoranz P., Babic A., Bangale P., Barres de Almeida U., Barrio J. A., Becerra González J., Bednarek W., Bernardini E., Biland A., Blanch O., Bonnefoy S., Bonnoli G., Borracci F., Bretz T., Carmona E., Carosi A., Carreto Fidalgo D., Colin P., Colombo E., Contreras J. L., Cortina J., Covino S., Da Vela P., Dazzi F., De Angelis A., De Caneva G., De Lotto B., Delgado Mendez C., Doert M., Domínguez A., Dominis Prester D., Dorner D., Doro M., Einecke S., Eisenacher D., Elsaesser D., Farina E., Ferenc D., Fonseca M. V., Font L., Frantzen K., Fruck C., García López R. J., Garczarczyk M., Garrido Terrats D., Gaug M., Godinović N., González Muñoz A., Gozzini S. R., Hadasch D., Hayashida M., Herrera J., Herrero A., Hildebrand D., Hose J., Hrupec D., Idec W., Kadenius V., Kellermann H., Kodani K., Konno Y., Krause J., Kubo H., Kushida J., La Barbera A., Lelas D., Lewandowska N., Lindfors E., Lombardi S., López M., López-Coto R., López-Oramas A., Lorenz E., Lozano I., Makariev M., Mallot K., Maneva G., Mankuzhiyil N., Mannheim K., Maraschi L., Marcote B., Mariotti M., Martínez M., Mazin D., Menzel U., Meucci M., Miranda J. M., Mirzoyan R., Moralejo A., Munar-Adrover P., Nakajima D., Niedzwiecki A., Nilsson K., Nishijima K., Noda K., Nowak N., Orito R., Overkemping A., Paiano S., Palatiello M., Paneque D., Paoletti R., Paredes J. M., Paredes-Fortuny X., Partini S., Persic M., Prada F., Prada Moroni P. G., Prandini E., Preziuso S., Puljak I., Reinthal R., Rhode W., Ribó M., Rico J., Rodriguez Garcia J., Rügamer S., Saggion A., Saito T., Saito K., Satalecka K., Scalzotto V., Scapin V., Schultz C., Schweizer T., Shore S. N., Sillanpää A., Sitarek J., Snidaric I., Sobczynska D., Spanier F., Stamatescu V., Stamerra A., Steinbring T., Storz J., Strzys M., Sun S., Surić T., Takalo L., Takami H., Tavecchio F., Temnikov P., Terzić T., Tescaro D., Teshima M., Thaele J., Tibolla O., Torres D. F., Toyama T., Treves A., Uellenbeck M., Vogler P., Wagner R. M., Zandanel F., Zanin R.	2014, A&A 569, AA46
1912	First observation of the thermal Sunyaev-Zel'dovich effect with kinetic inductance detectors	Adam R., Comis B., Macías-Pérez J. F., Adane A., Ade P., André P., Beelen A., Belier B., Benoît A., Bideaud A., Billot N., Boudou N., Bourrion O., Calvo M., Catalano A., Coiffard G., D'Addabbo A., Désert F.-X., Doyle S., Goupy J., Kramer C., Leclercq S., Martino J., Mauskopf P., Mayet F., Monfardini A., Pajot F., Pascale E., Perotto L., Pointecouteau E., Ponthieu N., Revéret V., Rodriguez L., Savini G., Schuster K., Sievers A., Tucker C., Zylka R.	2014, A&A 569, AA66
1913	The dark nature of GRB 130528A and its host galaxy	Jeong S., Castro-Tirado A. J., Bremer M., Winters J. M., Gorosabel J., Guziy S., Pandey S. B., Jelínek M., Sánchez-Ramírez R., Sokolov I. V., Orekhova N. V., Moskvitin A. S., Tello J. C., Cunniffe R., Lara-Gil O., Oates S. R., Pérez-Ramírez D., Bai J., Fan Y., Wang C., Park I. H.	2014, A&A 569, AA93
1914	Revised spectroscopic parameters of SH^+ from ALMA and IRAM 30 m observations	Müller H. S. P., Goicoechea J. R., Cernicharo J., Agúndez M., Pety J., Cuadrado S., Gerin M., Dumas G., Chapillon E.	2014, A&A 569, LL5
1915	The W43-MM1 mini-starburst ridge, a test for star formation efficiency models	Louvet F., Motte F., Hennebelle P., Maury A., Bonnell I., Bontemps S., Gusdorf A., Hill T., Gueth F., Peretto N., Duarte-Cabral A., Stephan G., Schilke P., Csengeri T., Nguyen Luong Q., Lis D. C.	2014, A&A 570, AA15
1916	Molecular line emission in NGC 1068 imaged with ALMA. II. The chemistry of the dense molecular gas	Viti S., García-Burillo S., Fuente A., Hunt L. K., Usero A., Henkel C., Eckart A., Martin S., Spaans M., Muller S., Combes F., Krips M., Schinnerer E., Casasola V., Costagliola F., Marquez I., Planesas P., van der Werf P. P., Aalto S., Baker A. J., Boone F., Tacconi L. J.	2014, A&A 570, AA28
1917	New molecules in IRC +10216: confirmation of C_5S and tentative identification of MgCCH, NCCP, and SiH_3CN	Agúndez M., Cernicharo J., Guélin M.	2014, A&A 570, AA45
1918	Dense molecular globulettes and the dust arc toward the runaway O star AE Aurigae (HD 34078)	Gratier P., Pety J., Boissé P., Cabrit S., Lesaffre P., Gerin M., Pineau des Forêts G.	2014, A&A 570, AA71
1919	Origin of the ionized wind in MWC 349A	Báez-Rubio A., Martín-Pintado J., Thum C., Planesas P., Torres-Redondo J.	2014, A&A 571, LL4
1920	Molecular Jet of IRAS 04166+2706	Wang L.-Y., Shang H., Su Y.-N., Santiago-García J., Tafalla M., Zhang Q., Hirano N., Lee C.-F.	2014, ApJ 780, 49
1921	An ALMA Survey of Sub-millimeter Galaxies in the Extended Chandra Deep Field South: Sub-millimeter Properties of Color-selected Galaxies	Decarli R., Smail I., Walter F., Swinbank A. M., Chapman S., Coppin K. E. K., Cox P., Dannerbauer H., Greve T. R., Hodge J. A., Ivison R., Karim A., Knudsen K. K., Lindroos L., Rix H.-W., Schinnerer E., Simpson J. M., van der Werf P., Weiß A.	2014, ApJ 780, 115
1922	The Afterglow of GRB 130427A from 1 to 10^{16} GHz	Perley D. A., Cenko S. B., Corsi A., Tanvir N. R., Levan A. J., Kann D. A., Sonbas E., Wiersema K., Zheng W., Zhao X.-H., Bai J.-M., Bremer M., Castro-Tirado A. J., Chang L., Clubb K. I., Frail D., Fruchter A., Göğüş E., Greiner J., Güver T., Horesh A., Filippenko A. V., Klose S., Mao J., Morgan A. N., Pozanenko A. S., Schmidl S., Stecklum B., Tanga M., Volnova A. A., Volvach A. E., Wang J.-G., Winters J.-M., Xin Y.-X.	2014, ApJ 781, 37
1923	A Molecular Line Scan in the Hubble Deep Field North	Decarli R., Walter F., Carilli C., Riechers D., Cox P., Neri R., Aravena M., Bell E., Bertoldi F., Colombo D., Da Cunha E., Daddi E., Dickinson M., Downes D., Ellis R., Lentati L., Maiolino R., Menten K. M., Rix H.-W., Sargent M., Stark D., Weiner B., Weiss A.	2014, ApJ 782, 78
1924	A Molecular Line Scan in the Hubble Deep Field North: Constraints on the CO Luminosity Function and the Cosmic H_2 Density	Walter F., Decarli R., Sargent M., Carilli C., Dickinson M., Riechers D., Ellis R., Stark D., Weiner B., Aravena M., Bell E., Bertoldi F., Cox P., Da Cunha E., Daddi E., Downes D., Lentati L., Maiolino R., Menten K. M., Neri R., Rix H.-W., Weiss A.	2014, ApJ 782, 79
1925	Varying [C II]/[N II] Line Ratios in the Interacting System BR1202-0725 at z = 4.7	Decarli R., Walter F., Carilli C., Bertoldi F., Cox P., Ferkinhoff C., Groves B., Maiolino R., Neri R., Riechers D., Weiss A.	2014, ApJ 782, LL17
1926	An Observational Investigation of the Identity of B11244 ($l\text{-}C_3H^+/C_3H^+$)	McGuire B. A., Carroll P. B., Gratier P., Guzmán V., Pety J., Roueff E., Gerin M., Blake G. A., Remijan A. J.	2014, ApJ 783, 36
1927	The PdBI Arcsecond Whirlpool Survey (PAWS): Environmental Dependence of Giant Molecular Cloud Properties in M51	Colombo D., Hughes A., Schinnerer E., Meidt S. E., Leroy A. K., Pety J., Dobbs C. L., García-Burillo S., Dumas G., Thompson T. A., Schuster K. F., Kramer C.	2014, ApJ 784, 3

1928	The PdBI Arcsecond Whirlpool Survey (PAWS): Multi-phase Cold Gas Kinematic of M51	Colombo D., Meidt S. E., Schinnerer E., García-Burillo S., Hughes A., Pety J., Leroy A. K., Dobbs C. L., Dumas G., Thompson T. A., Schuster K. F., Kramer C.	2014, ApJ 784, 4
1929	Search for [C II] Emission in z = 6.5-11 Star-forming Galaxies	González-López J., Riechers D. A., Decarli R., Walter F., Vallini L., Neri R., Bertoldi F., Bolatto A. D., Carilli C. L., Cox P., da Cunha E., Ferrara A., Gallerani S., Infante L.	2014, ApJ 784, 99
1930	The Heating of Mid-infrared Dust in the Nearby Galaxy M33: A Testbed for Tracing Galaxy Evolution	Calapa M. D., Calzetti D., Draine B. T., Boquien M., Kramer C., Xilouris M., Verley S., Braine J., Relaño M., van der Werf P., Israel F., Hermelo I., Albrecht M.	2014, ApJ 784, 130
1931	Localized SiO Emission Triggered by the Passage of the W51C Supernova Remnant Shock	Dumas G., Vaupré S., Ceccarelli C., Hily-Blant P., Dubus G., Montmerle T., Gabici S.	2014, ApJ 786, LL24
1932	PdBI Cold Dust Imaging of Two Extremely Red H - [4.5] >4 Galaxies Discovered with SEDS and CANDELS	Caputi K. I., MichaŃowski M. J., Krips M., Geach J. E., Ashby M. L. N., Huang J.-S., Fazio G. G., Koekemoer A. M., Popping G., Spaans M., Castellano M., Dunlop J. S., Fontana A., Santini P.	2014, ApJ 788, 126
1933	The GISMO Two-millimeter Deep Field in GOODS-N	Staguhn J. G., Kovács A., Arendt R. G., Benford D. J., Decarli R., Dwek E., Fixsen D. J., Hilton G. C., Irwin K. D., Jhabvala C. A., Karim A., Leclercq S., Maher S. F., Miller T. M., Moseley S. H., Sharp E. H., Walter F., Wollack E. J.	2014, ApJ 790, 77
1934	The Identification of Filaments on Far-infrared and Submillimiter Images: Morphology, Physical Conditions and Relation with Star Formation of Filamentary Structure	Schisano E., Rygl K. L. J., Molinari S., Busquet G., Elia D., Pestalozzi M., Polychroni D., Billot N., Carey S., Paladini R., Noriega-Crespo A., Moore T. J. T., Plume R., Glover S. C. O., Vázquez-Semadeni E.	2014, ApJ 791, 27
1935	η Carinae Baby Homunculus Uncovered by ALMA	Abraham Z., Falceta-Gonçalves D., Beaklini P. P. B.	2014, ApJ 791, 95
1936	ALMA Observation of 158 μm [C II] Line and Dust Continuum of a z = 7 Normally Star-forming Galaxy in the Epoch of Reionization	Ota K., Walter F., Ohta K., Hatsukade B., Carilli C. L., da Cunha E., González-López J., Decarli R., Hodge J. A., Nagai H., Egami E., Jiang L., Iye M., Kashikawa N., Riechers D. A., Bertoldi F., Cox P., Neri R., Weiss A.	2014, ApJ 792, 34
1937	Fueling Active Galactic Nuclei. II. Spatially Resolved Molecular Inflows and Outflows	Davies R. I., Maciejewski W., Hicks E. K. S., Emsellem E., Erwin P., Burtscher L., Dumas G., Lin M., Malkan M. A., Müller-Sánchez F., Orban de Xivry G., Rosario D. J., Schnorr-Müller A., Tran A.	2014, ApJ 792, 101
1938	Mapping the Release of Volatiles in the Inner Comae of Comets C/2012 F6 (Lemmon) and C/2012 S1 (ISON) Using the Atacama Large Millimeter/Submillimeter Array	Cordiner M. A., Remijan A. J., Boissier J., Milam S. N., Mumma M. J., Charnley S. B., Paganini L., Villanueva G., Bockelée-Morvan D., Kuan Y.-J., Chuang Y.-L., Lis D. C., Biver N., Crovisier J., Minniti D., Coulson I. M.	2014, ApJ 792, LL2
1939	Circumbinary Ring, Circumstellar Disks, and Accretion in the Binary System UY Aurigae	Tang Y.-W., Dutrey A., Guilloteau S., Piétu V., Di Folco E., Beck T., Ho P. T. P., Boehler Y., Gueth F., Bary J., Simon M.	2014, ApJ 793, 10
1940	Tentative Detection of the Nitrosylium Ion in Space	Cernicharo J., Bailleux S., Alekseev E., Fuente A., Roueff E., Gerin M., Tercero B., Treviño-Morales S. P., Marcelino N., Bachiller R., Lefloch B.	2014, ApJ 795, 40
1941	Spitzer/Infrared Spectrograph Investigation of MIPSGAL 24 μm Compact Bubbles: Low-resolution Observations	Nowak M., Flagey N., Noriega-Crespo A., Billot N., Carey S. J., Paladini R., Van Dyk S. D.	2014, ApJ 796, 116
1942	Discovery of Time Variation of the Intensity of Molecular Lines in IRC+10216 in the Submillimeter and Far-Infrared Domains	Cernicharo J., Teyssier D., Quintana-Lacaci G., Daniel F., Agúndez M., Velilla-Prieto L., Decin L., Guélin M., Encrenaz P., García-Lario P., de Beck E., Barlow M. J., Groenewegen M. A. T., Neufeld D., Pearson J.	2014, ApJ 796, LL21
1943	Detection of significant cm to sub-mm band radio and γ-ray correlated variability in Fermi bright blazars	Fuhrmann L., Larsson S., Chiang J., Angelakis E., Zensus J. A., Nestoras I., Krichbaum T. P., Ungerechts H., Sievers A., Pavlidou V., Readhead A. C. S., Max-Moerbeck W., Pearson T. J.	2014, MNRAS 441, 1899
1944	ALLSMOG: an APEX Low-redshift Legacy Survey for MOlecular Gas - I. Molecular gas scaling relations, and the effect of the CO/H_2 conversion factor	Bothwell M. S., Wagg J., Cicone C., Maiolino R., Møller P., Aravena M., De Breuck C., Peng Y., Espada D., Hodge J. A., Impellizzeri C. M. V., Martín S., Riechers D., Walter F.	2014, MNRAS 445, 2599
1945	First CO(17-16) emission line detected in a z>6 quasar	Gallerani S., Ferrara A., Neri R., Maiolino R.	2014, MNRAS 445, 2848
1946	Two families of exocomets in the β Pictoris system	Kiefer F., Lecavelier des Etangs A., Boissier J., Vidal-Madjar A., Beust H., Lagrange A.-M., Hébrard G., Ferlet R.	2014, Nature 514, 462
1947	Possible planet formation in the young, low-mass, multiple stellar system GG Tau A	Dutrey A., di Folco E., Guilloteau S., Boehler Y., Bary J., Beck T., Beust H., Chapillon E., Gueth F., Huré J.-M., Pierens A., Piétu V., Simon M., Tang Y.-W.	2014, Nature 514, 600
1948	Stellar feedback as the origin of an extended molecular outflow in a starburst galaxy	Geach J. E., Hickox R. C., Diamond-Stanic A. M., Krips M., Rudnick G. H., Tremonti C. A., Sell P. H., Coil A. L., Moustakas J.	2014, Nature 516, 68
1949	What Microwave Astronomical Spectroscopy can tell you about the Carriers of the DIBs	Liszt H., Lucas R., Pety J., Gerin M.	2014, Proc. IAU 297, 163
1950	Unbiased line surveys of molecular clouds in the Galactic center region	Riquelme D., Aladro R., Martín S., Requena-Torres M., Martín-Pintado J., Güsten R., Mauersberger R., Harada N., Hochgürtel S., Menten K. M.	2014, Proc. IAU 303, 117
1951	Disk-halo interactions: molecular clouds in the Galactic center	Riquelme D., Martín-Pintado J., Mauersberger R., Martín S., Bronfman L.	2014, Proc. IAU 303, 177
1952	The Herschel-PACS photometer calibration. Point-source flux calibration for scan maps	Balog Z., Müller T., Nielbock M., Altieri B., Klaas U., Blommaert J., Linz H., Lutz D., Moór A., Billot N., Sauvage M., Okumura K.	2014, Exp. Astronomy. 37, 129
1953	PACS photometer calibration block analysis	Moór A., Müller T. G., Kiss C., Balog Z., Billot N., Marton G.	2014, Exp. Astronomy 37, 225
1954	Gas and dust productions of Comet 103P/Hartley 2 from millimetre observations: Interpreting rotation-induced time variations	Boissier J., Bockelée-Morvan D., Biver N., Colom P., Crovisier J., Moreno R., Zakharov V., Groussin O., Jorda L., Lis D. C.	2014, Icarus 228, 197
1955	Superconductor-Insulator-Superconductor Mixers for the 2 mm Band (129-174 GHz)	Navarrini A., Fontana A. L., Maier D., Serres P., Billon-Pierron D.	2014, J. of Infrared, mm and THz Waves 35, 536
1956	MicroSQUID Force Microscopy in a Dilution Refrigerator	Hykel D. J., Wang Z. S., Castellazzi P., Crozes T., Shaw G., Schuster K., Hasselbach K.	2014, J. of low Temp. Physics 175, 861
1957	Latest NIKA Results and the NIKA-2 Project	Monfardini A., Adam R., Adane A., Ade P., André P., Beelen A., Belier B., Benoit A., Bideaud A., Billot N., Bourrion O., Calvo M., Catalano A., Coiffard G., Comis B., D'Addabbo A., Désert F.-X., Doyle S., Goupy J., Kramer C., Leclercq S., Macias-Perez J., Martino J., Mauskopf P., Mayet F., Pajot F., Pascale E., Ponthieu N., Revéret V., Rodriguez L., Savini G., Schuster K., Sievers A., Tucker C., Zylka R.	2014, J. of low Temp. Physics 176, 787
1958	Design and Expected Performance of GISMO-2, a Two Color Millimeter Camera for the IRAM 30-meter telescope	Staguhn J., Benford D., Dwek E., Hilton G., Fixsen D., Irwin K., Jhabvala C., Kovacs A., Leclercq S., Maher S., Miller T., Moseley S. H., Sharp E., Wollack E.	2014, J. of low Temp. Physics. 176, 829

1959	FLASH(+) - A Dual-Channel Wide-Band Spectrometer for APEX	Klein T., Ciechanowicz M., Leinz C., Heyminck S., Gusten R., Kasemann C., Wunsch J., Maier D., Sekimoto Y.	2014, IEEE Trans. on THz Science and Technology 4, 588
1960	The European ALMA Regional Centre: a model of user support	Andreani P., Stoehr F., Zwaan M., Hatziminaoglou E., Biggs A., Diaz-Trigo M., Humphreys E., Petry D., Randall S., Stanke T., van Kampen E., Bárta M., Brand J., Gueth F., Hogerheijde M., Bertoldi F., Muxlow T., Richards A., Vlemmings W.	2014, SPIE 9149, 91490Y
1961	A 3mm band SIS receiver for the Sardinia Radio Telescope	Ladu A., Pisanu T., Navarrini A., Marongiu P., Valente G.	2014, SPIE 9153, 91532J
1962	Optimization of kinetic inductance detectors for millimeter and submillimeter wave detection	Coiffard G., Schuster K. F., Monfardini A., Adane A., Barbier B., Boucher C., Calvo M., Goupy J., Leclercq S., Pignard S.	2014, SPIE 9153, 91530S
1963	Local oscillator development for focal plane array and supra-THz astronomy receivers	Henry M., Ellison B., Aryathilaka P., Brewster N., Huggard P., Yassin G., Withington S., Maier D.	2014, SPIE 9153, 91530O
1964	The NIKA 2013-2014 observation campaigns: control of systematic effects and results	Catalano A., Adam R., Adane A., Ade P., André P., Beelen A., Belier B., Benoît A., Bideaud A., Billot N., Boudou N., Bourrion O., Calvo M., Coiffard G., Comis B., D'Addabbo A., Désert F.-X., Doyle S., Goupy J., Kramer C., Leclercq S., Macías-Pérez J.-F., Martino J., Mauskopf P., Mayet F., Monfardini A., Pajot F., Pascale E., Perotto L., Pointecouteau E., Ponthieu N., Revéret V., Ritacco A., Rodriguez L., Savini G., Schuster K., Sievers A., Tucker C., Zylka R.	2014, SPIE 9153, 915302
1965	Future mmVLBI Research with ALMA: A European vision	Tilanus R. P. J., Krichbaum T. P., Zensus J. A., Baudry A., Bremer M., Falcke H., Giovannini G., Laing R., van Langevelde H. J., Vlemmings W., Abraham Z., Afonso J., Agudo I., Alberdi A., Alcolea J., Altamirano D., Asadi S., Assaf K., Augusto P., Baczko A., Boeck M., Boller T., Bondi M., Boone F., Bourda G., Brajsa R., Brand J., Britzen S., Bujarrabal V., Cales S., Casadio C., Casasola V., Castangia P., Cernicharo J., Charlot P., Chemin L., Clenet Y., Colomer F., Combes F., Cordes J., Coriat M., Cross N., D'Ammando F., Dallacasa D., Desmurs J., Eatough R., Eckart A., Eisenacher D., Etoka S., Felix M., Fender R., Ferreira M., Freeland E., Frey S., Fromm C., Fuhrmann L., Gabanyi K., Galvan-Madrid R., Giroletti M., Goddi C., Gomez J., Gourgoulhon E., Gray M., di Gregorio I., Greimel R., Grosso N., Guirado J., Hada K., Hanslmeier A., Henkel C., Herpin F., Hess P., Hodgson J., Horns D., Humphreys E., Hutawarakorn Kramer B., Ilyushin V., Impellizzeri V., Ivanov V., Julião M., Kadler M., Kerins E., Klaassen P., van 't Klooster K., Kording E., Kozlov M., Kramer M., Kreikenbohm A., Kurtanidze O., Lazio J., Leite A., Leitzinger M., Lepine J., Levshakov S., Lico R., Lindqvist M., Liuzzo E., Lobanov A., Lucas P., Mannheim K., Marcaide J., Markoff S., Martí-Vidal I., Martins C., Masetti N., Massardi M., Menten K., Messias H., Migliari S., Mignano A., Miller-Jones J., Minniti D., Molaro P., Molina S., Monteiro A., Moscadelli L., Mueller C., Müller A., Muller S., Niederhofer F., Odert P., Olofsson H., Orienti M., Paladino R., Panessa F., Paragi Z., Paumard T., Pedrosa P., Pérez-Torres M., Perrin G., Perucho M., Porquet D., Prandoni I., Ransom S., Reimers D., Rejkuba M., Rezzolla L., Richards A., Ros E., Roy A., Rushton A., Savolainen T., Schulz R., Silva M., Sivakoff G., Soria-Ruiz R., Soria R., Spaans M., Spencer R., Stappers B., Surcis G., Tarchi A., Temmer M., Thompson M., Torrelles J., Truestedt J., Tudose V., Venturi T., Verbiest J., Vieira J., Vielzeuf P., Vincent F., Wex N., Wiik K., Wiklind T., Wilms J., Zackrisson E., Zechlin H.	2014, arXiv 1406.4650
1966	Chemical complexity in the Horsehead photodissociation region	Guzmán V. V., Pety J., Gratier P., Goicoechea J. R., Gerin M., Roueff E., Le Petit F., Le Bourlot J.	2014, Faraday Discussions 168, 103
1967	Planet formation in multiple stellar systems: GG Tau A	Di Folco E., Dutrey A., Guilloteau S., Le Bouquin J.-B., Lacour S., Berger J.-P., Köhler R., Piétu V.	2014, SF2A 135
1968	PdBI high-resolution high-sensitivity imaging of a strongly lensed submillimeter source at z=5.24	Boone F., Combes F., Krips M., Richard J., Rawle T., Egami E., Kneib J.-P., Schaerer D., Dessauges-Zavadsky M., Pello R., Clément B.	2014, SF2A 381
1969	High-redshift star formation efficiency as uncovered by the IRAM PHIBSS programs	Freundlich J., Salomé P., Combes F., Tacconi L., Neri R., Garcia-Burillo S., Genzel R., Contini T., Lilly S.	2014, SF2A 387
1970	Identification of protostellar clusters in the inner part of the milky way : Interaction between the ISM and star forming regions.	Beuret M., Billot N., Cambrésy L., Elia D., Molinari S., Pezzuto S., Pestalozzi M., Schisano E.	2014, SF2A 457
1971	CALYPSO: An IRAM Plateau de Bure Survey of Class 0 Protostars	Maury A. J., André P., Maret S., Codella C., Gueth F., Belloche A., Cabrit S., Bacmann A.	2014, Astrophys. and Space Science Proc. 36, 233
1972	First Cometary Observations with ALMA: C/2012 F6 (Lemmon) and C/2012 S1 (ISON)	Cordiner M. A., Milam S. N., Mumma M. J., Charnley S. B., Remijan A. J., Villanueva G., Paganini L., Boissier J., Bockelee-Morvan D., Biver N., Lis D. C., Kuan Y. J., Crovisier J., Coulson I. M., Minniti D.	2014, Lunar and Planetary Science Conf. 45, 2609
1973	Rotating and expanding gas in post-AGB nebulae	Bujarrabal V., Alcolea J., Castro-Carrizo A., van Winckel H., Santander-Garcia M., Neri R., Lucas R.	2014, Asymmetrical Planet. Nebulae VI Conf., 9
1974	Properties of the molecular gas around the most massive evolved stars	Quintana-Lacaci G., Cernicharo, J., Bujarrabal, V., Castro-Carrizo, A., Sanchez-Contreras, C., Agundez, M., Alcolea J.	2014, Asymmetrical Planet. Nebulae VI Conf., 72
1975	Spatio-kinematics of the optical nebula M1-92 with HST/STIS	Ramos-Medina J., Sánchez-Contreras C., Sahai R., Bujarrabal V., Castro-Carrizo A., Morris M.	2014, Asymmetrical Planet. Nebulae VI Conf., 74
1976	Mm-wave and far-IR Molecular line survey of OH 231.8+4.2: Hard-boiled rotten eggs	Sánchez Contreras C., Velilla L., Alcolea J., Quintana-Lacaci G., Cernicharo J., Agundez M., Teyssier D., Bujarrabal V., Castro-Carrizo A., Daniel F., Fonfria J. P., Garcia-Lario P., Goicoechea J. R., Herpin F., Barlow M., Cherchneff I., Comito C., Cordiner M., Decin L., Halfen D. ~., Justtanont K., Latter W., Malloci G., Matsuura M., Menten K., Mulas G., Muller H. S. P., Pardo J. R., Pearson J., Swinyward B., Tenenbaum E., Wesson R., Wyrowski F., Ziurys L.	2014, Asymmetrical Planet. Nebulae VI Conf. 88
1977	The Molecular Gas Properties of M100 as seen by ALMA	Vlahakis C., Martin S., Zwaan M., Bendo G. J., Leon S., Garcia D.	2014, AAS 223, #453.22
1978	Probing the Molecular Complexity of Cometary Volatiles: The Case of C/2012 K1 (PanSTARRS)	Milam S. N., Cordiner M., Remijan A., Gicquel A., Charnley S., Colom P., Crovisier J., Mumma M., Boissier J., Bockelee-Morvan D., Biver N., Villanueva G., Paganini L., Lis D., Kuan Y.-J., Coulson I.	2014, DPS 46, #110.01
1979	GRB 141026A: IRAM 30-meter telescope millimetre observations.	Castro-Tirado A. J., Tello J. C., Gorosabel J., Kramer C., Hermelo I., Paubert G., Sievers A., Staguhn J. G.	2014, GCN 16974

Annex III – Committee Members

EXECUTIVE COUNCIL

R. Bachiller, OAN-IGN, Spain
A. Barcia Cancio, CAY, Spain
R. Genzel, MPE, Germany
J. Gomez-Gonzalez, IGN, Spain
S. Guilloteau, CNRS, France
K. Menten, MPIfR, Germany
D. Mourard, CNRS-INSU, France
J.L. Puget, IAS, France
M. Schleier, MPG, Germany

SCIENTIFIC ADVISORY COMMITTEE

L. Tacconi, MPE, Germany
F. Boulanger, IAS, France
M. Tafalla, OAN-IGN, Spain
D. Jaffe, University of Texas, USA
R. Moreno, LESIA, France
A. Weiss, MPIfR, Germany
F. Wyrowski, MPIfR, Germany
M. Gerin, LERMA, France
P. Planesas, OAN-IGN, Spain

PROGRAM COMMITTEE

H. Beuther, MPIA, Germany
A. Blain, University of Leicester, UK
J. Goicoechea, CSIC/INTA, Spain
S. Bontemps, Obs. Bordeaux, France
C. Henkel, MPIfR, Germany
V. Bujarrabal, OAN-IGN, Spain
C. Codella, INAF, Italy
R. Dave, Univ. of Western Cape, South Africa
A. Usero, OAN, Spain
R. Davies, MPE, Germany
C. Vastel, IRAP, France
A. Beelen, IAS, France
N. Brouillet, LAB, France

AUDIT COMMISSION

M.L. Inisan-Ehret, CNRS, France
G. Maar, MPG, Germany

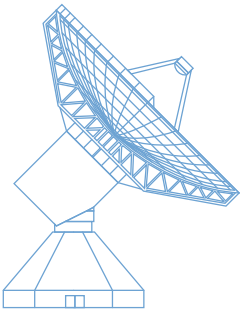

30-meter diameter telescope, Pico Veleta

7 x 15-meter interferometer, NOEMA

The Institut de Radioastronomie Millimétrique (IRAM) is a multi-national scientific institute covering all aspects of radio astronomy at millimeter wavelengths: the operation of two high-altitude observatories – a 30-meter diameter telescope on Pico Veleta in the Sierra Nevada (southern Spain), and an interferometer of six 15 meter diameter telescopes on the Plateau de Bure in the French Alps – the development of telescopes and instrumentation, radio astronomical observations and their interpretation. NOEMA will transform the Plateau de Bure observatory by doubling its number of antennas, making it the most powerful millimeter radiotelescope of the Northern Hemisphere.

IRAM was founded in 1979 by two national research organizations: the CNRS and the Max-Planck-Gesellschaft – the Spanish Instituto Geográfico Nacional, initially an associate member, became a full member in 1990.

The technical and scientific staff of IRAM develops instrumentation and software for the specific needs of millimeter radioastronomy and for the benefit of the astronomical community. IRAM's laboratories also supply devices to several European partners, including for the ALMA project.

IRAM's scientists conduct forefront research in several domains of astrophysics, from nearby star-forming regions to objects at cosmological distances.

IRAM Partner Organizations:
Centre National de la Recherche Scientifique (CNRS) – Paris, France
Max-Planck-Gesellschaft (MPG) – München, Deutschland
Instituto Geografico Nacional (IGN) – Madrid, España

iram
Institut de
Radioastronomie
Millimétrique